Space Science School 2012 (ISWI, SERC)
(Bandung, 2012.9.17-26)

Physics of the Geospace
(magnetosphere-ionosphere current system)

Takashi Kikuchi
Emeritus
Solar-Terrestrial Environment Laboratory, Nagoya University

Current circuit

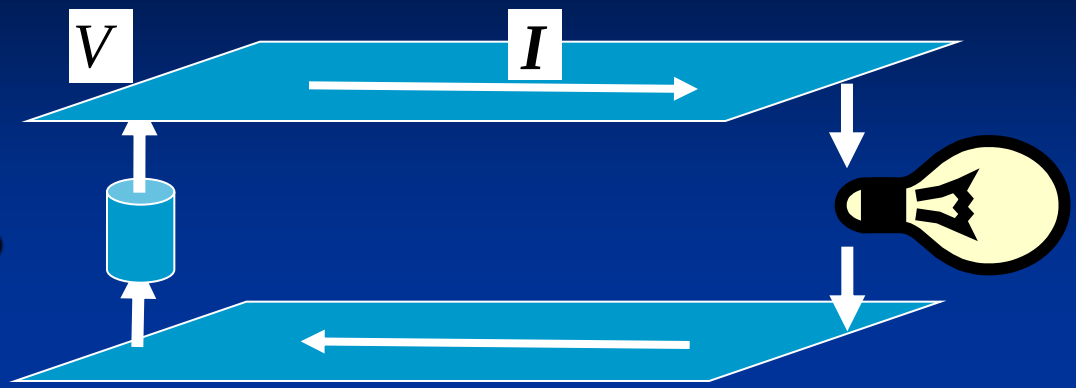

Dynamo

Load

The current system is an energy transmission system.

Energy $W = V \cdot I$

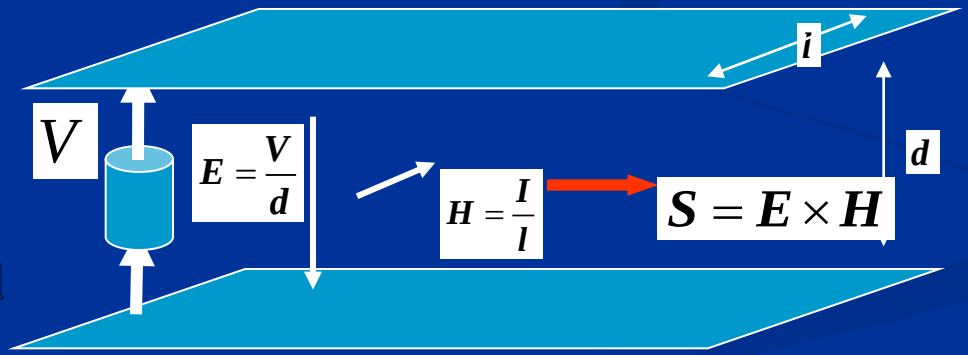

In the dynamo, J and E are in opposite direction.

Therefore, $J \cdot E < 0$

Energy $W = ld \cdot S$

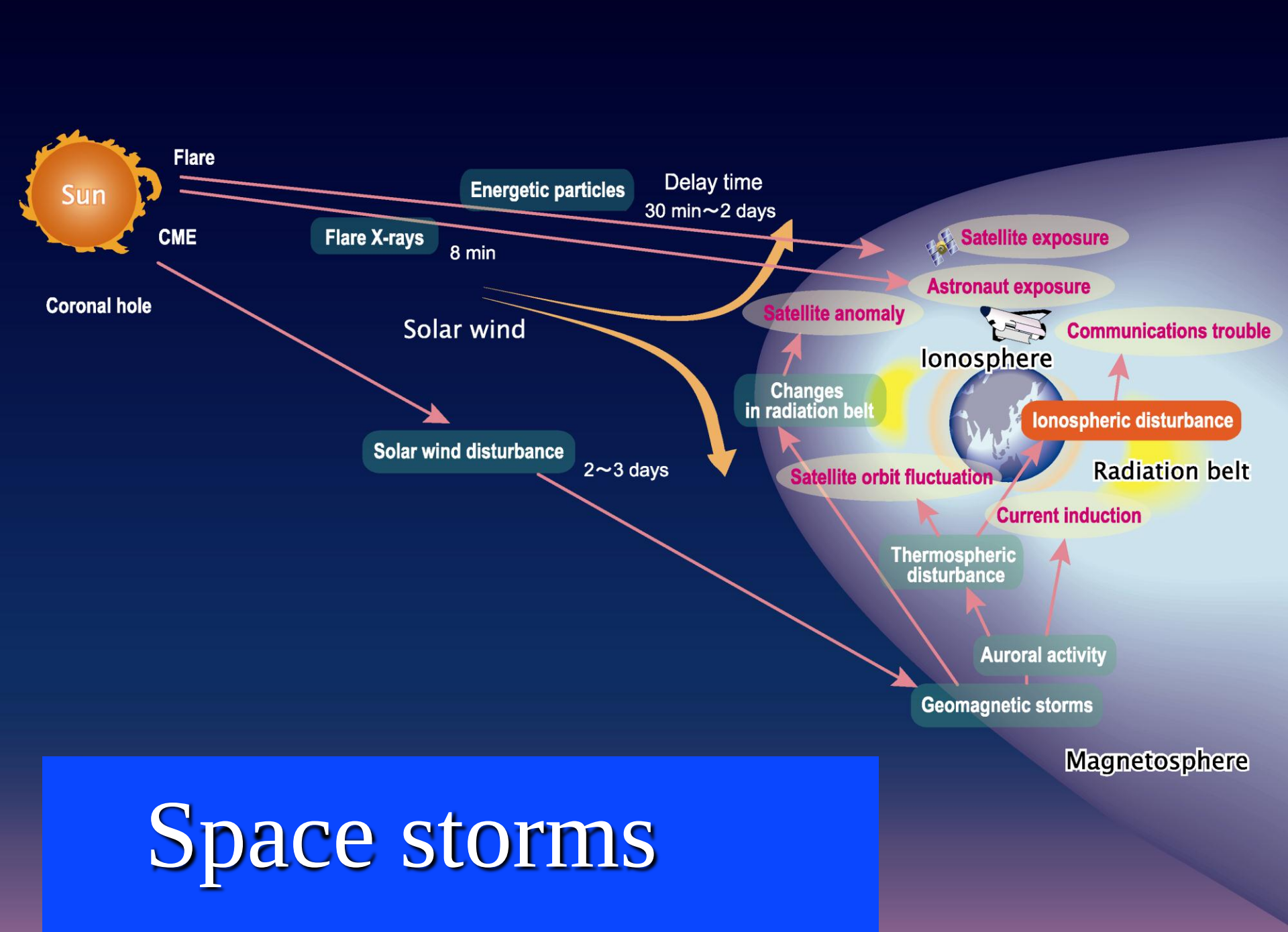

Space storms

Solar flare on 28 October 2003 (SOHO)

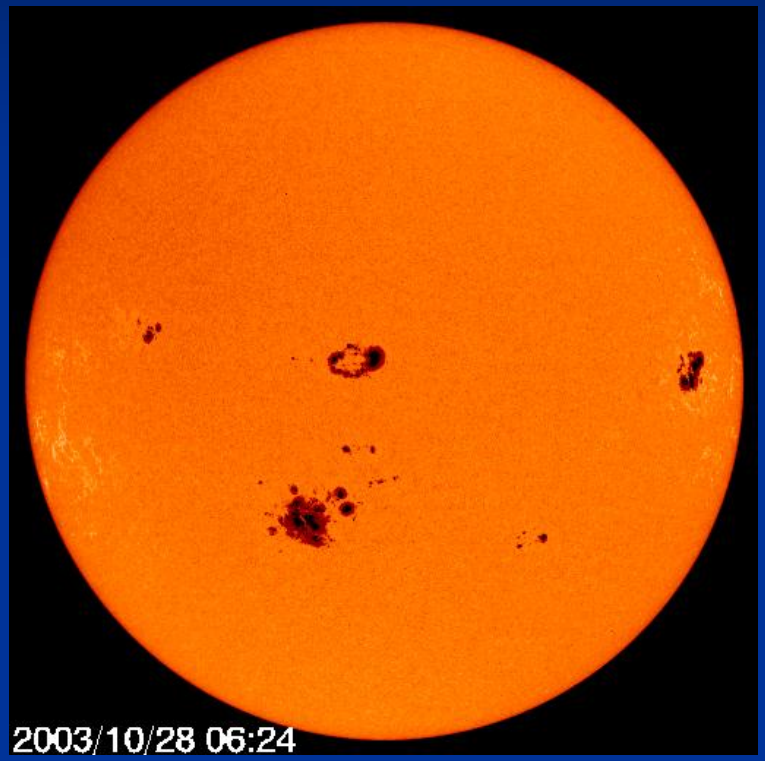

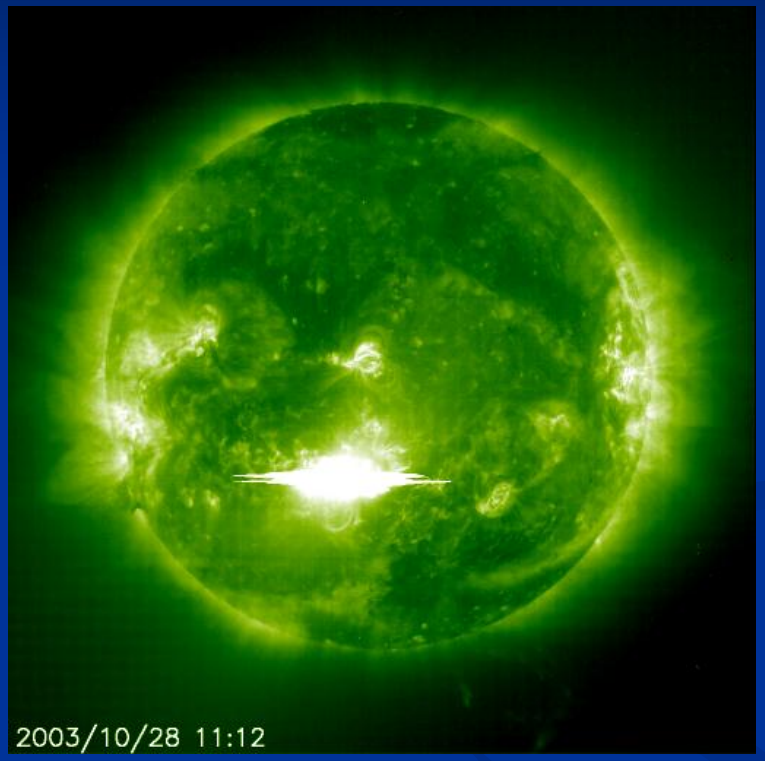

Solar flare on 28 October 2003 (SOHO)

Coronal mass ejection (CME)

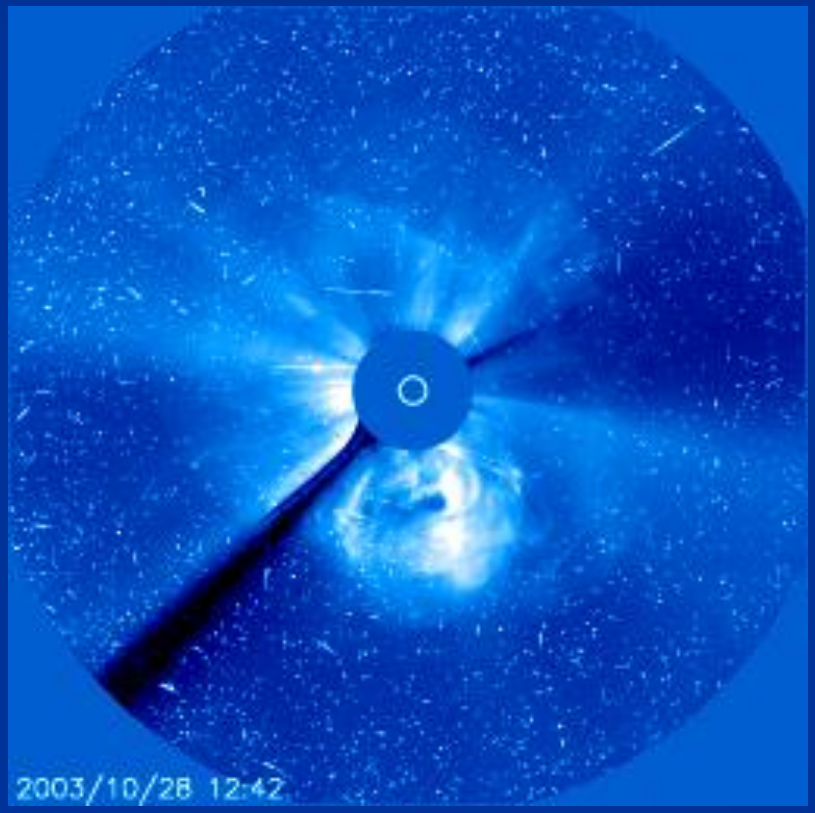

Solar energetic particles

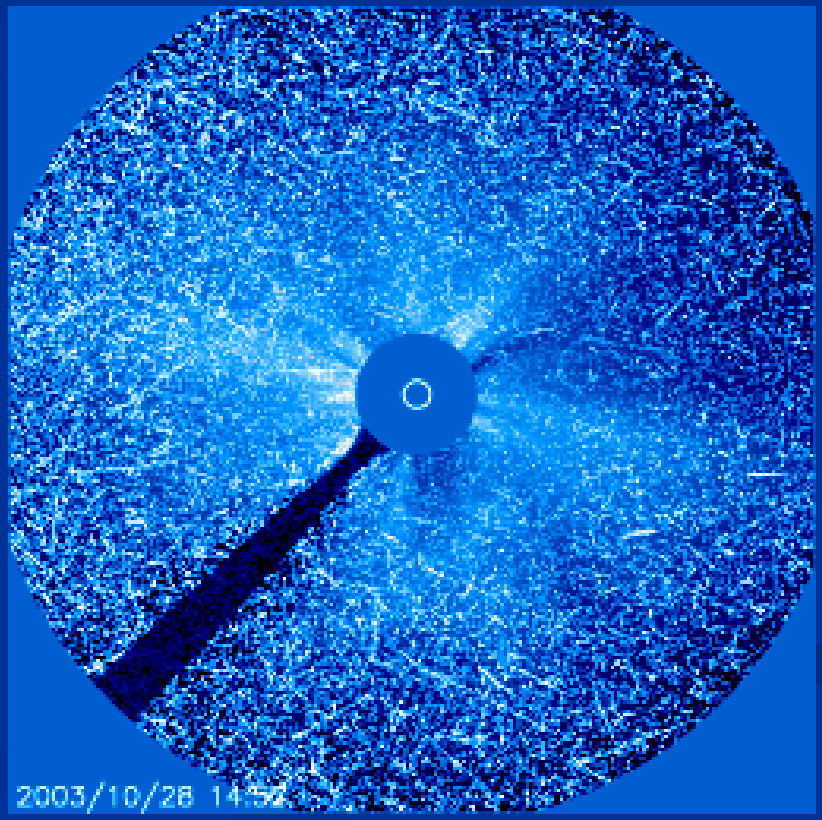

Geomagnetic storms at low latitude (Okinawa)

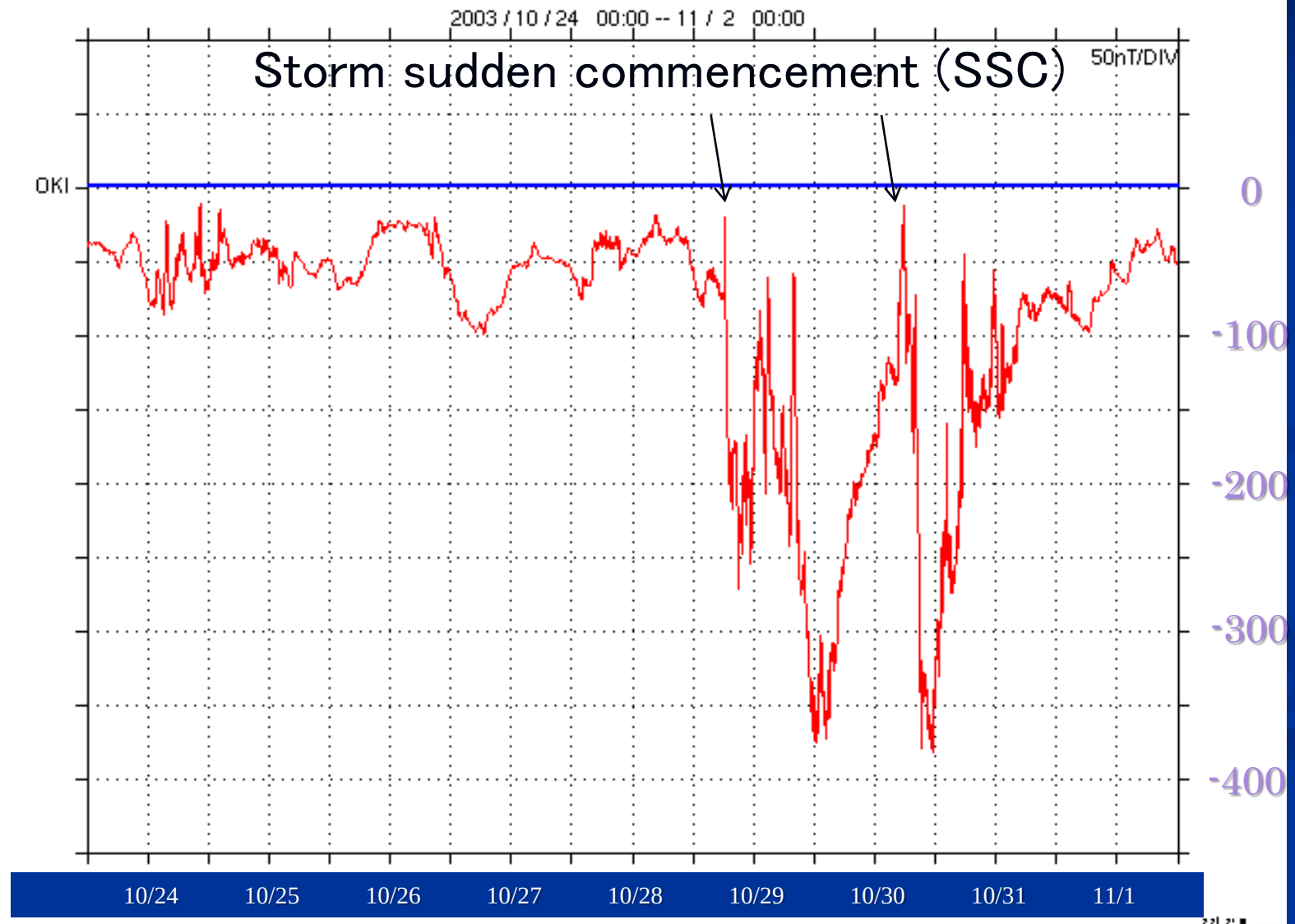

Mid latitude aurora during the major storm in April 1981 in Boulder, Colorado

Low latitude aurora during the major storm in October 1989 in Hokkaido, Japan

31年ぶりに北海道で観測された赤色のオーロラ

Earth observation satellite “Midori” suffered fatal damages during auroral substorms

(1) 30min before, passed over the evening auroral region
(2) 10min before, passed over the morning auroral region

NOAA17(41N,78W)

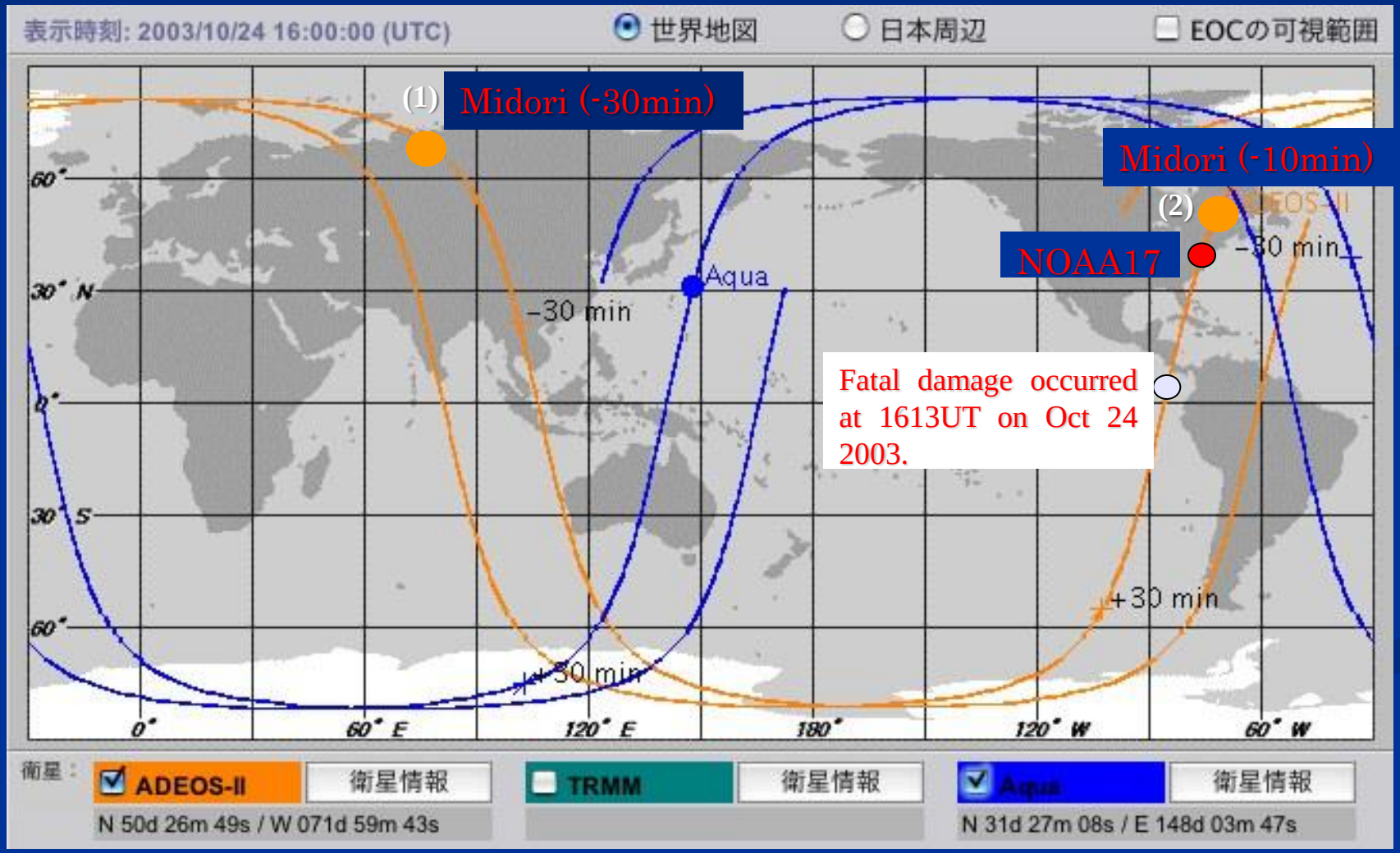

Auroral electrons detected by NOAA
(E>30keV)
(lat > 50度)
(altitude>800km)

磁気インパルスに伴い大量の高エネルギー電子がオーロラ帯に降下した

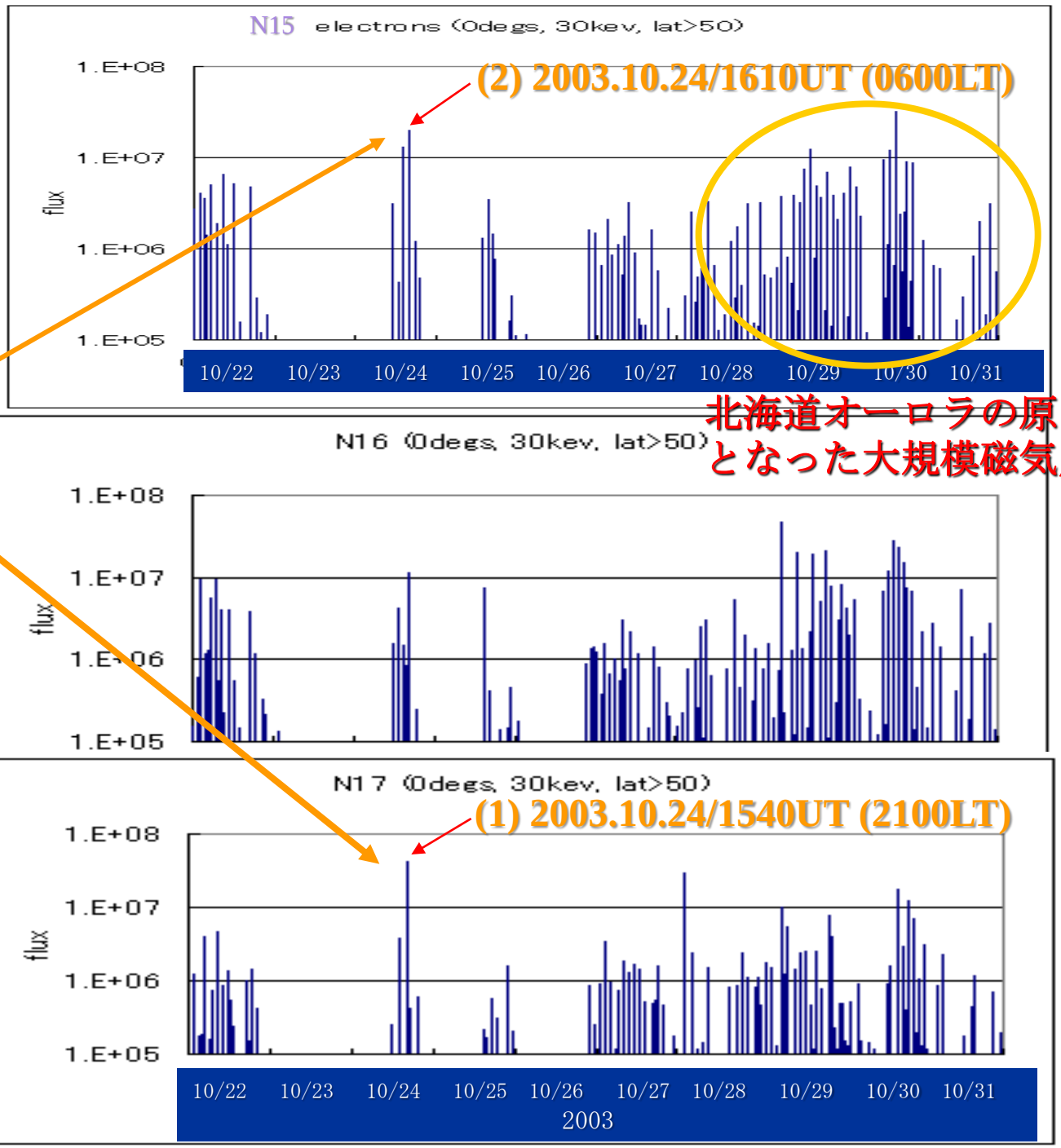

北海道オーロラの原因となった大規模磁気嵐

Satellite drag due to heating of the thermosphere

Asuka lost its attitude control during the major storm in July 2000.

Asahi　2001.1.27

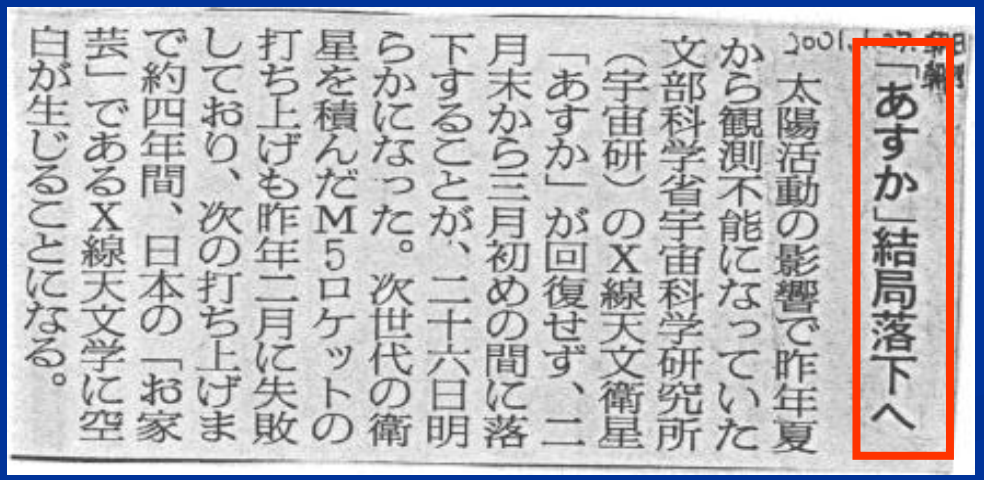

「あすか」結局落下へ

太陽活動の影響で昨年夏から観測不能になっていた文部科学省宇宙科学研究所（宇宙研）のX線天文衛星「あすか」が回復せず、二月末から三月初めの間に落下することが、二十六日明らかになった。次世代の衛星を積んだM5ロケットの打ち上げも昨年二月に失敗しており、次の打ち上げまで約四年間、日本の「お家芸」であるX線天文学に空白が生じることになる。

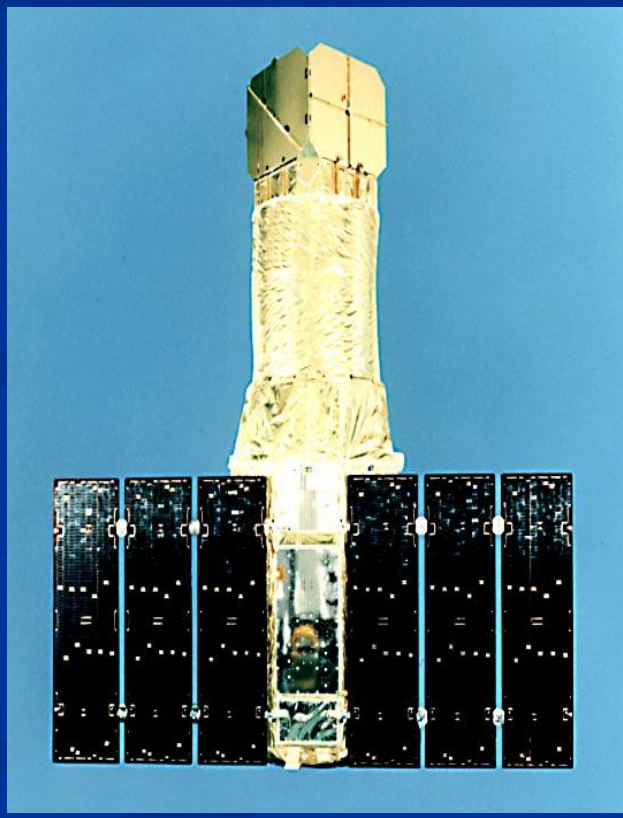

Scintillations on the signal of the meteorological satellite Himawari during the storm in April 2001

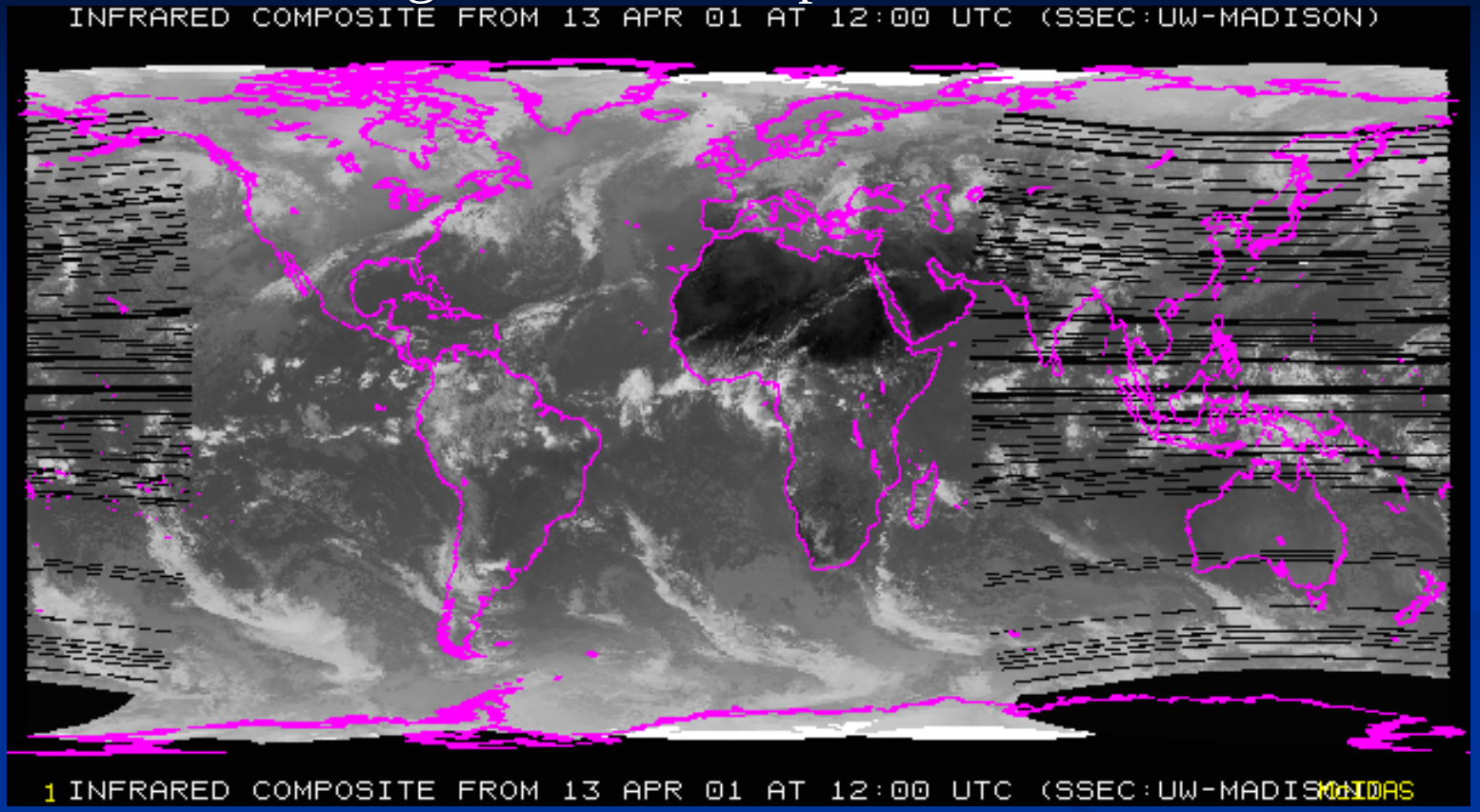

Geomagnetic storm

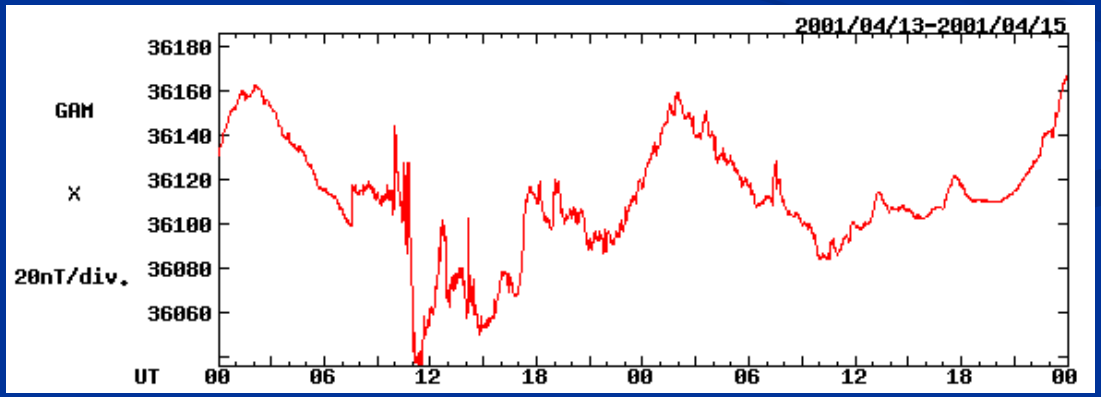

Geomagnetically induced currents on 13 March 1989

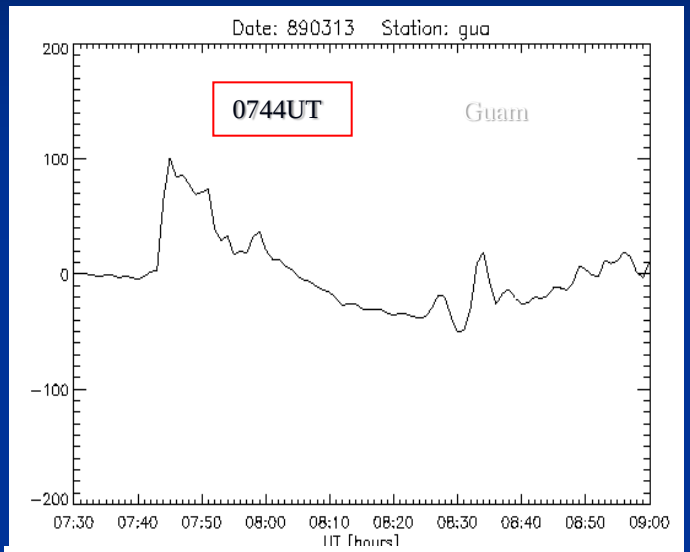

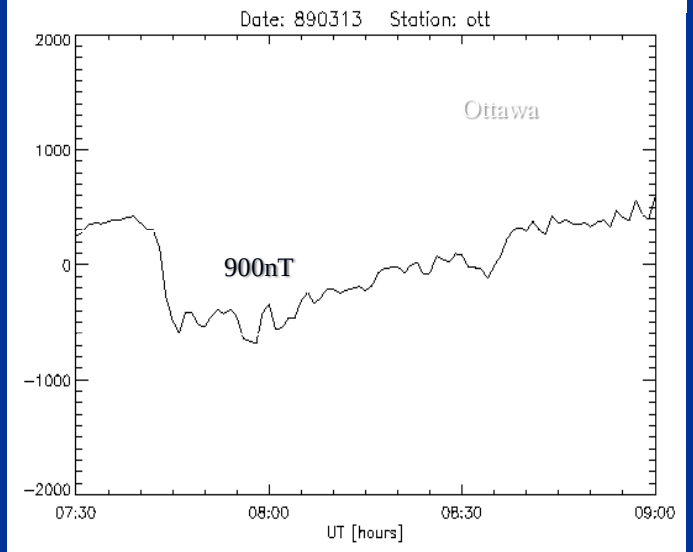

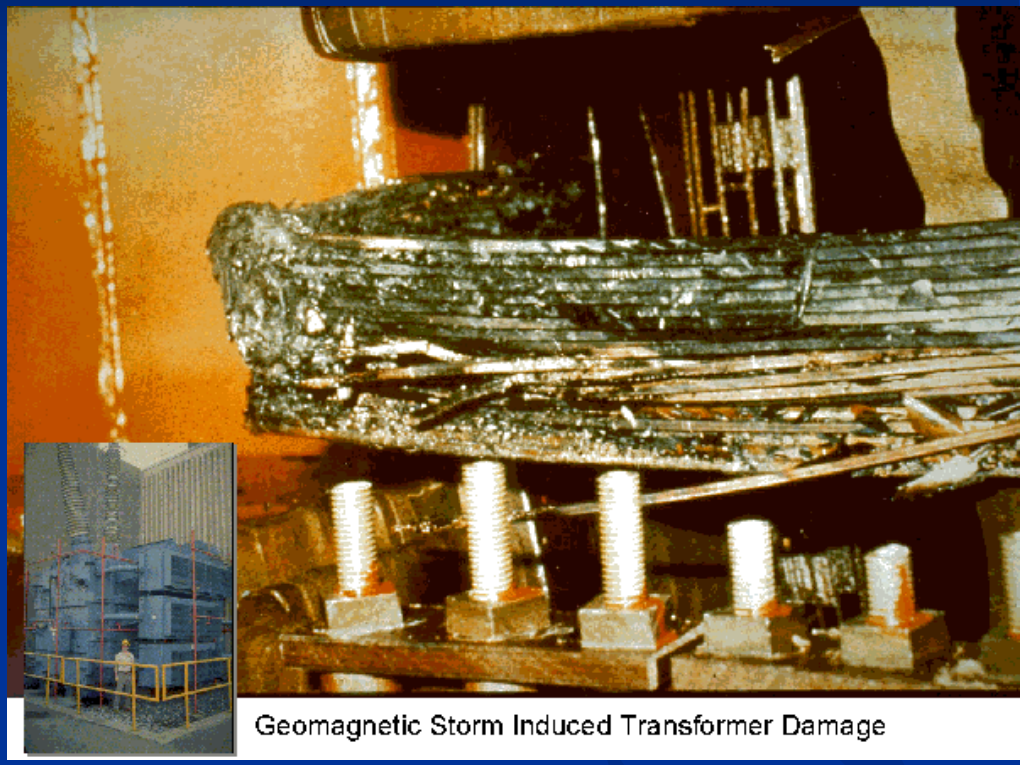

- *March 13, 1989*
- *0744UT:17s*

  Over current, 40s after the onset of dayside SC.
- *0744UT:33s*

  Stop SVC

Contents

- *Magnetosphere-ionosphere current systems during the storm sudden commencements (SSC), geomagnetic storms and substorms*
- *Dynamos of the electric field and currents due to the solar wind dynamic pressure and IMF.*
- *Transmission mechanism of the EM energy to the magnetosphere and ionosphere*

Magnetosphere

Courtesy of T. Tanaka

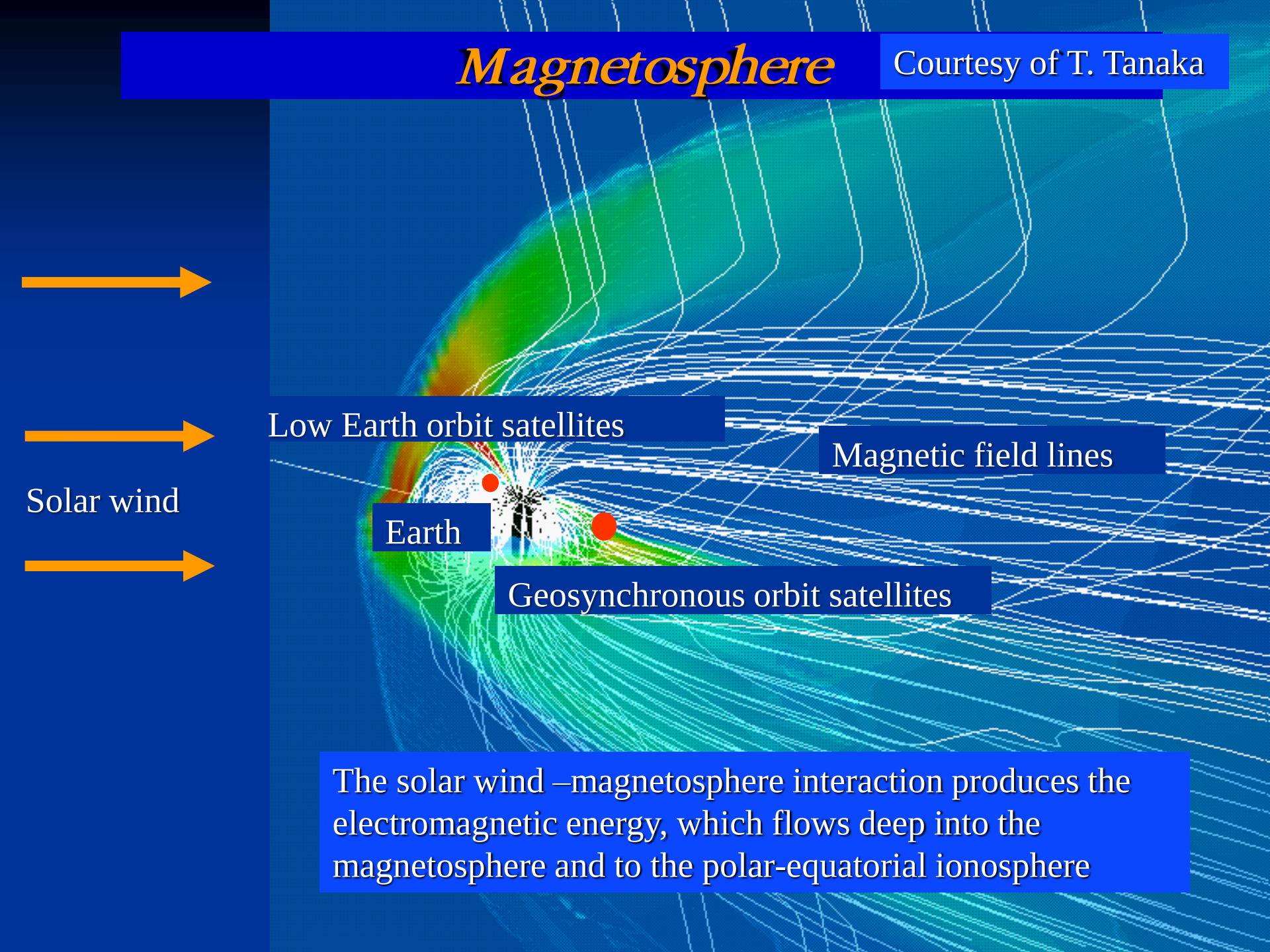

The solar wind –magnetosphere interaction produces the electromagnetic energy, which flows deep into the magnetosphere and to the polar-equatorial ionosphere

Storm sudden commencement (SSC)

Pressure balance

$$2\rho v^2 = \frac{B^2}{2\mu_0}$$

CME

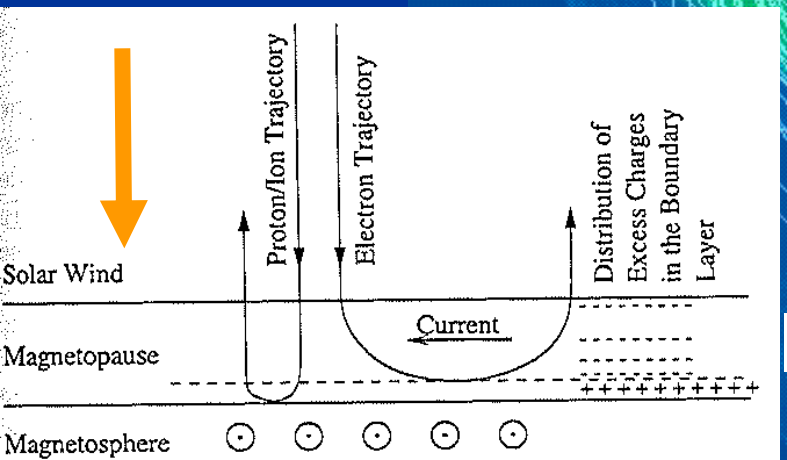

Magnetopause current

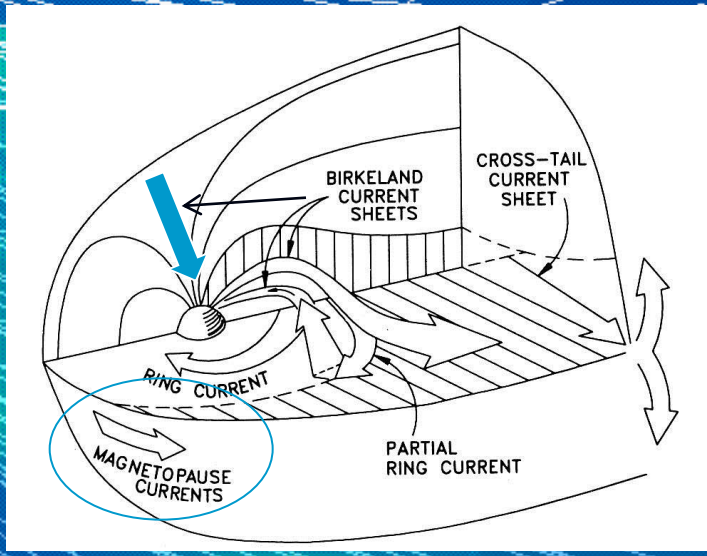

MHD simulation of the PI currents

The magnetopause current is intensified by the CME, which drives the field-aligned current.

Tanaka [2007]

Magnetopause current

Field-aligned currents

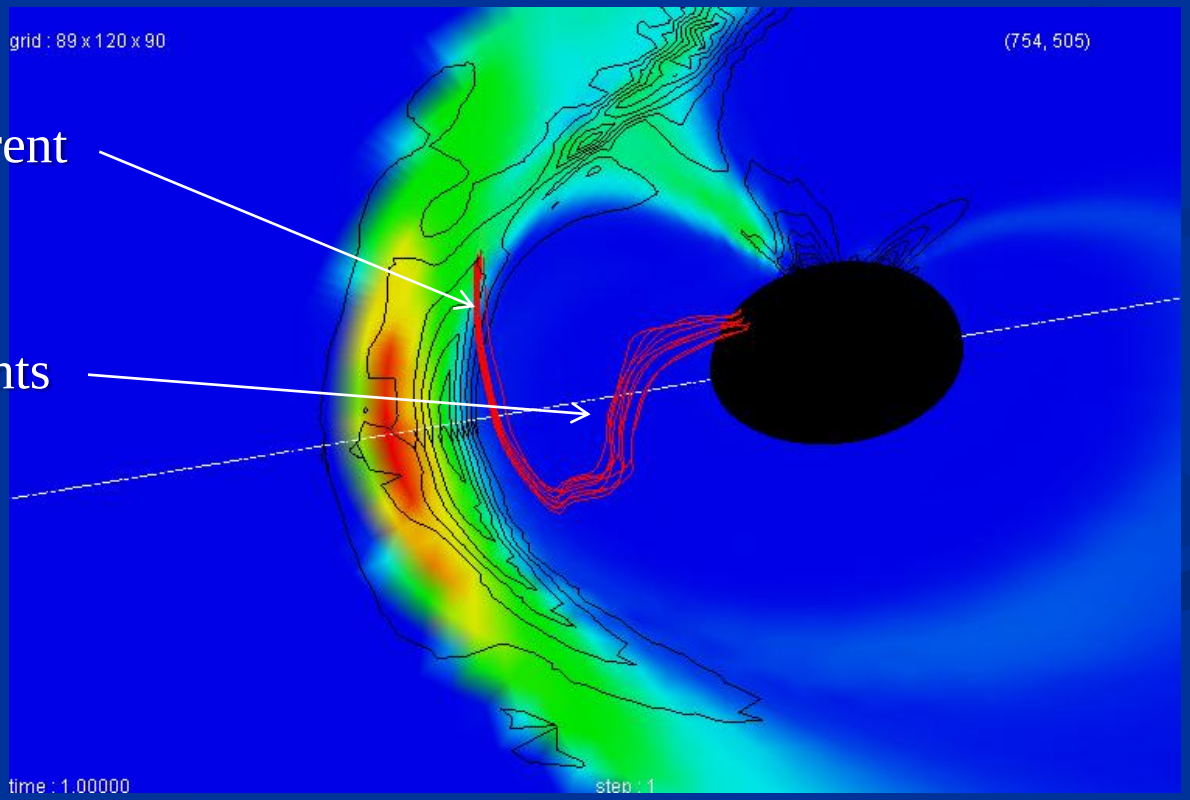

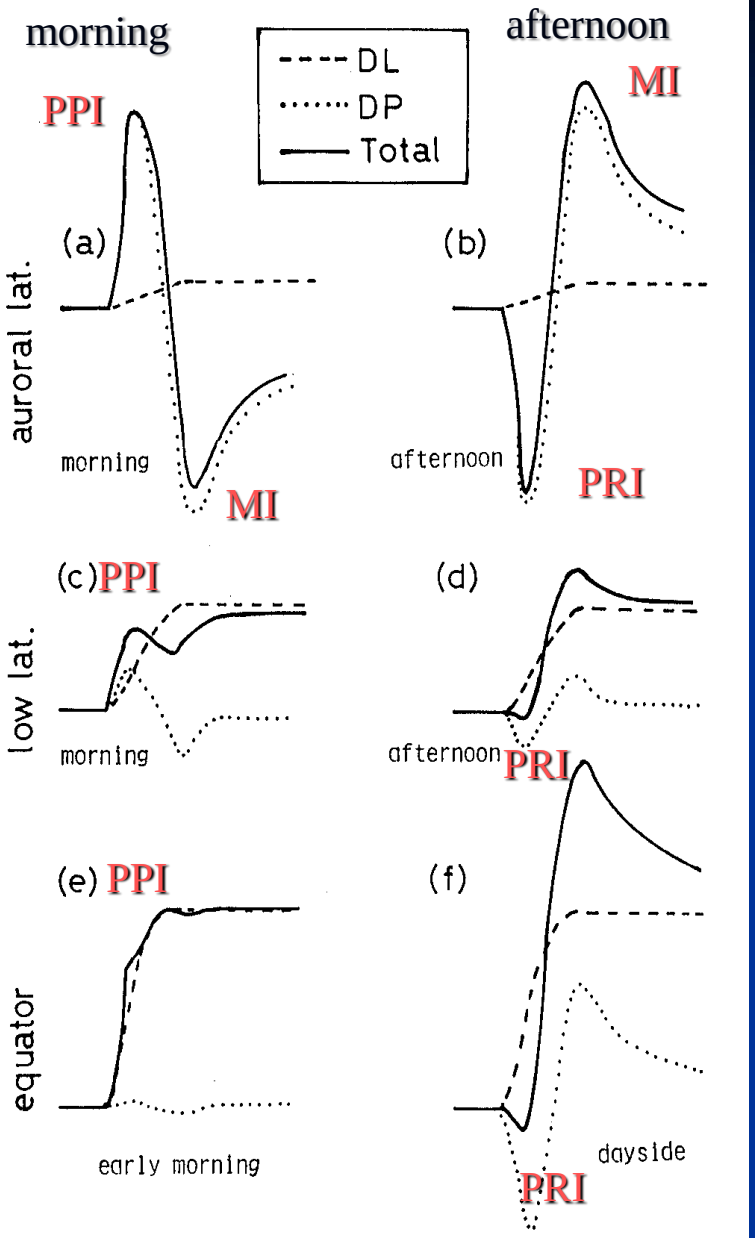

Fig. 11. Decomposition of the SC disturbance field into *DP*- and *DL*-sub-fields.

Local time and latitudinal features of SSC (Araki, 1994)

The preliminary impulse (PI) preceding the main impulse (MI) appears as the preliminary reverse impulse (PRI) and the preliminary positive impulse (PPI), depending on the local time and latitude.

The complicated latitude and local time dependence are explained by means of ionospheric currents caused by the dusk-to-dawn (PRI/PPI) and dawn-to-dusk (MI) electric fields.

Storm sudden commencement (SSC)

SSC: storm sudden commencement
PI: preliminary impulse (1min)
PPI: preliminary positive impulse
PRI: preliminary reverse impulse
MI: main impulse (10min)

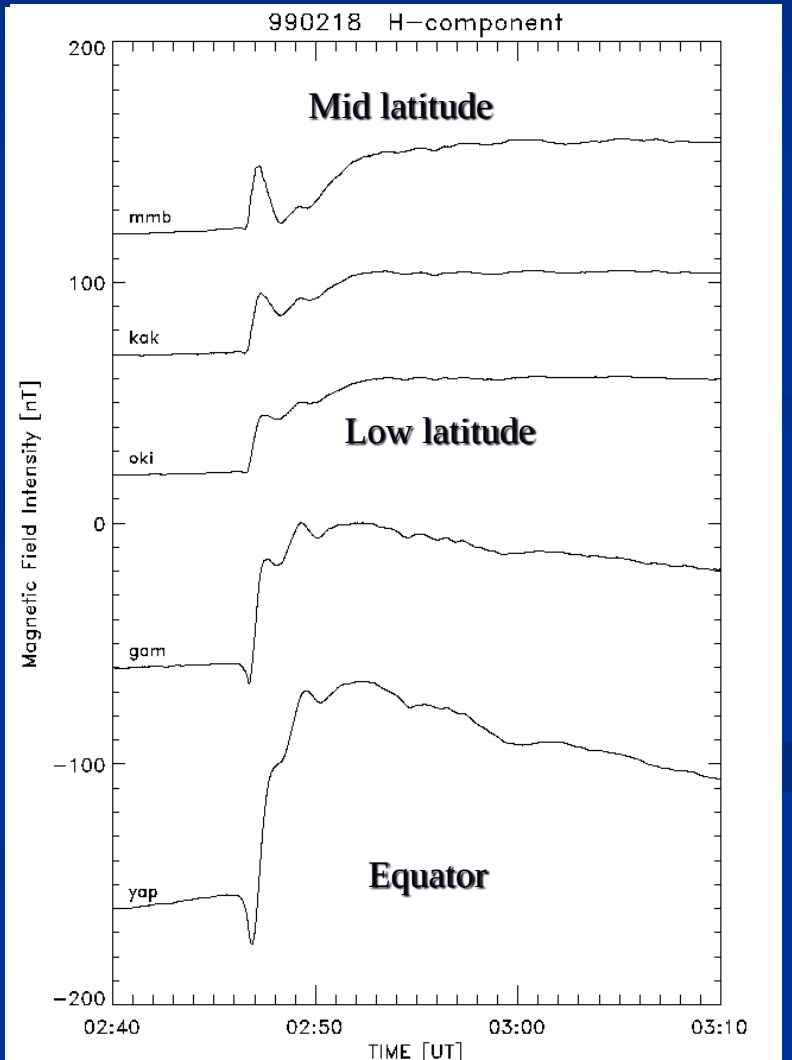

(Kikuchi et al., JGR 2001)

PI Current System in the Magnetosphere and Ionosphere

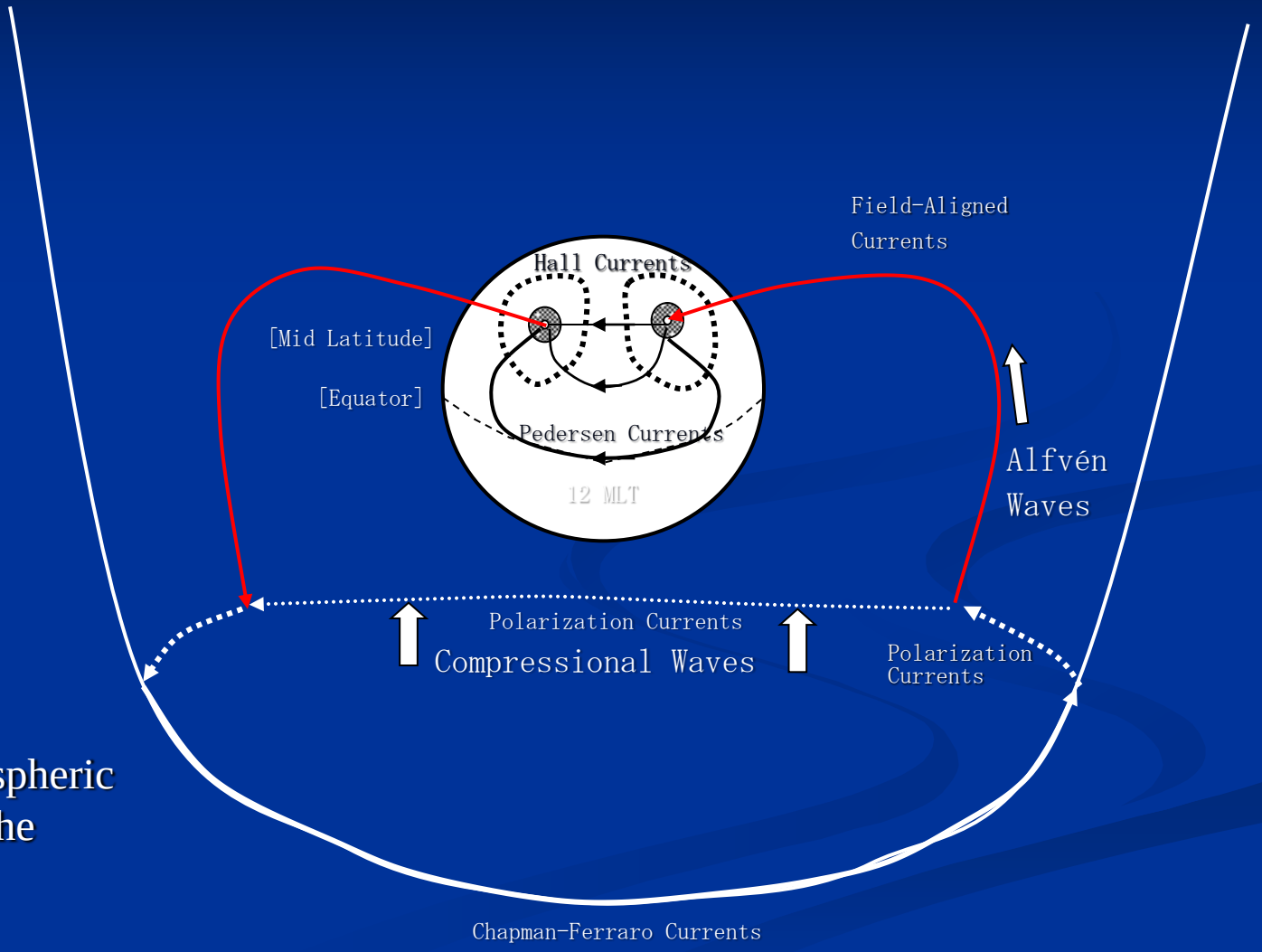

At the equator, the ionospheric current is enhanced by the Cowling effect.

$$\sigma_C = \sigma_P + \frac{\sigma_{H^2}}{\sigma_P}$$

FACs of the PI on the polar ionosphere (MHD simulation)

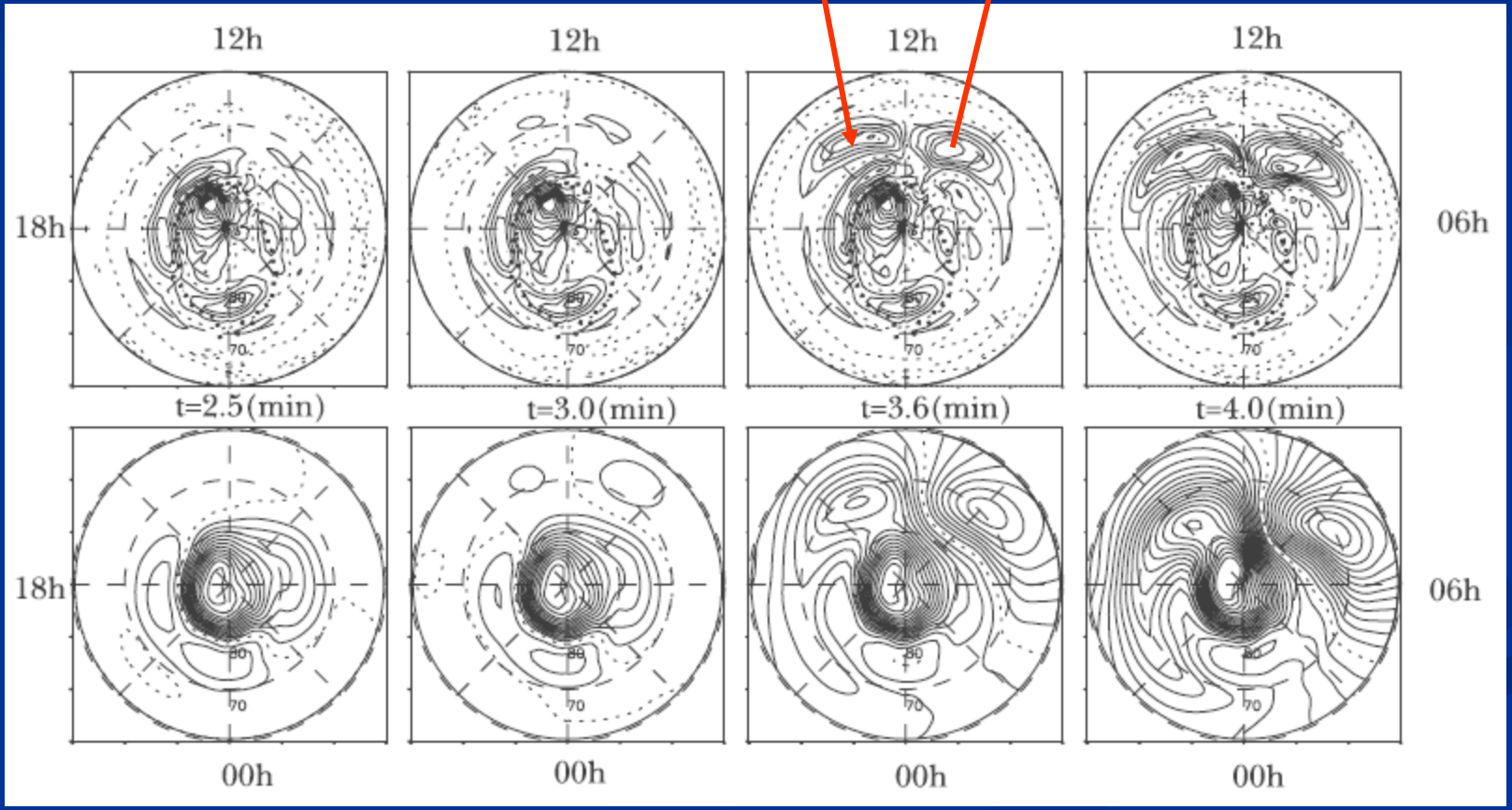

(Fujita et al., JGR 2003)

Near-instantaneous transmission of the PI currents from high latitude to the equator. The PI started within a few seconds.

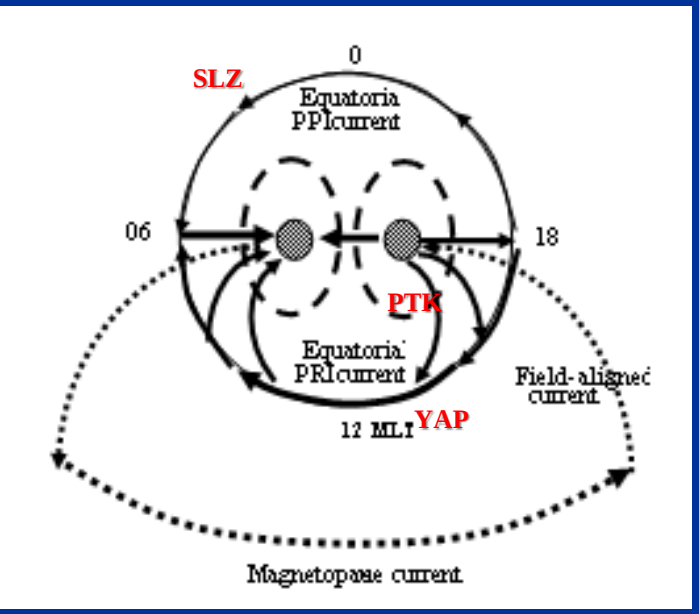

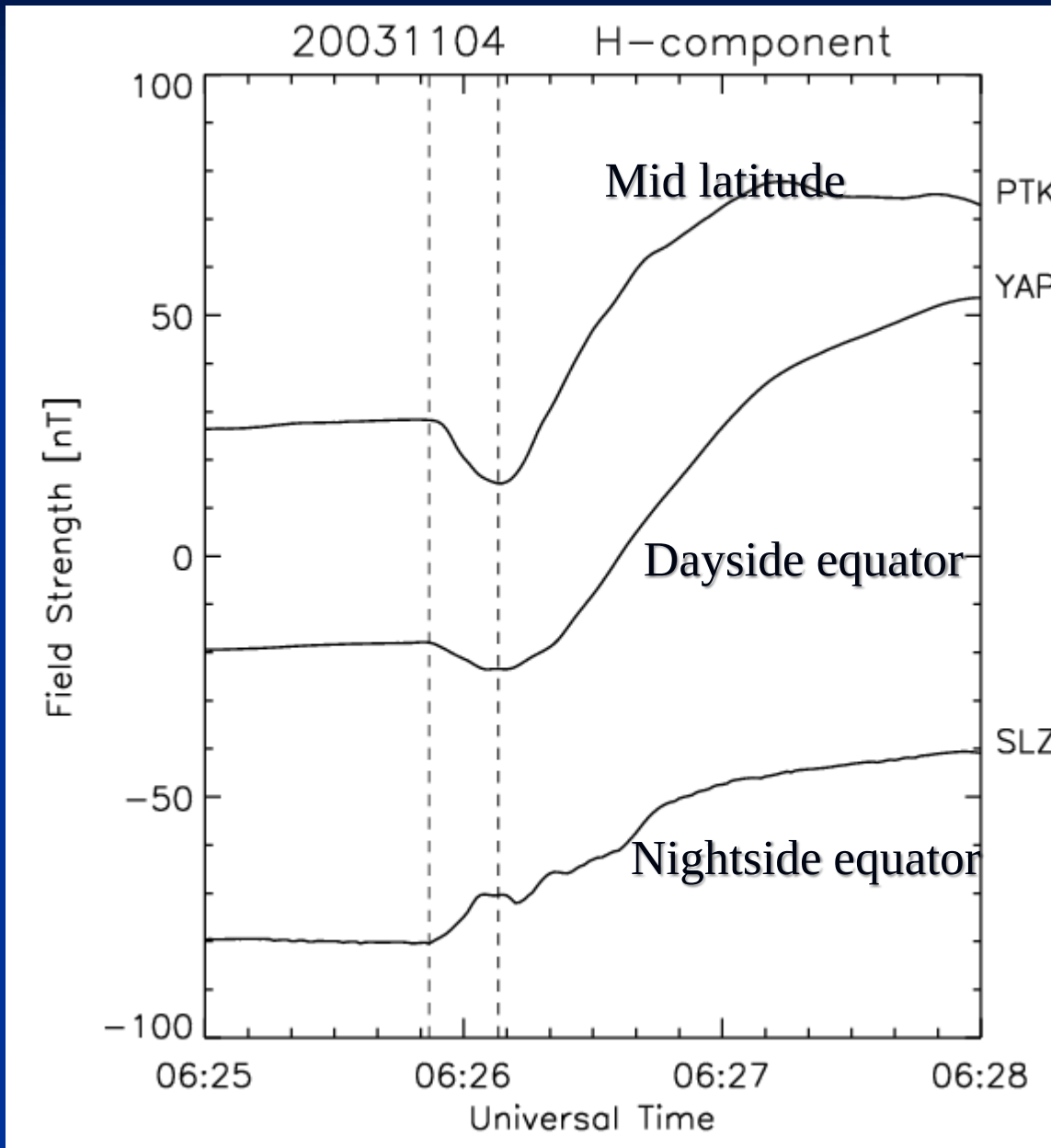

PRI electric field at nightside low latitude (HF Doppler observation)

SCF (SC-associated Frequency deviation) is preceded by a negative PFD (Preliminary Frequency Deviation) in the midnight.

The PFD occurs simultaneously with the high latitude PRI within a time resolution of 10 sec.

(Kikuchi, JGR 1986)

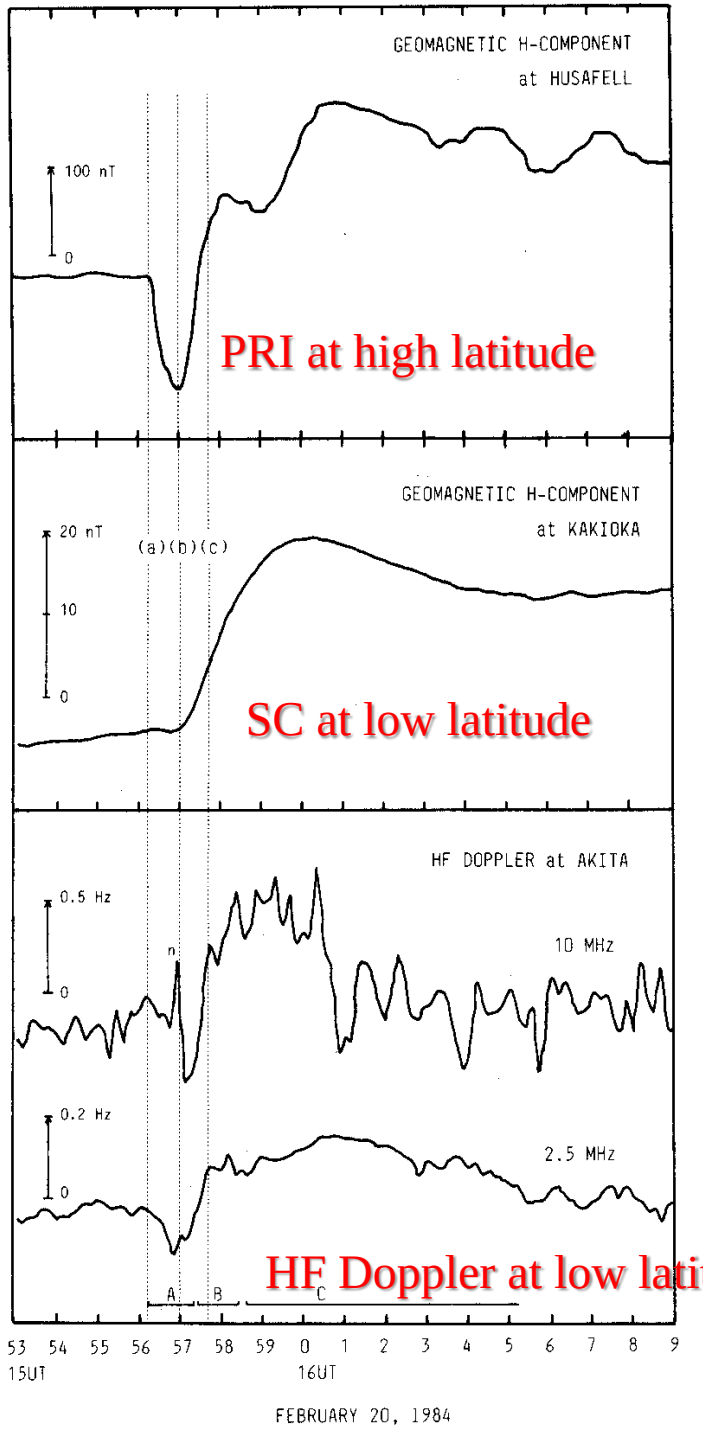

Global PC5 at high-equatorial latitudes (morning sector)

Motoba et al.(JGR 2003)

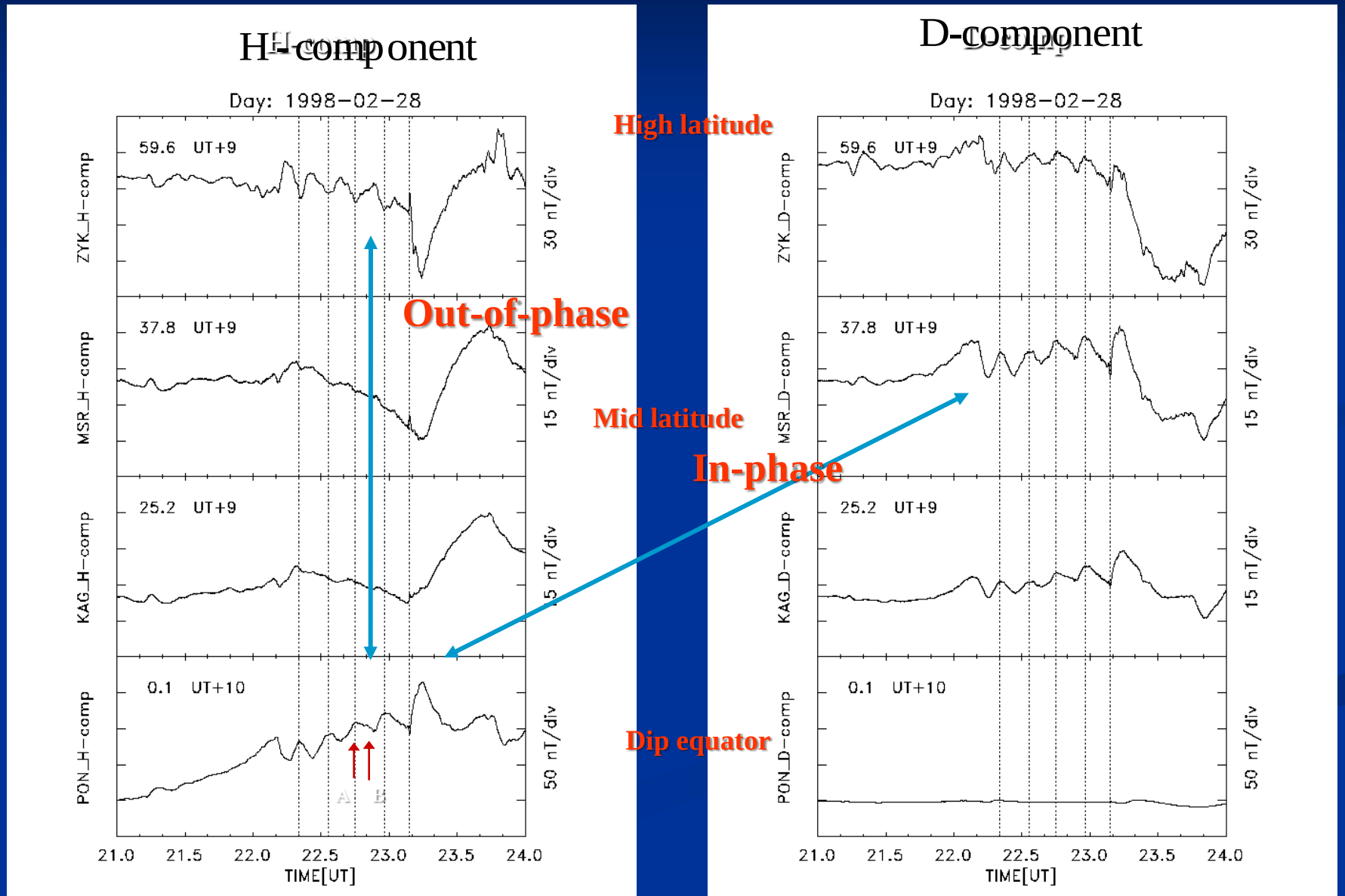

Global PC5 at high-equatorial latitudes (afternoon sector)

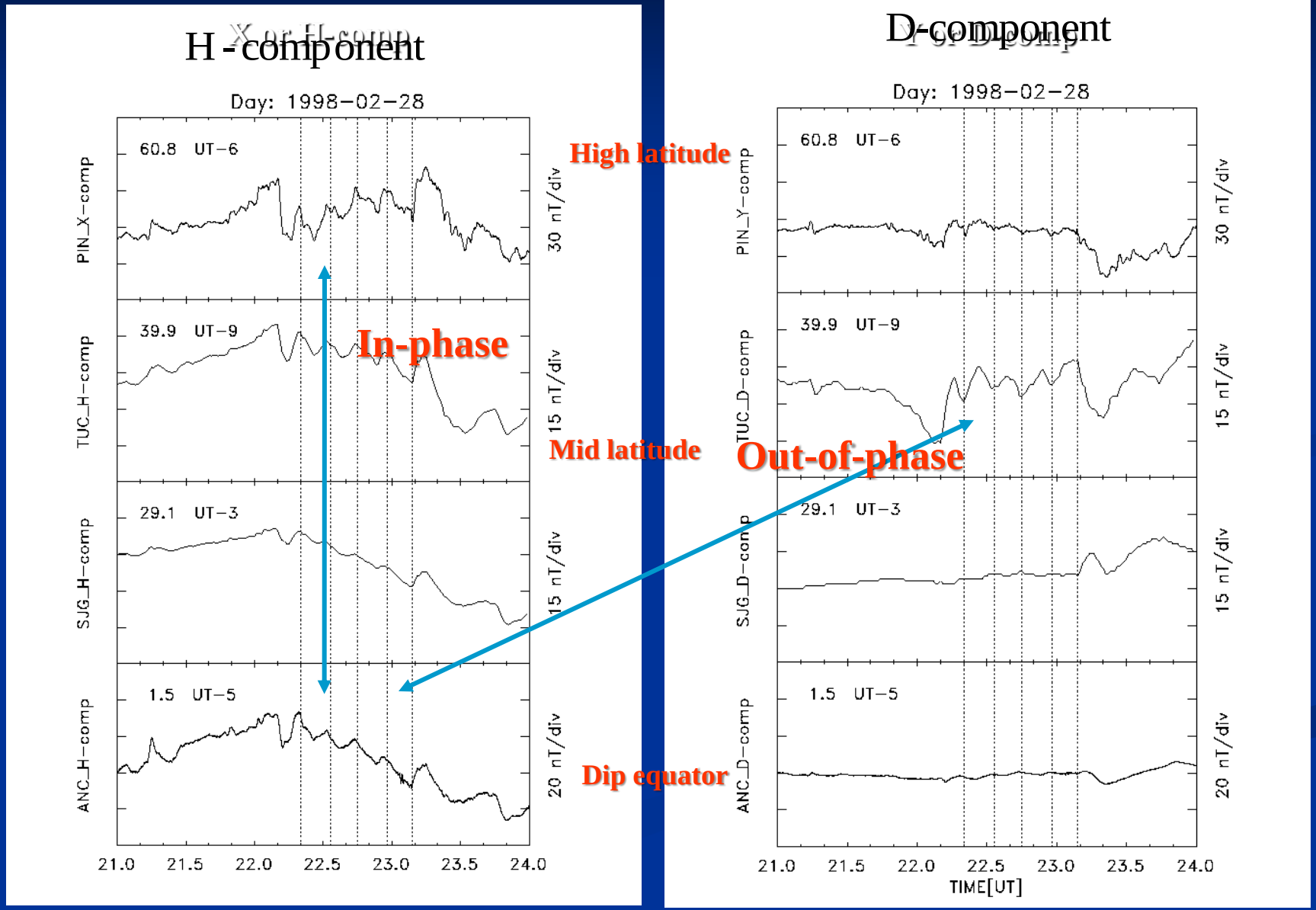

Magnetospheric convection

When the IMF is southward, the magnetic reconnection at the dayside magnetopause put the solar wind energy into the magnetosphere.

Magnetic reconnection

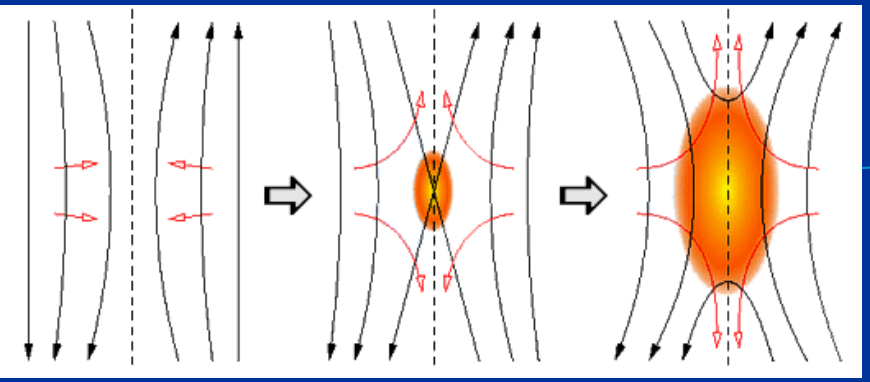

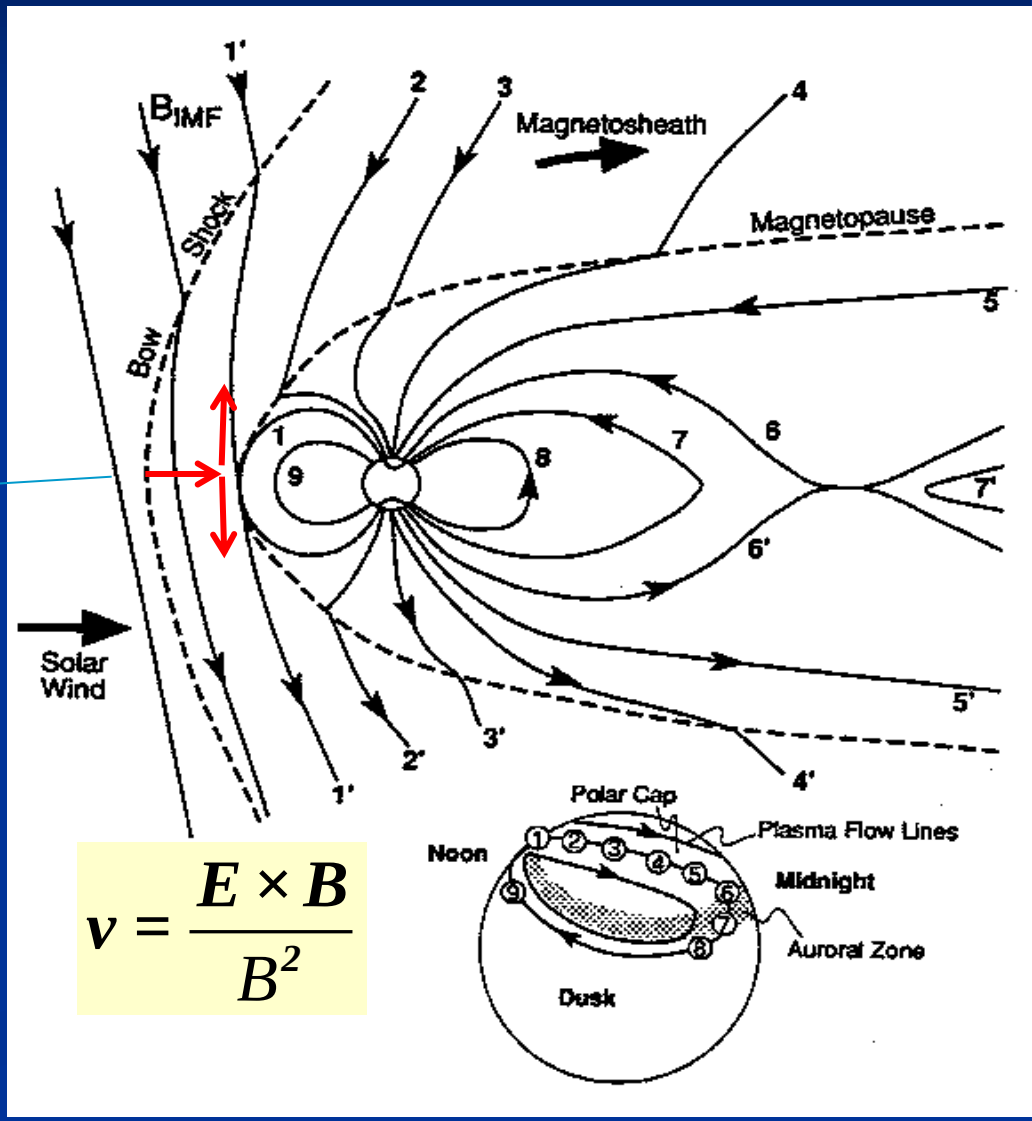

$$v = \frac{E \times B}{B^2}$$

Dungey (1961)

The magnetic reconnection creates the high pressure plasma regime around the cusp (MHD simulation by Tanaka [JGR 1995])

IMF Bz < 0

The red/white color indicates high pressure plasma.

$$\rho \frac{dV}{dt} = J \times B - \nabla p$$

The pressure generates diamagnetic currents.

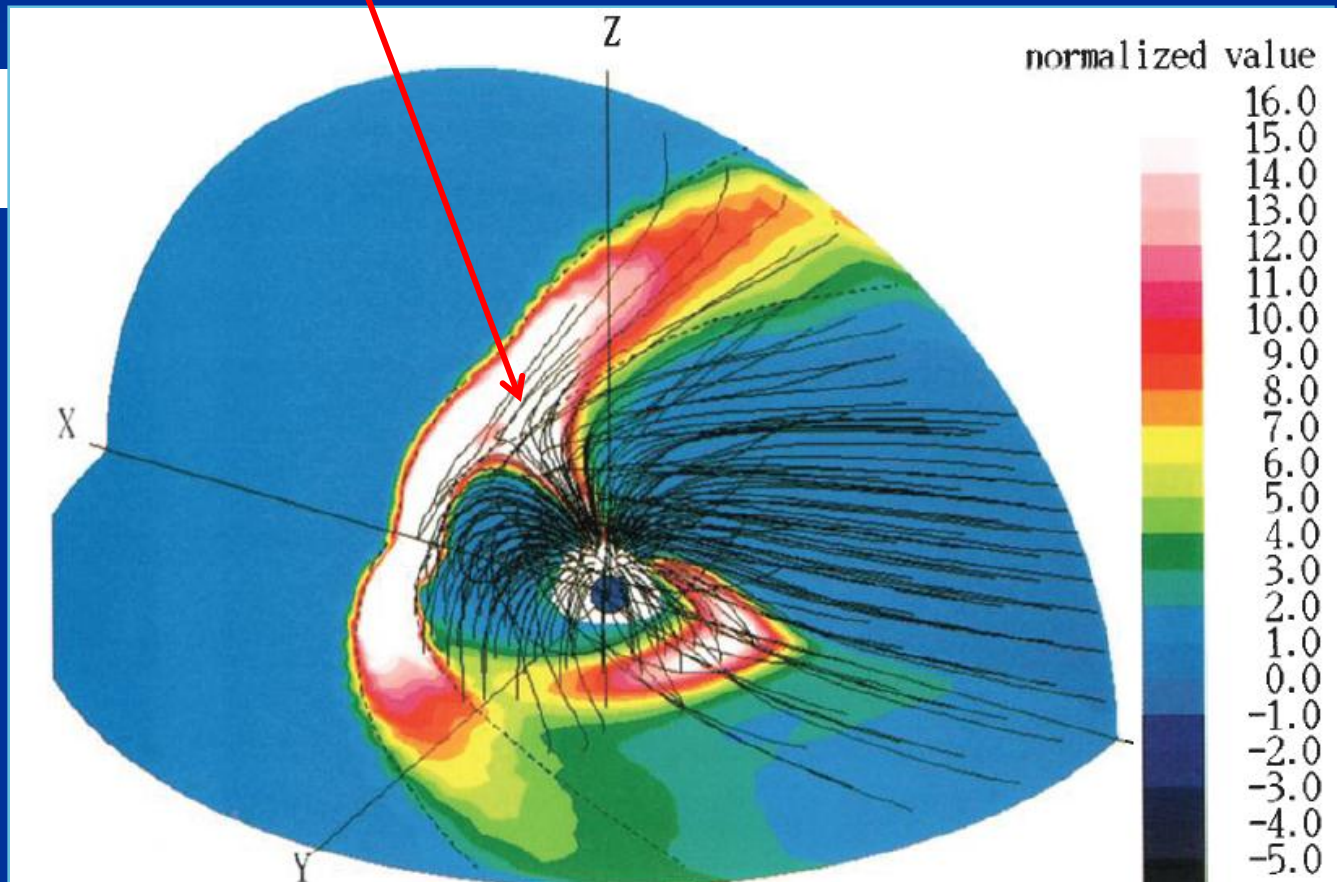

Dynamos of the convection electric field and the Region-1 field-aligned currents
(MHD simulation by Tanaka [JGR 1995])

EM energy = cross polar cap potential × field-aligned currents

Bz < 0

The red/white color represents J□E<0.

The electric currents are generated by the pressure gradient.

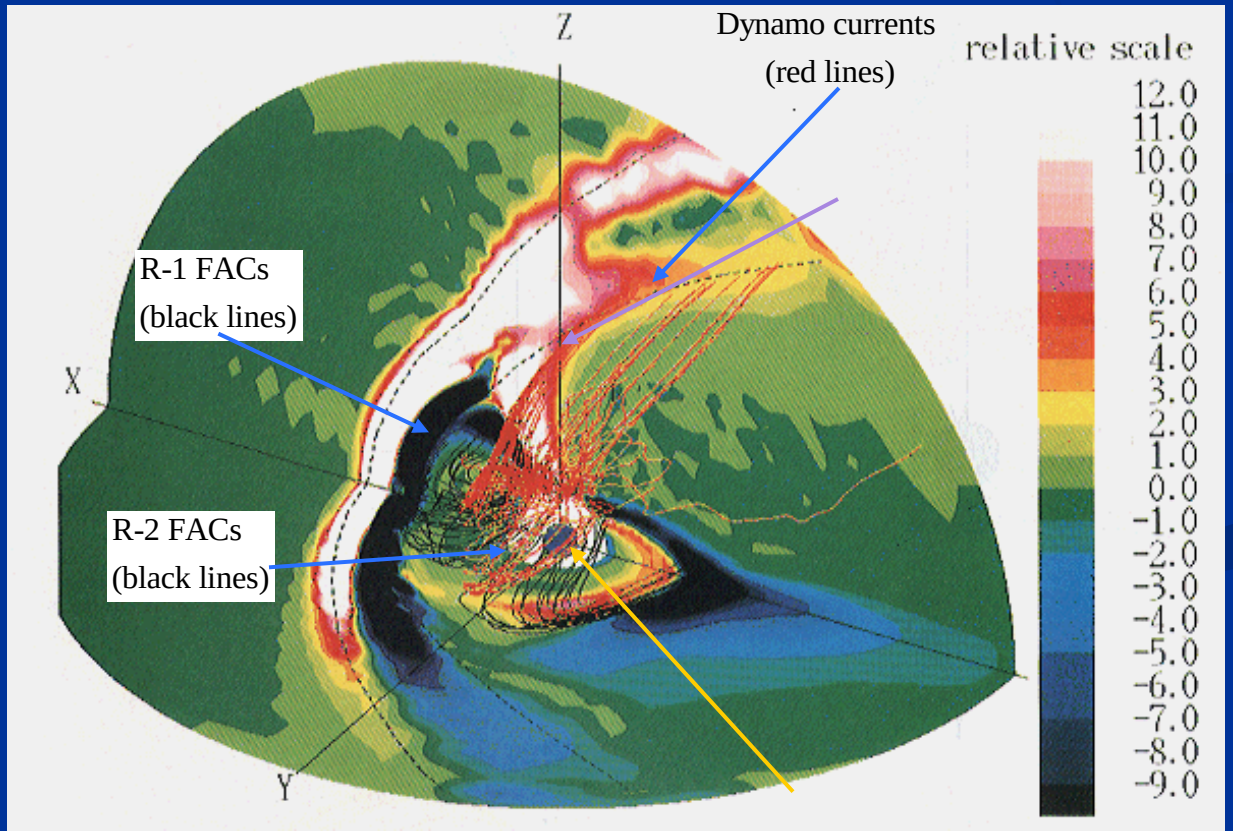

Dynamo currents in the outer magnetosphere (red) and the R1 FACs (black) flowing into the polar ionosphere

The red color indicates J□E<0.

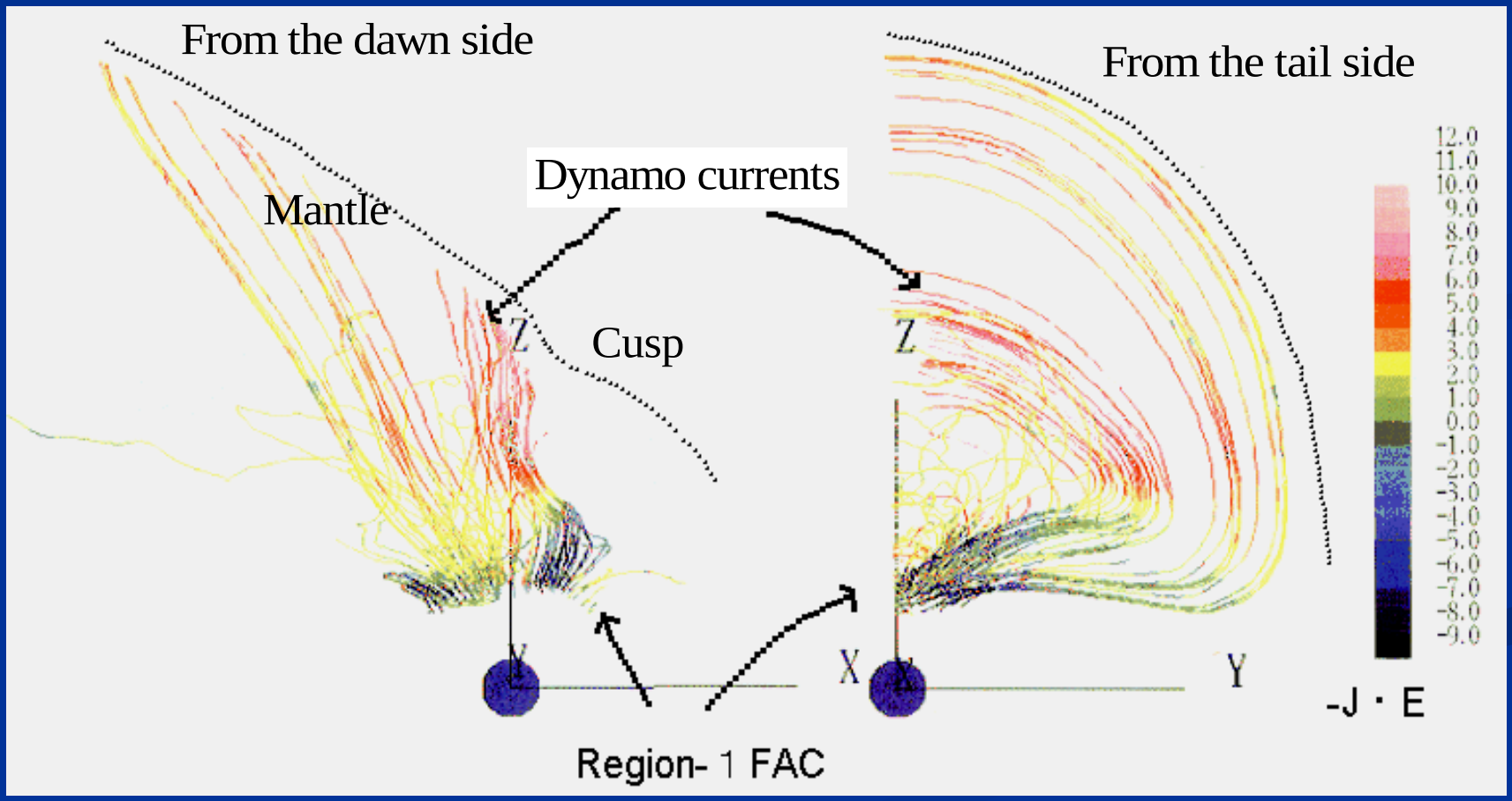

[Tanaka, JGR 1995]

Region-1 and Region-2 field-aligned currents on the polar ionosphere (Tanaka, JGR 1995)

The ionospheric plasma flows along the potential lines.
The ionospheric Hall currents flow in opposite direction to the plasma flow.

100 kV ×100 MA=100 GW

Bz < 0

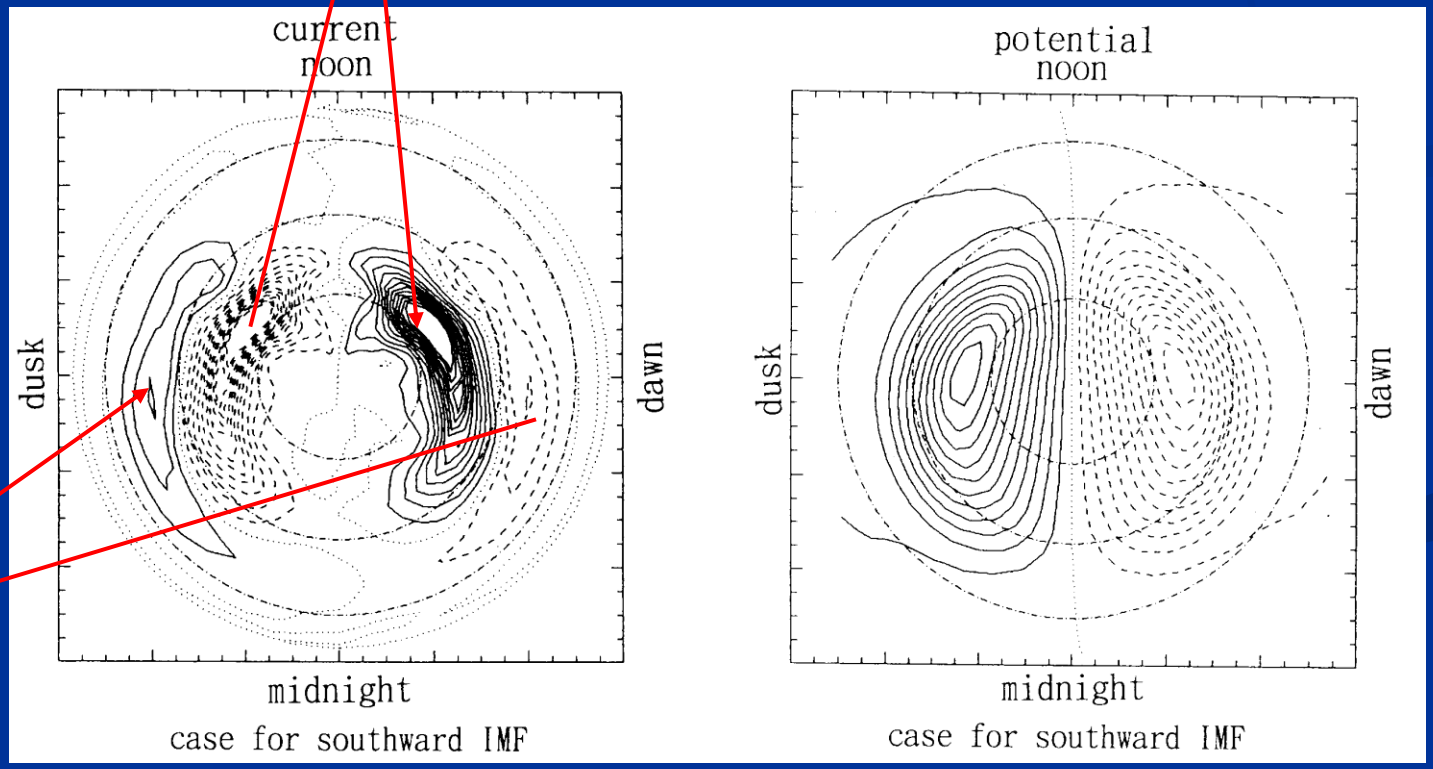

Quasi-periodic DP2 magnetic fluctuations at high latitude and equator correlated with the IMF

Quasi-periodic DP2 magnetic fluctuations are caused by convection electric fields controlled by the IMF.

(Nishida, JGR 1968)

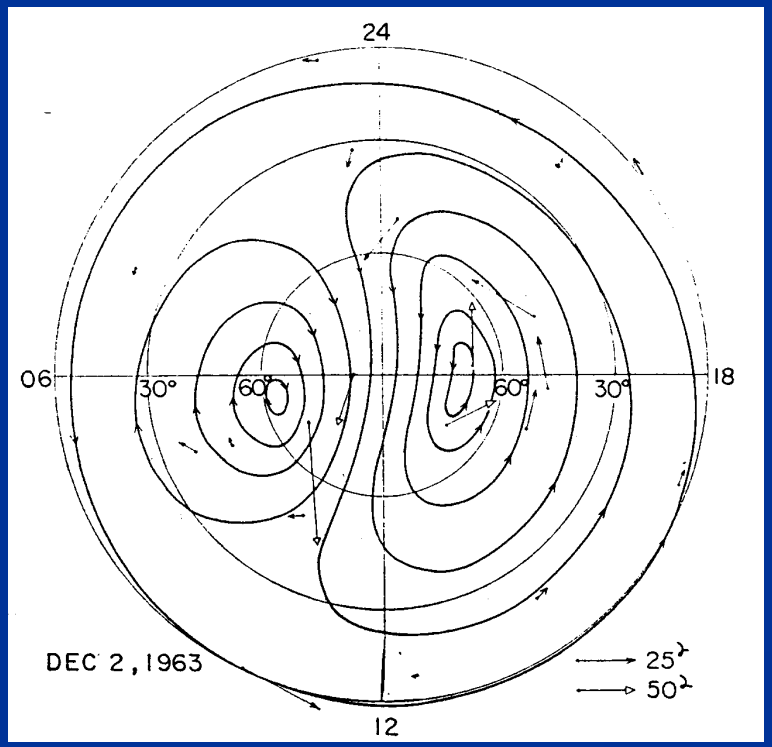

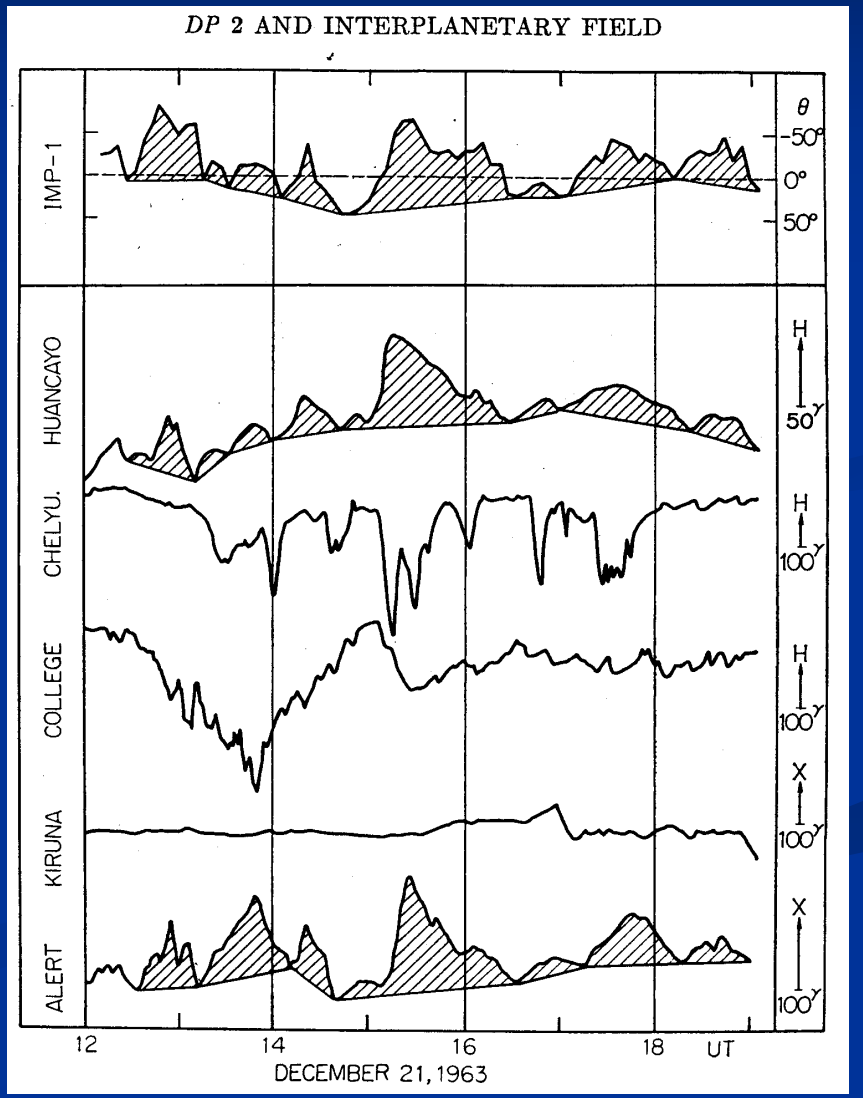

Near-instantaneous transmission of the convection electric field to the equator (R1 FACs - EEJ current circuit)

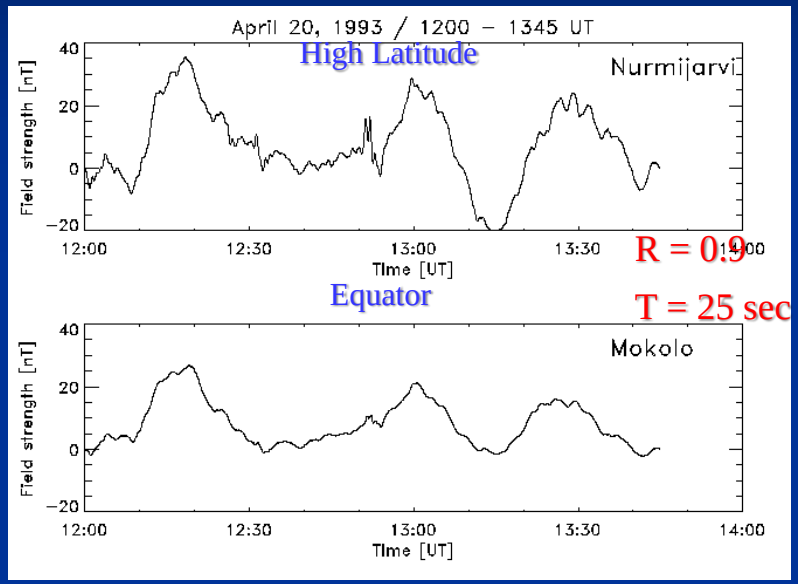

The excellent correlation between the high latitude and equatorial DP2 suggests near-instantaneous transmission of the electric field and current to the equator.

A current circuit is completed between the R1 FACs and the equatorial currents.

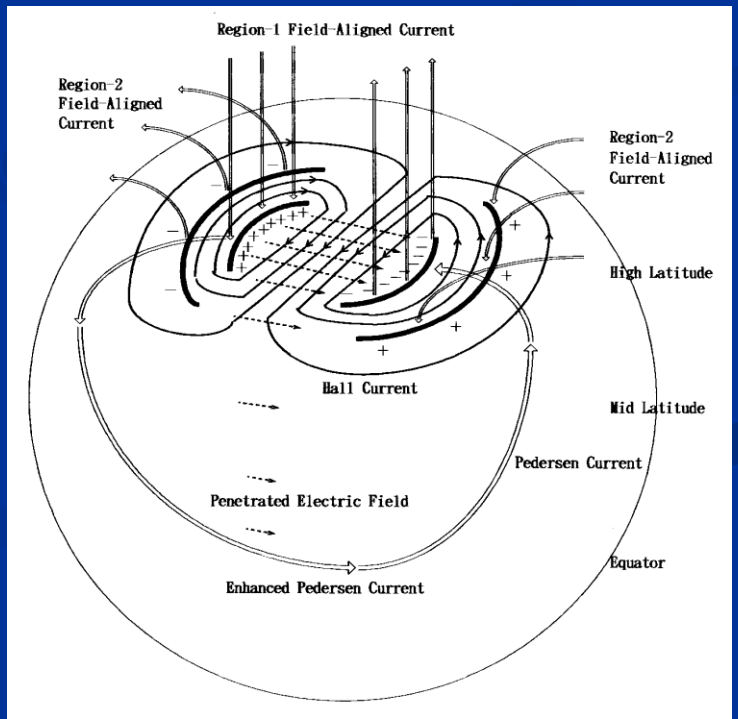

(Kikuchi et al., JGR 1996)

SuperDARN observation of the large-scale ionospheric convection

The sunward convection in the afternoon sector is intensified at the onset of substorm.

The anti-sunward convection appears equatorward of the sunward convection.

The latitudinal features of the convection flow implies development of the R2 FACs.

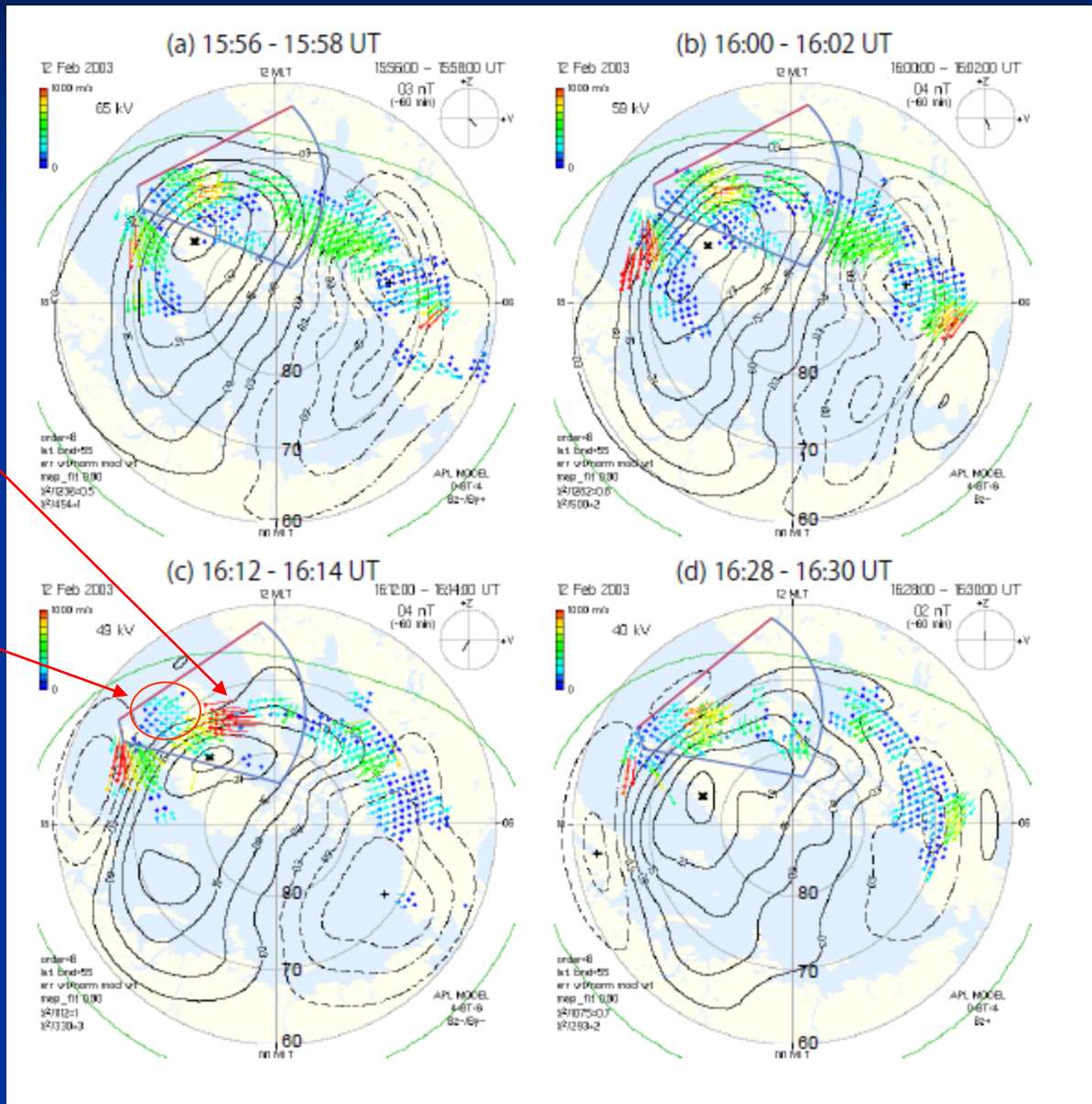

Magnetosphere-ionosphere current circuit

Force balance in the dynamo

$$\rho \frac{dV}{dt} = J \times B - \nabla p$$

Generation of EM energy

$$J \cdot E = (J \times B) \times V < 0$$

Radiation of EM energy

$$\nabla \cdot S = -J \cdot E > 0$$

$$S = E \times \Delta B_{\perp} / \mu_0 \text{ (Poynting flux)}$$

FAC (Charge accumulation)

$$\frac{e_B}{B} \cdot (\nabla \times v) = -\left(\frac{1}{B^2}\right) \nabla \cdot E$$

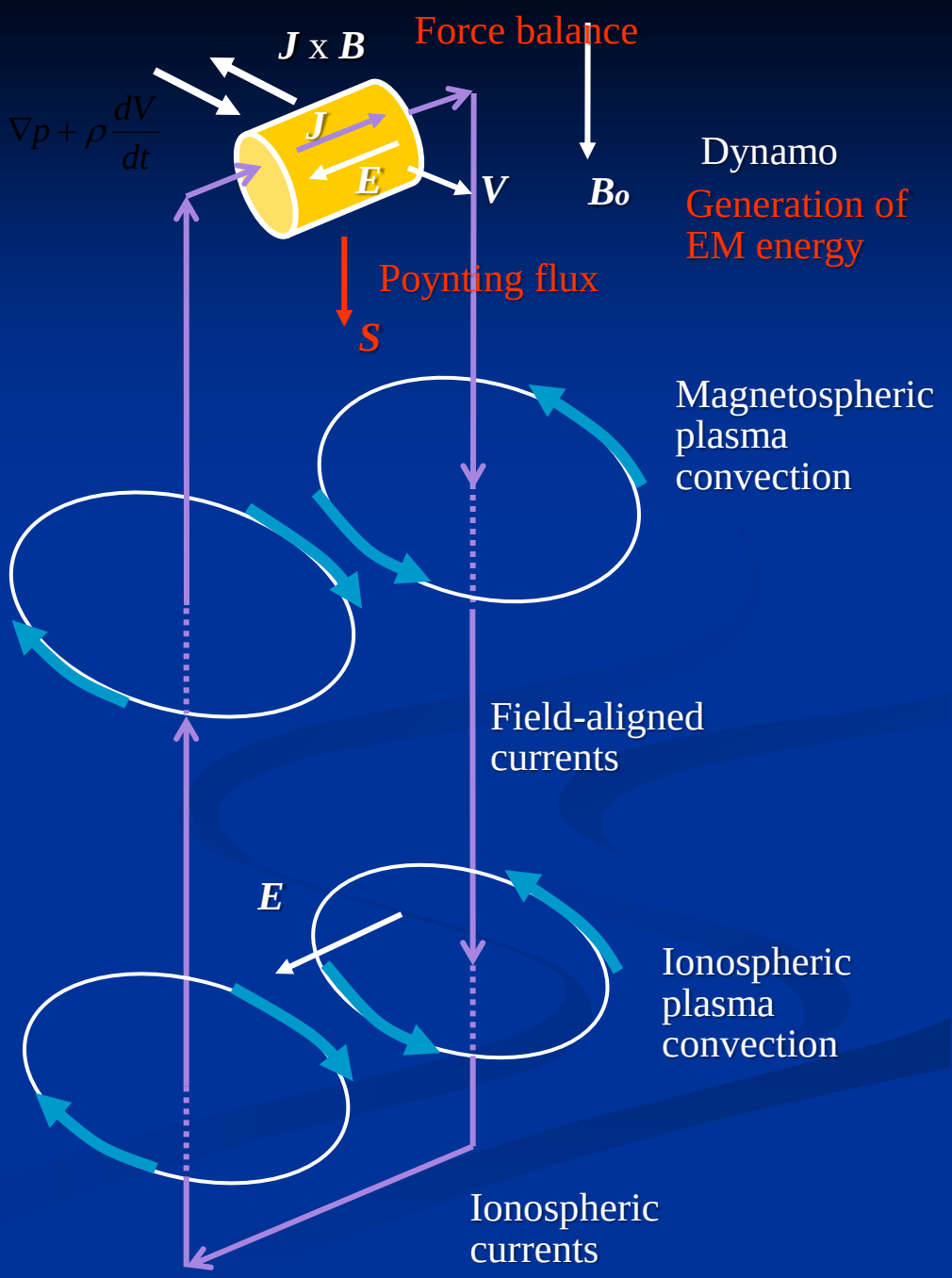

Transmission in the ionospheric F-region

The ionospheric waveguide centered at the F-region peak has a lower cutoff frequency at 0.5 Hz [Manchester, 1966], which can be applied to the PC1 but NOT to the PRI.

F-region waveguide mode is the fast mode described by the Schroedinger equation. (Tepley and Landshoff, 1966)

$$\frac{d^2 E_y(z)}{\partial z^2} - \left[k_n^2 - \frac{\omega^2}{V_a(z)^2} \right] E_y(z) = 0$$

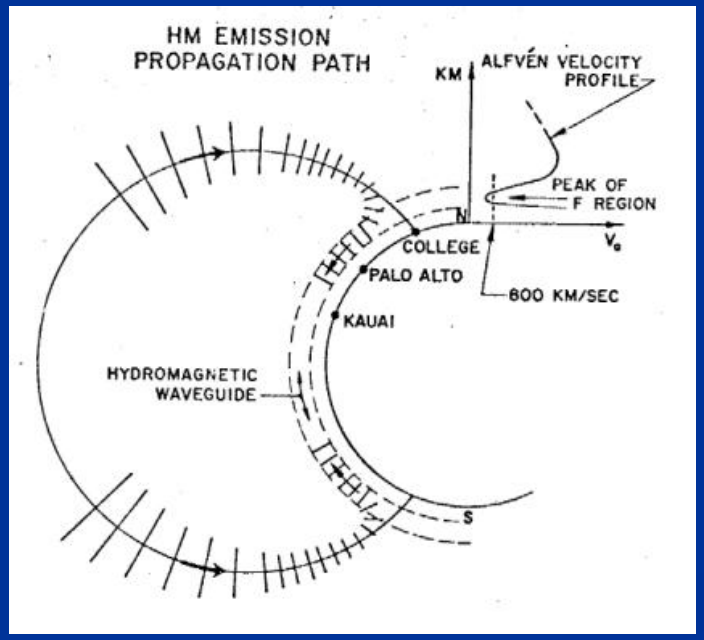

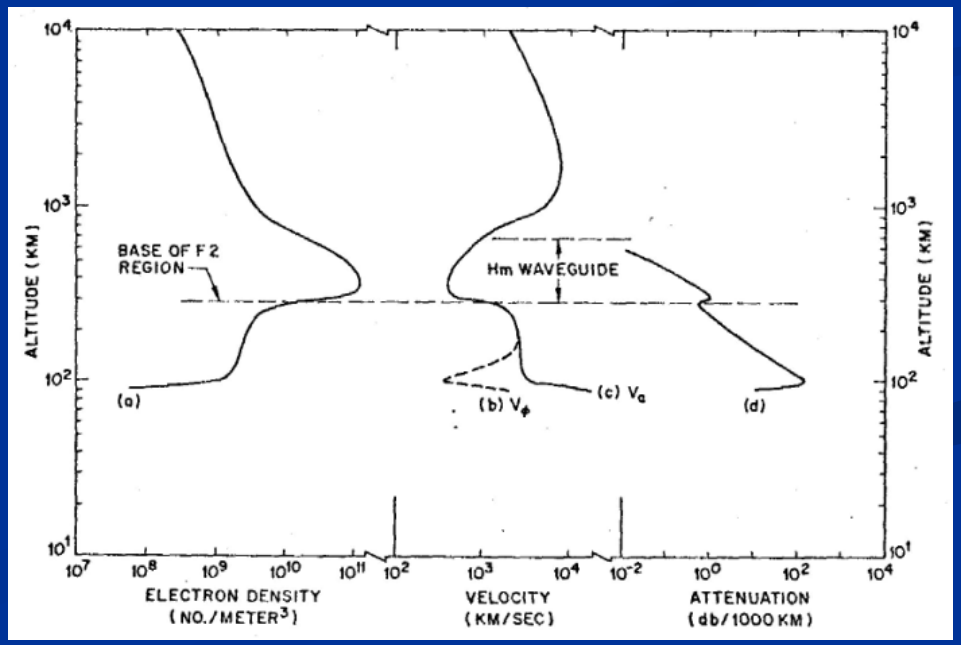

Transmission in the ionospheric E-region

The propagation mode is a diffusion mode in the E-region, which requires 1 h to make obervable effects at the equator. (Kikuchi and Araki, JATP 1979a)

$$H_y = A_y\left(\operatorname{erfc}\left(\frac{x\sqrt{\mu_0\sigma_{c1}}}{2\sqrt{t}}\right) - \operatorname{erfc}\left(\frac{x\sqrt{\mu_0\sigma_{c2}}}{2\sqrt{t}}\right)\right),$$

$$H_z = A_{z1}\operatorname{erfc}\left(\frac{x\sqrt{\mu_0\sigma_{c1}}}{2\sqrt{t}}\right) + A_{z2}\operatorname{erfc}\left(\frac{x\sqrt{\mu_0\sigma_{c2}}}{2\sqrt{t}}\right)$$

$$\sigma_{c1} = \tfrac{1}{2}\sigma_I^2(C - \sqrt{D}),$$

$$\sigma_{c2} = \tfrac{1}{2}\sigma_I^2(C + \sqrt{D}),$$

$$A_y = -\frac{R_2 \cos I}{\sqrt{D}},$$

$$A_{z1} = \frac{1}{2}\left(1 + \frac{(R_1 - R_0)\sin^2 I}{\sqrt{D}}\right),$$

$$A_{z2} = \frac{1}{2}\left(1 - \frac{(R_1 - R_0)\sin^2 I}{\sqrt{D}}\right),$$

with

$$\sigma_I^2 = \frac{1}{R_0 R_1 \sin^2 I + (R_1^2 + R_2^2)\cos^2 I},$$

$$C = R_0 \sin^2 I + R_1(1 + \cos^2 I),$$

$$D = (R_1 - R_0)^2 \sin^4 I - 4R_2^2 \cos^2 I.$$

$$R_0 = \frac{1}{\sigma_0},$$

$$R_1 = \frac{\sigma_1}{\sigma_1^2 + \sigma_2^2} = \frac{1}{\sigma_3},$$

$$R_2 = \frac{\sigma_2}{\sigma_1^2 + \sigma_2^2},$$

Parallel propagation

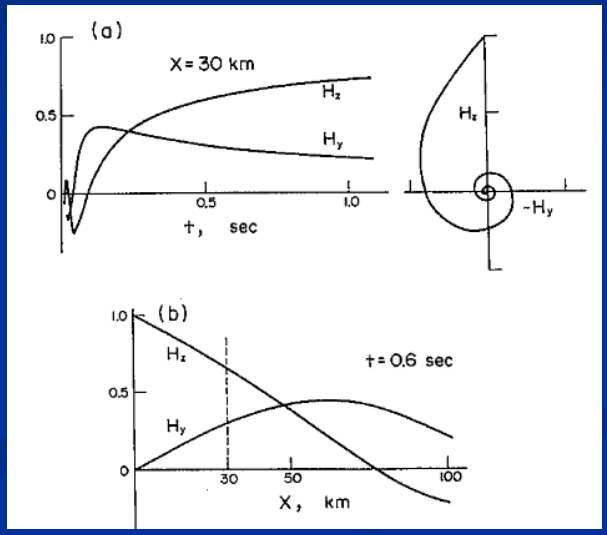

Perpendicular propagation

$$E_y = E_0 Erfc\left(\frac{x\sqrt{\mu_0\sigma}}{2\sqrt{t}}\right)$$

$x = 5000km$

$\sigma = 10^{-4}\, mho/m$

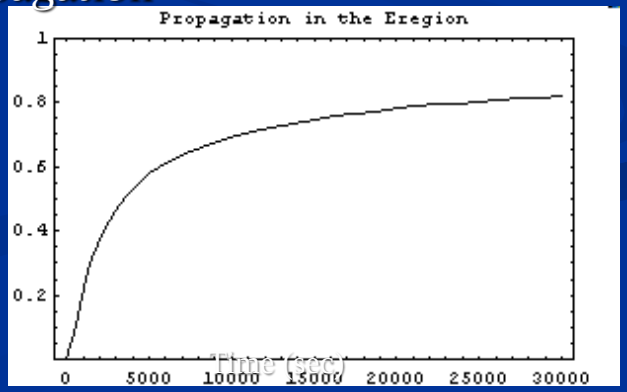

Earth-ionosphere waveguide model

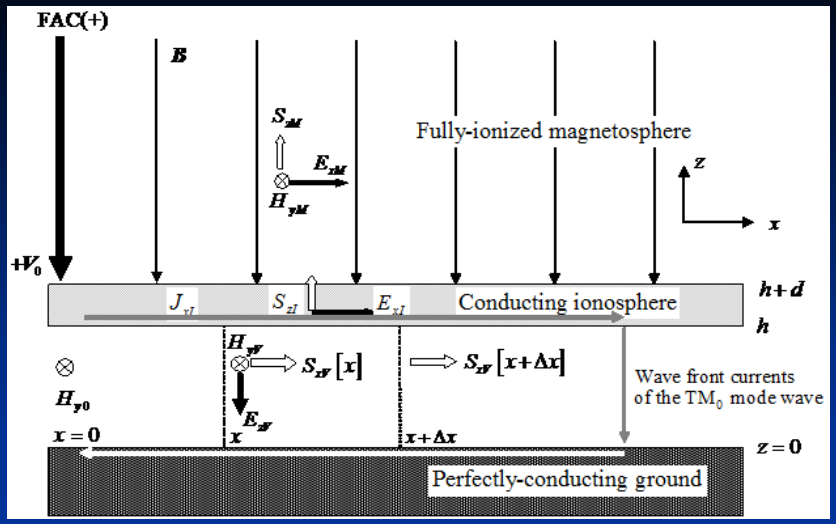

Magnetosphere

$$\overline{h_{yM}}[z,s] = A_{M1}e^{-\frac{(z-d)}{V_A}s} + A_{M2}e^{\frac{(z-d)}{V_A}s}, \quad (2\text{-}19)$$

$$\overline{e_{xM}}[z,s] = \mu_0 V_a\left(A_{M1}e^{-\frac{(z-d)}{V_A}s} - A_{M2}e^{\frac{(z-d)}{V_A}s}\right), \quad (2\text{-}20)$$

Upward propagating Alfven wave

Ionosphere

$$\overline{h_{yI}}[\beta,s] = \sqrt{\frac{2}{\pi}}\frac{\beta}{s\left(\beta^2+\mu_0\sigma\cdot s\right)} + A_{I1}e^{-z\sqrt{\beta^2+\mu_0\sigma s}} + A_{I2}e^{z\sqrt{\beta^2+\mu_0\sigma s}}, \quad (2\text{-}17)$$

$$\overline{e_{xI}}[\beta,s] = \frac{\sqrt{\beta^2+\mu_0\sigma\cdot s}}{\sigma}\left(A_{I1}e^{-z\sqrt{\beta^2+\mu_0\sigma s}} - A_{I2}e^{z\sqrt{\beta^2+\mu_0\sigma s}}\right), \quad (2\text{-}18)$$

Vertically propagating diffusion mode wave

Neutral atmosphere

$$\overline{h_{yV}}[\beta,s] = H_{y0}\sqrt{\frac{2}{\pi}}\frac{\beta}{s\left(\beta^2+\frac{s^2}{c^2}\right)} + A_{V1}e^{-z\sqrt{\beta^2+\frac{s^2}{c^2}}} + A_{V2}e^{z\sqrt{\beta^2+\frac{s^2}{c^2}}}, \quad (2\text{-}15)$$

$$\overline{e_{xV}}[\beta,s] = \frac{1}{\varepsilon_0 s}\sqrt{\beta^2+\frac{s^2}{c^2}}\left(A_{V1}e^{-z\sqrt{\beta^2+\frac{s^2}{c^2}}} - A_{V2}e^{z\sqrt{\beta^2+\frac{s^2}{c^2}}}\right), \quad (2\text{-}16)$$

Horizontally propagating TM0 mode wave

Excitation of the TM0 mode wave

The electric and magnetic fields are transmitted into the space below the ionosphere, exciting the TM0 mode waves in the Earth-ionosphere waveguide.

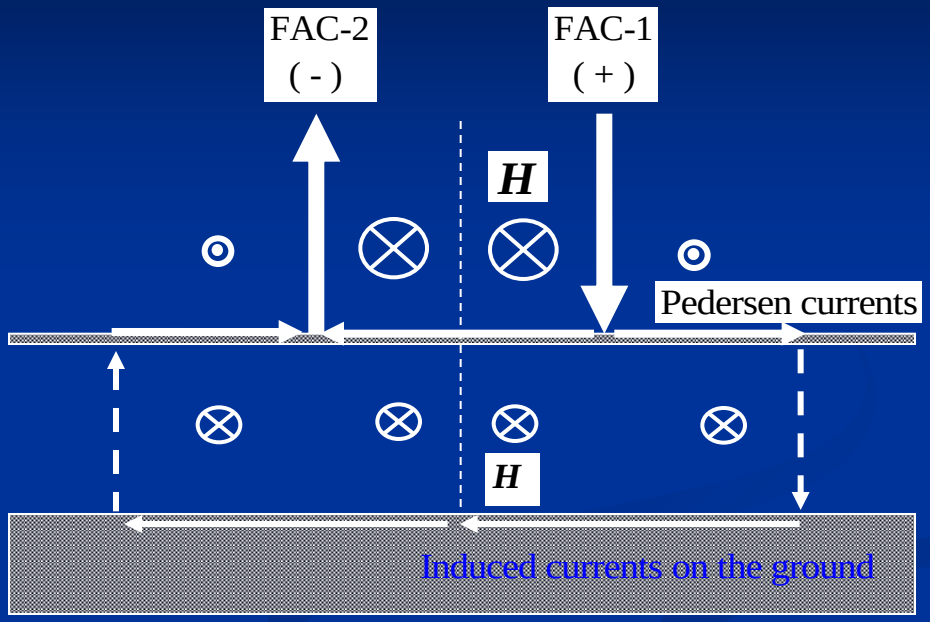

Reflection and transmission coefficients

$$C_r = \frac{R_1 Z_2 - Z_1(R_1 + Z_2)}{R_1 Z_2 + Z_1(R_1 + Z_2)} = -0.821$$

$$C_t = \frac{2R_1 Z_2}{R_1 Z_2 + Z_1(R_1 + Z_2)} = 0.179$$

Three-layered Earth-ionosphere waveguide

Magnetosphere

$$H_{yM}[x,t]=\frac{\Sigma_A}{\Sigma_A+\Sigma_I}H_{yV}[x]\cdot U\left(t-\frac{z}{V_A}\right)$$

$$E_{xM}[x,t]=\frac{1}{\Sigma_A+\Sigma_I}H_{yV}[x]\cdot U\left(t-\frac{z}{V_A}\right)$$

$$S_{z,M}(x,z)=\frac{\Sigma_A}{(\Sigma_A+\Sigma_I)^2}H_{yV}^2(x)\cdot U\left(t-\frac{z}{V_a}\right)$$

Ionosphere

$$H_{yI}[x,z]=\left(1-\frac{\sigma z}{\Sigma_A+\Sigma_I}\right)H_{yV}[x]\cdot U[t]$$

$$E_{xI}[x,z]=\frac{1}{\Sigma_A+\Sigma_I}H_{yV}[x]\cdot U[t]$$

$$S_{zI}[x,z]=\frac{\Sigma_A+\Sigma_I-\sigma\cdot z}{(\Sigma_A+\Sigma_I)^2}H_{yV}^2[x]$$

Neutral atmosphere

$$H_{yV}=H_{y0}U\left[t-\frac{x}{c}\right]$$

$$E_{zV}=-Z_0H_{y0}U\left[t-\frac{x}{c}\right]$$

$$V[x,t]=V_0U\left[t-\frac{x}{c}\right]$$

$$S_{xV}(x)=Z_0H_{yV}^{\ 2}(x)=E_{zV}^{\ 2}(x)/Z_0$$

The ionospheric potential propagates at the speed of light.

The ionospheric electric field is mapped upward into the F-region and to the inner magnetosphere.

$$E_{xM}(x)=\frac{1}{\Sigma_A+\Sigma_I}H_{yV}(x)\cdot U\left(t-\frac{z}{V_a}\right)$$

$$\Sigma_A=\frac{1}{\mu_0V_a}=\frac{1}{B_0}\sqrt{\frac{\rho}{\mu_0}}$$

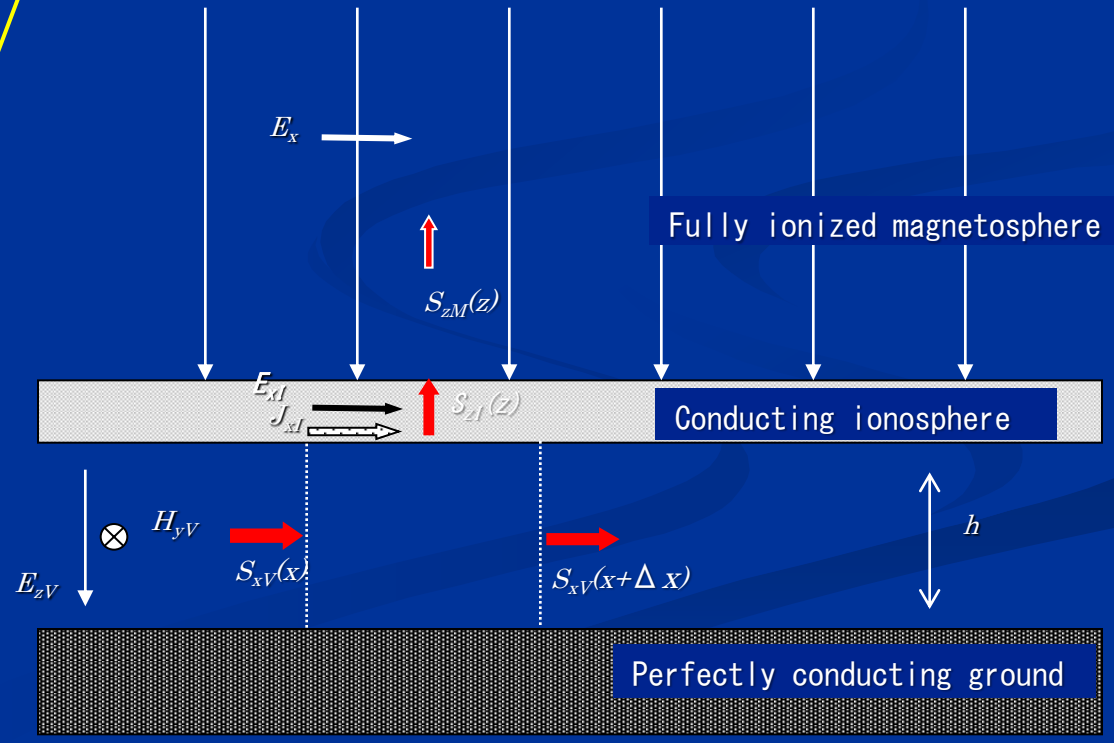

Kikuchi (AGU monograph, 2005)

Earth-ionosphere waveguide model

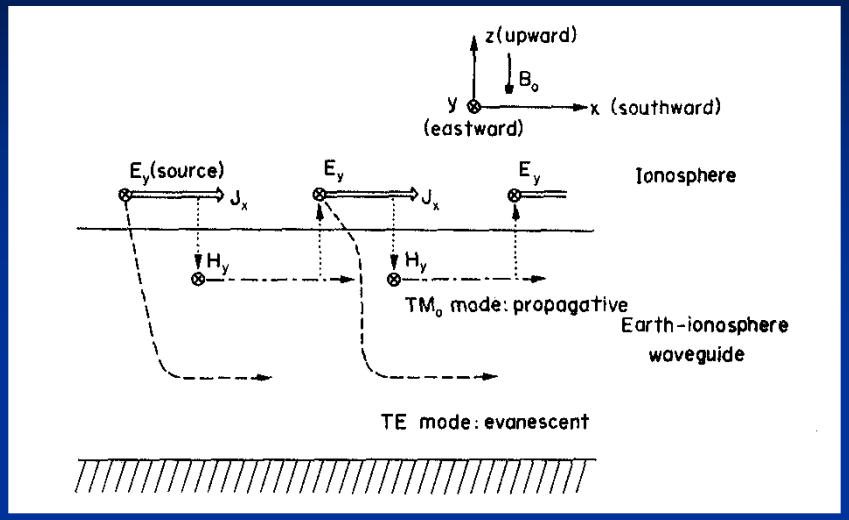

The polar electric field is transmitted to the equator at the speed of light by the TM0 mode wave in the Earth-ionosphere waveguide.
The TM0 mode wave has no lower cutoff frequency, which enables long-period disturbances to propagate to the equator.
The transmitted electric field suffers from geometrical attenuation, but the induced currents are enhanced at the dayside equator by the Cowling effect.

Kikuchi et al. [1978], Kikuchi and Araki [1979b]

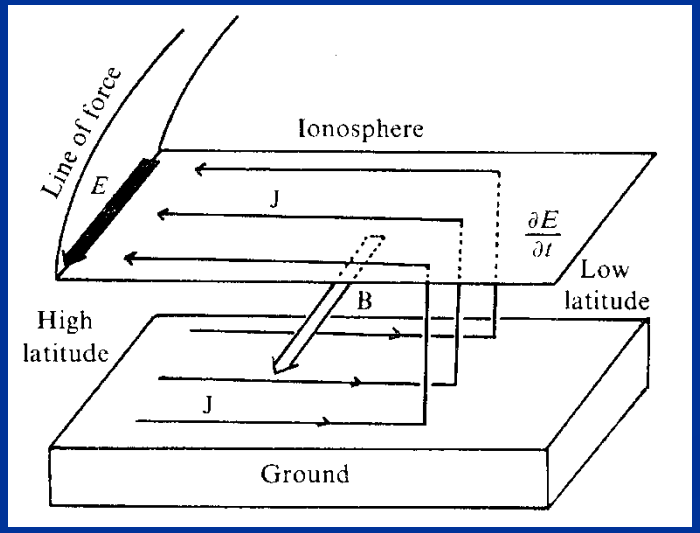

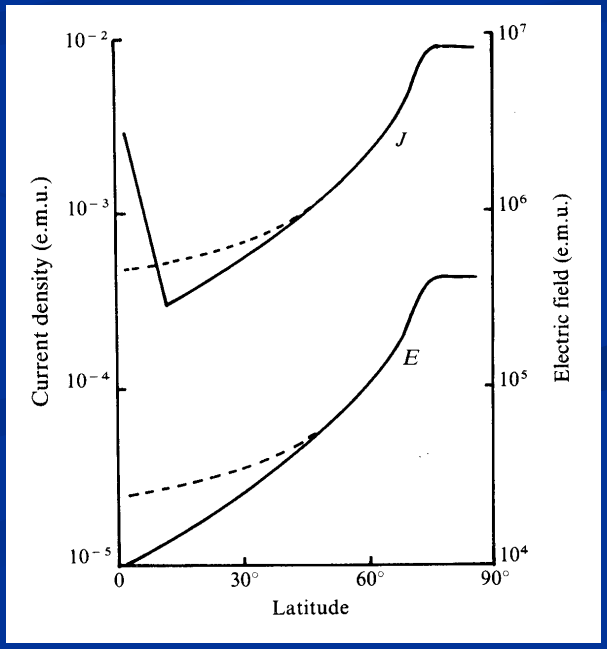

Upward Poynting flux from the ionosphere to the inner magnetosphere

PRI electric field is observed prior to the arrival of the compressional MHD wave.

Upward Poynting flux

Nishimura et al. (JGR 2010)

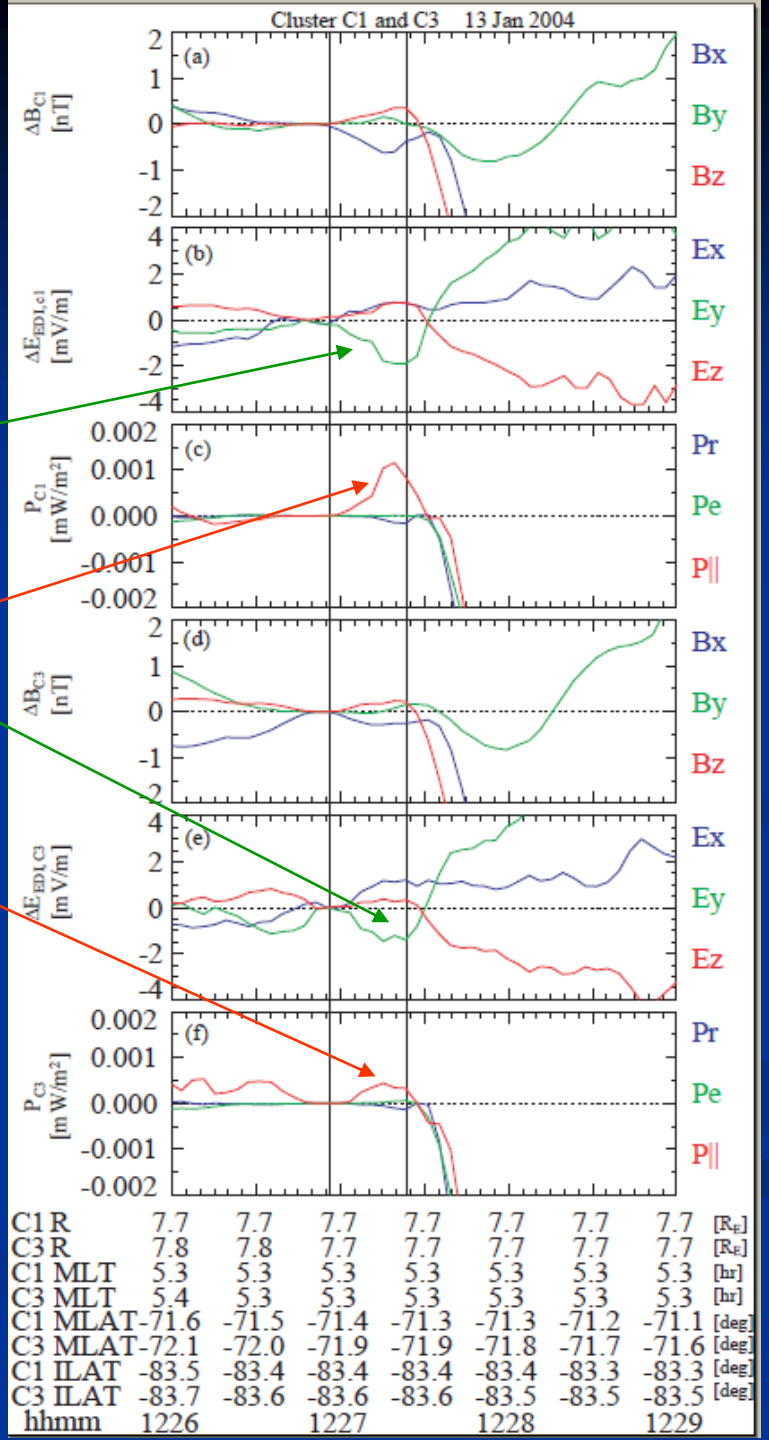

Geomagnetic storm

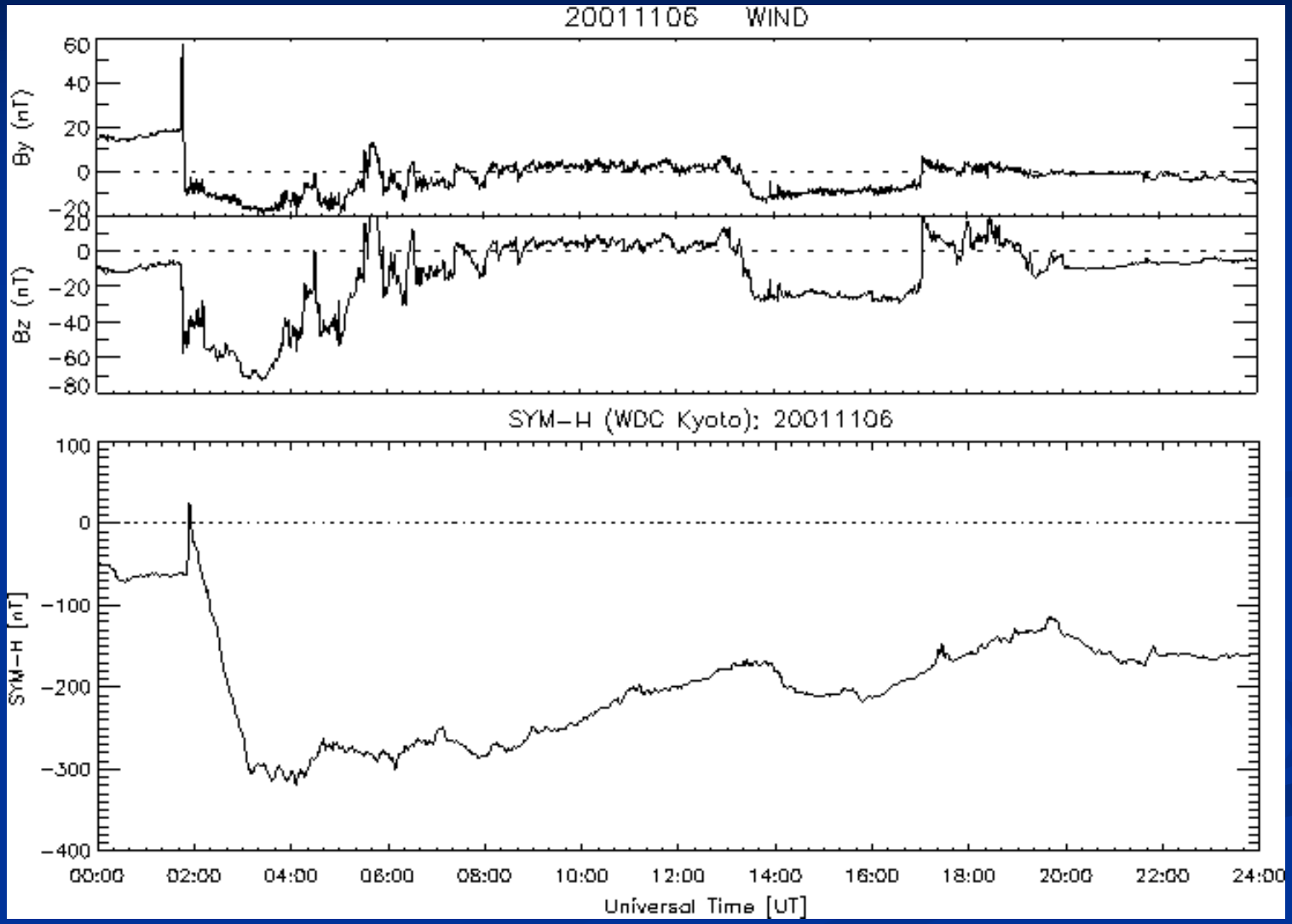

The partial ring current is developed by the convection electric field, which is the dynamo of the R2 FACs

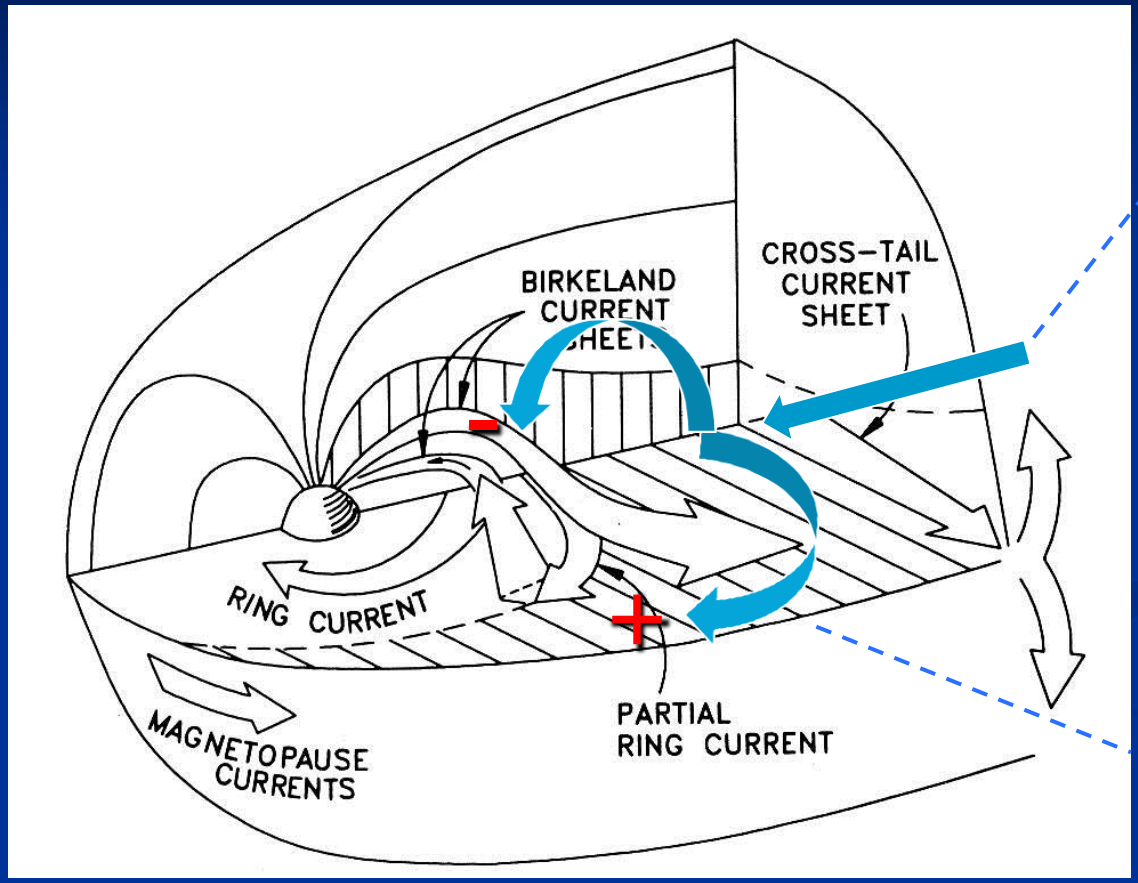

Earthward motion of plasma

$$\boldsymbol{v} = \frac{\boldsymbol{E} \times \boldsymbol{B}}{B^2}$$

Charge separation

$$\boldsymbol{v} = \frac{m v_{\perp}^{2}}{qB^4} \boldsymbol{B} \times \left(\boldsymbol{B} \cdot \nabla \right) \boldsymbol{B}$$

$$\boldsymbol{v} = \frac{m v_{\perp}^{2}}{2qB^3} \boldsymbol{B} \times \nabla B$$

The R2 FACs provide a dusk-to-dawn shielding/overshielding electric field to the ionosphere.

Geomagnetic storm at the low latitude (OKI) and equator (Yap)

(Kikuchi, Hashimoto, Nozaki, JGR 2008)

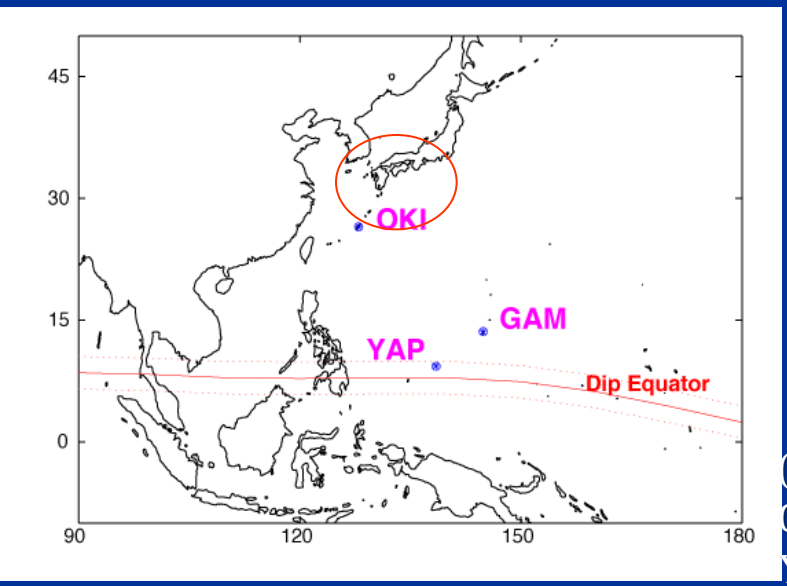

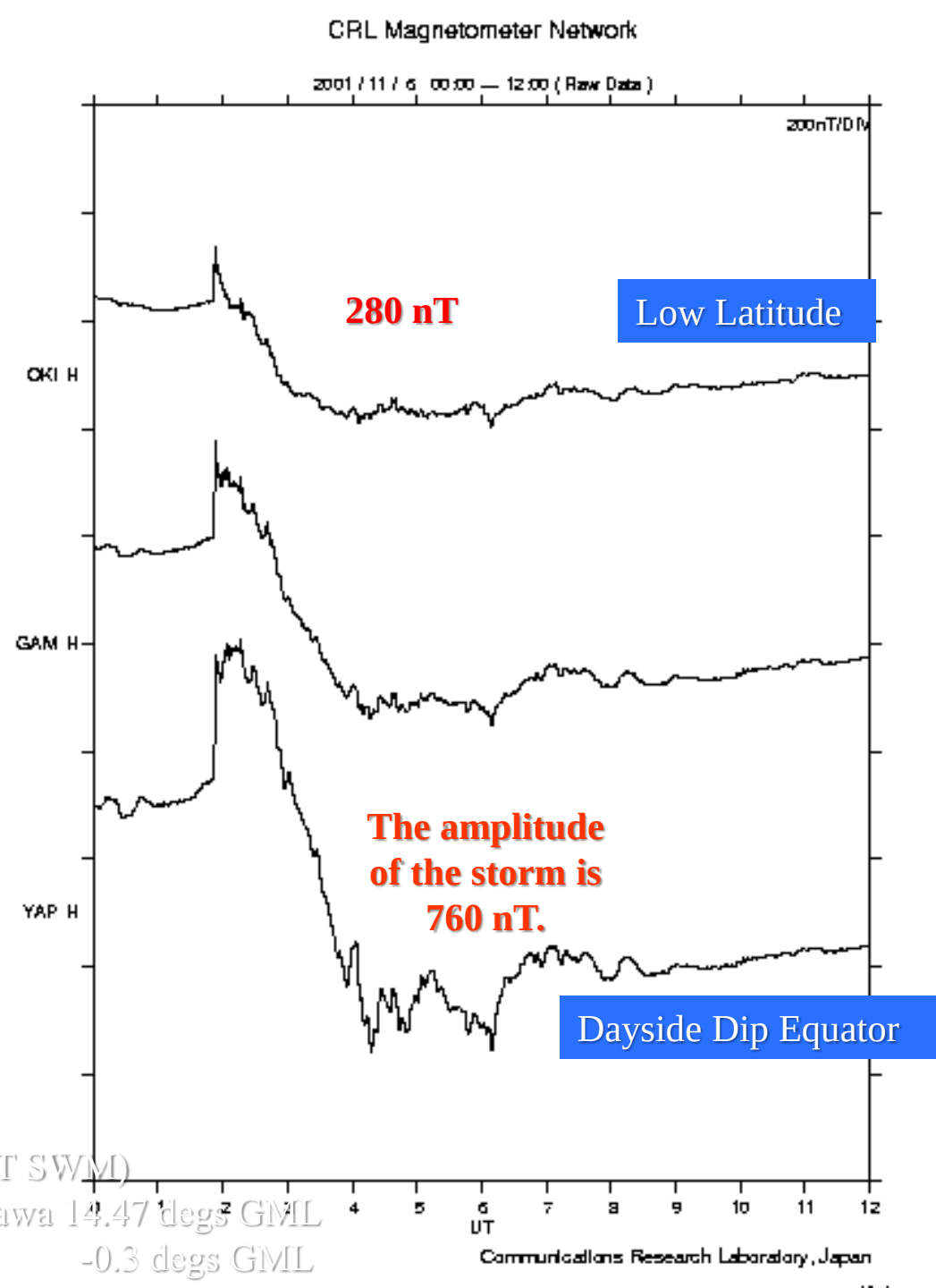

(NICT SWM)
Okinawa 14.47 degs GML
Yap -0.3 degs GML

Equatorial electrojet during the storm

EEJ: eastward electrojet
CEJ: counterelectrojet

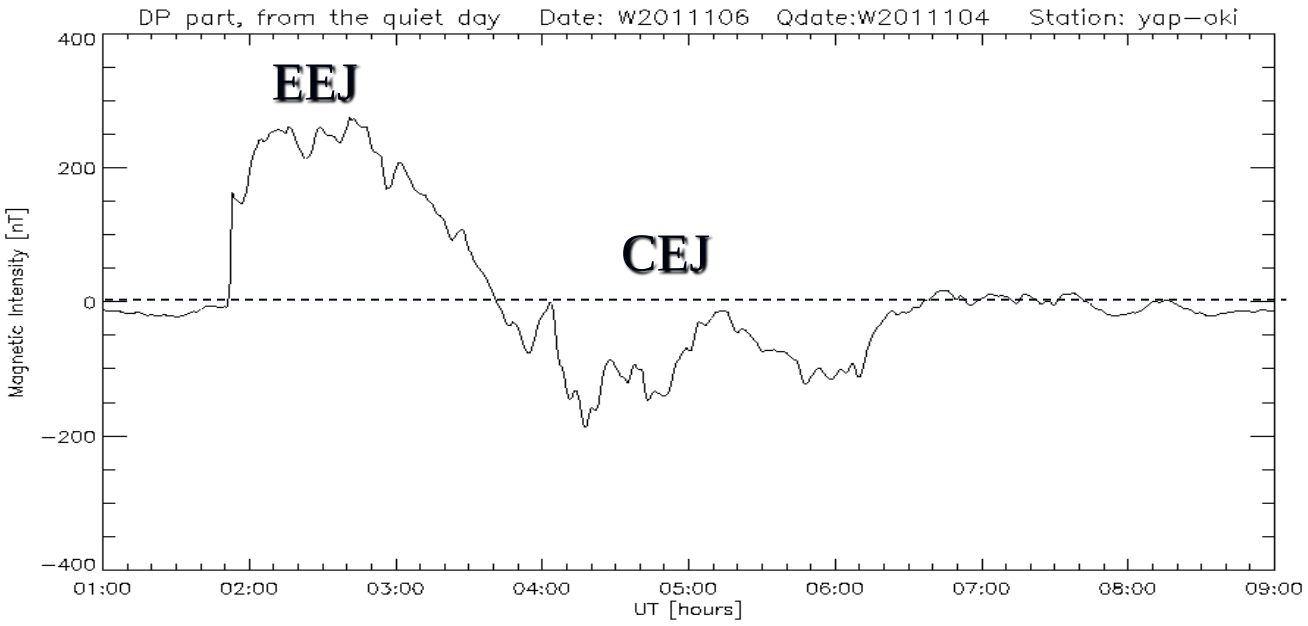

Convection electric field dominant

Shielding getting effective

Shielding dominant (overshielding)

(Kikuchi, Hashimoto, Nozaki, JGR 2008)

Geomagnetic storm on November 6, 2001

1. Equatorial DP2 developed around noon, simultaneously with ring current development.
2. Shielding effect appeared during late main phase.
3. Equatorial CEJ occurred at the beginning of storm recovery phase, when the auroral AEJ moved rapidly poleward.

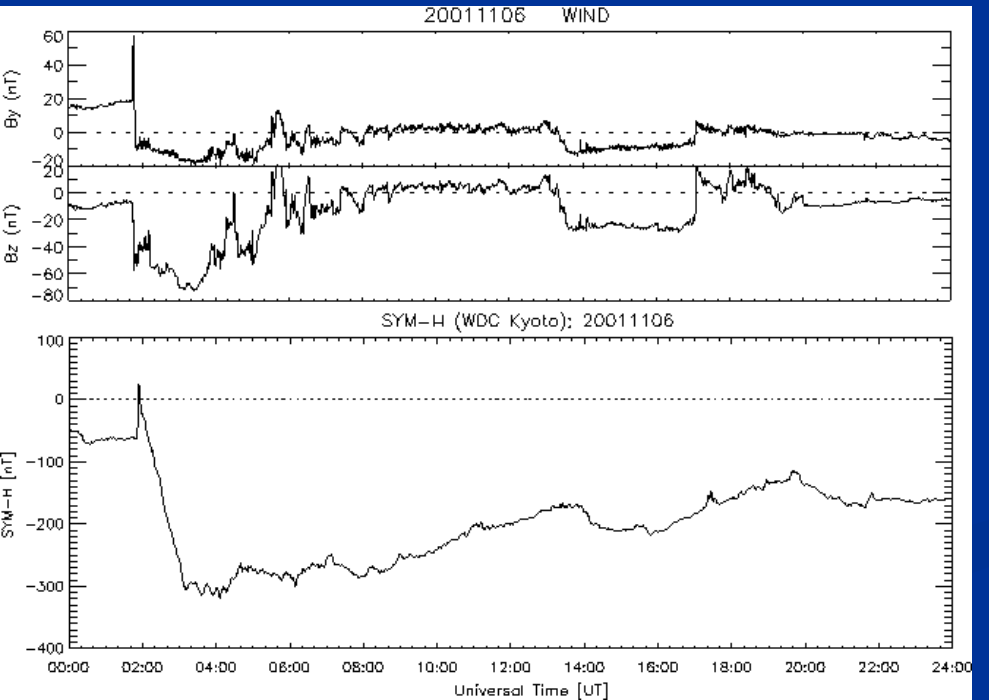

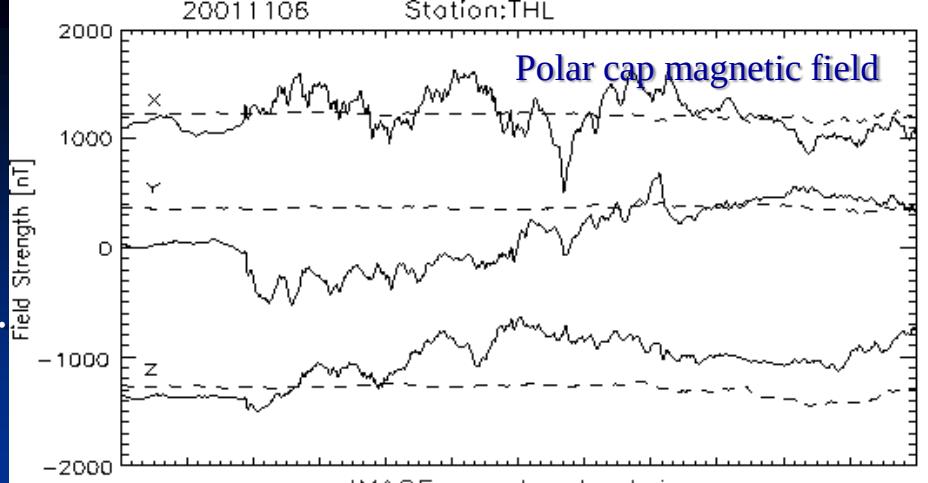

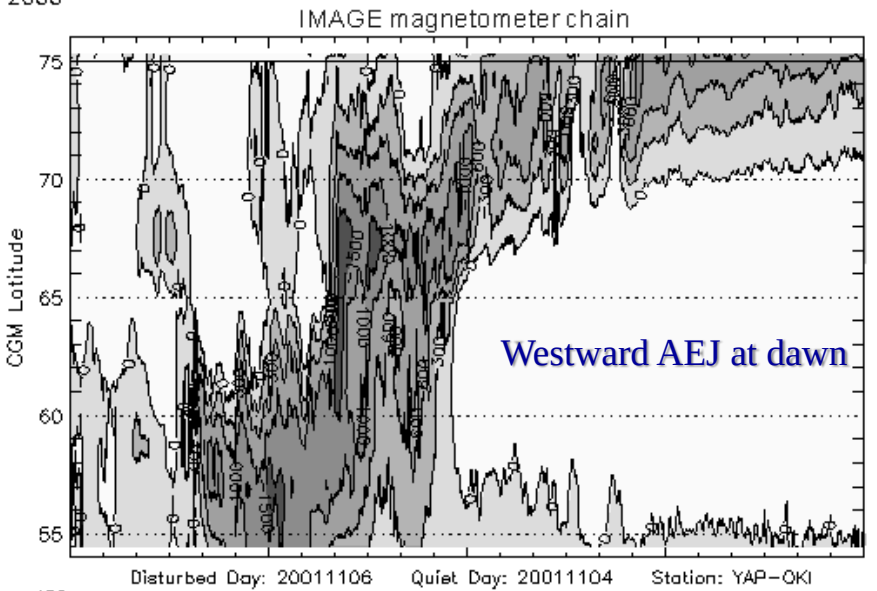

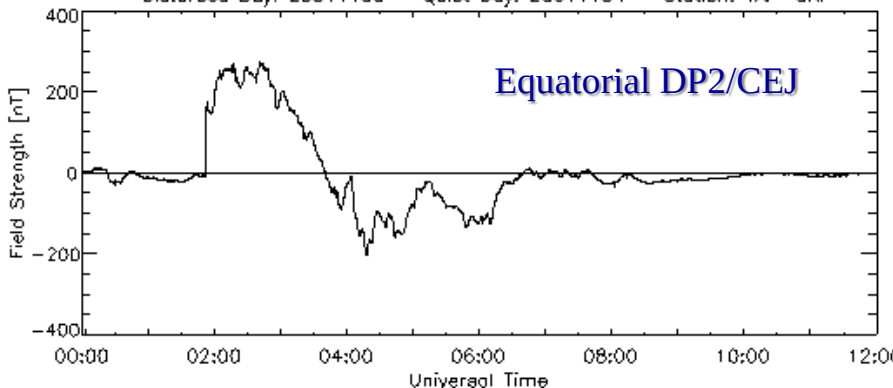

Low latitude ionograms during Nov. 6, 2001 storm

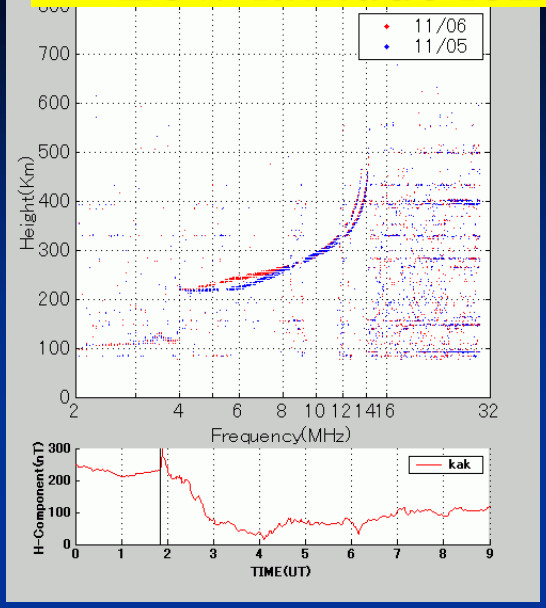

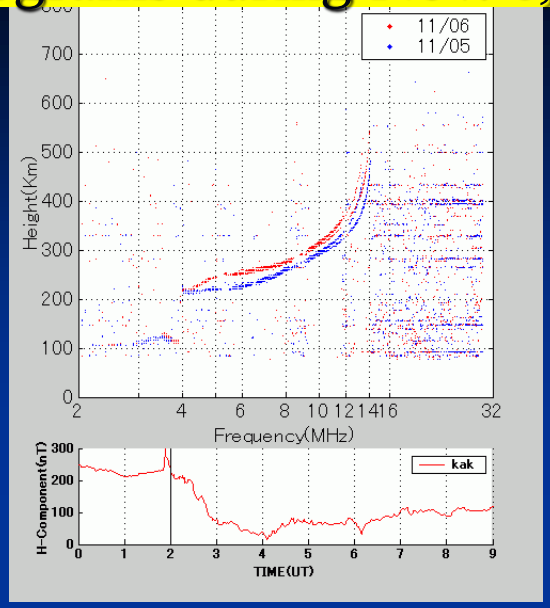

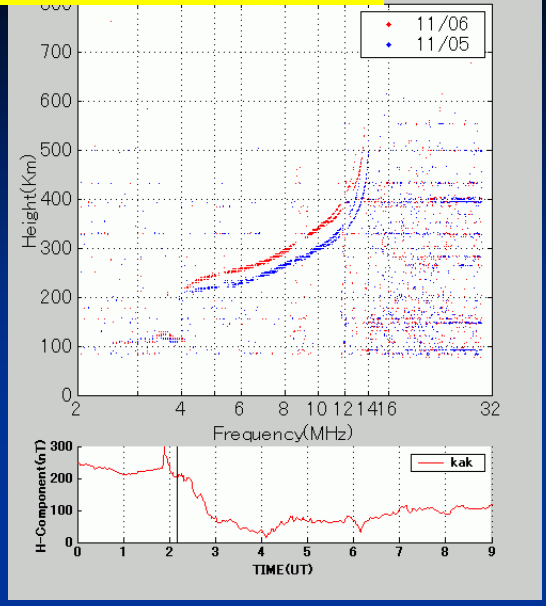

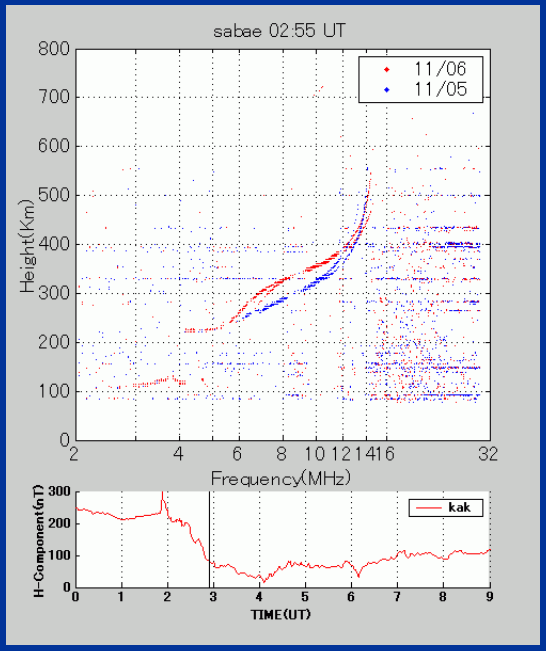

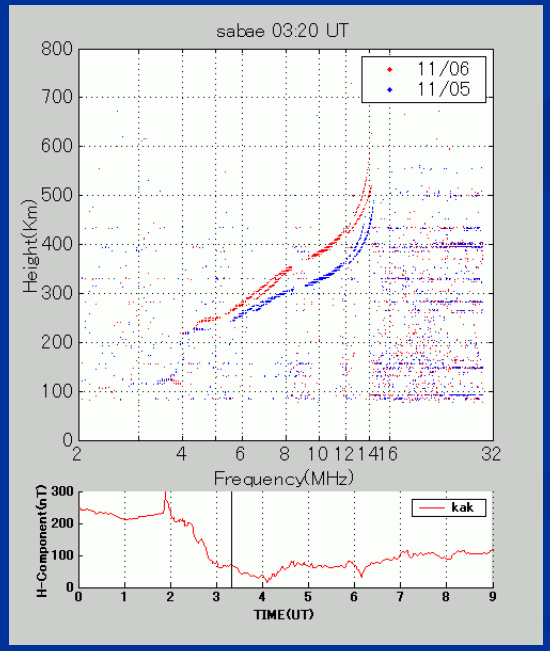

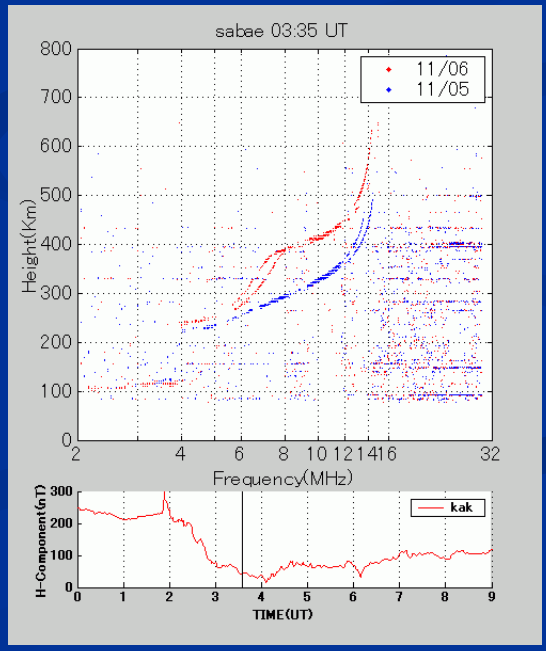

Low latitude ionograms during Nov. 6, 2001 storm (contd)

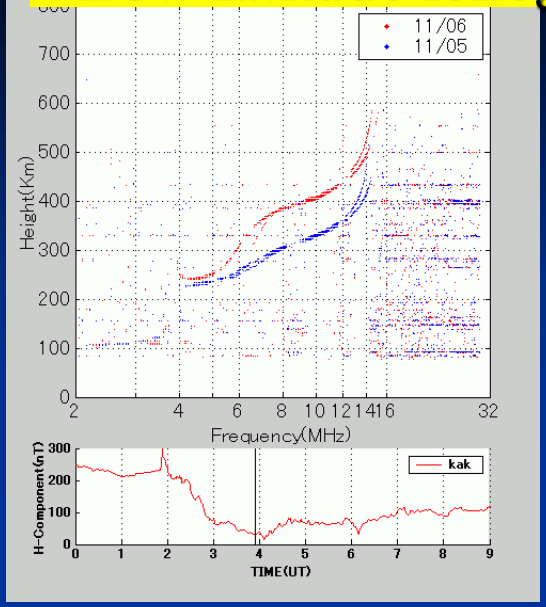

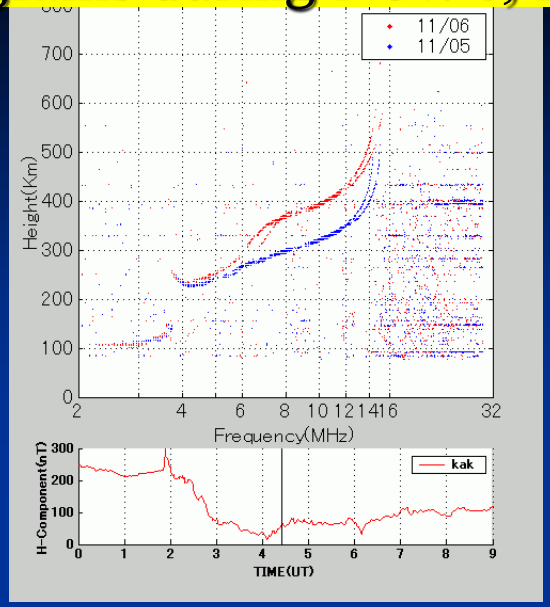

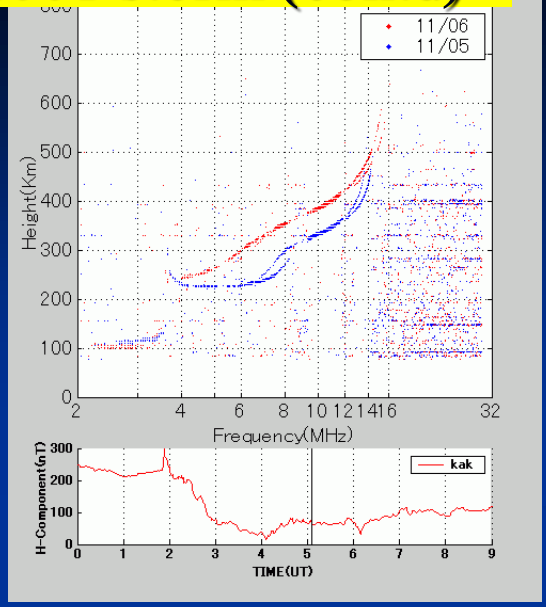

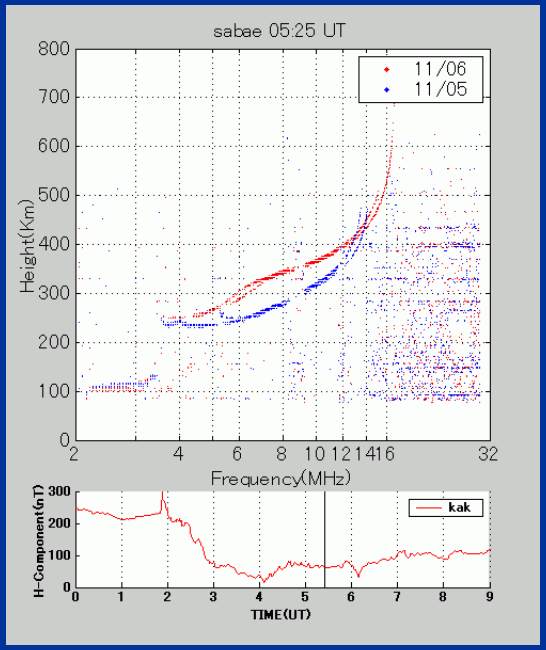

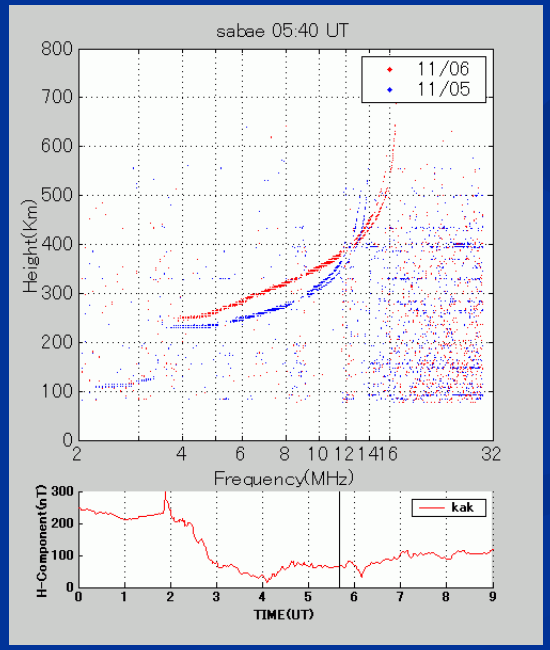

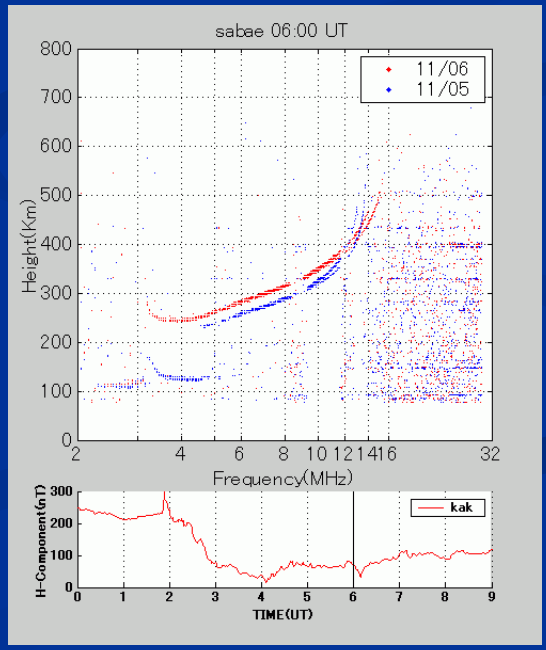

Enhancement of the total electron content (TEC)

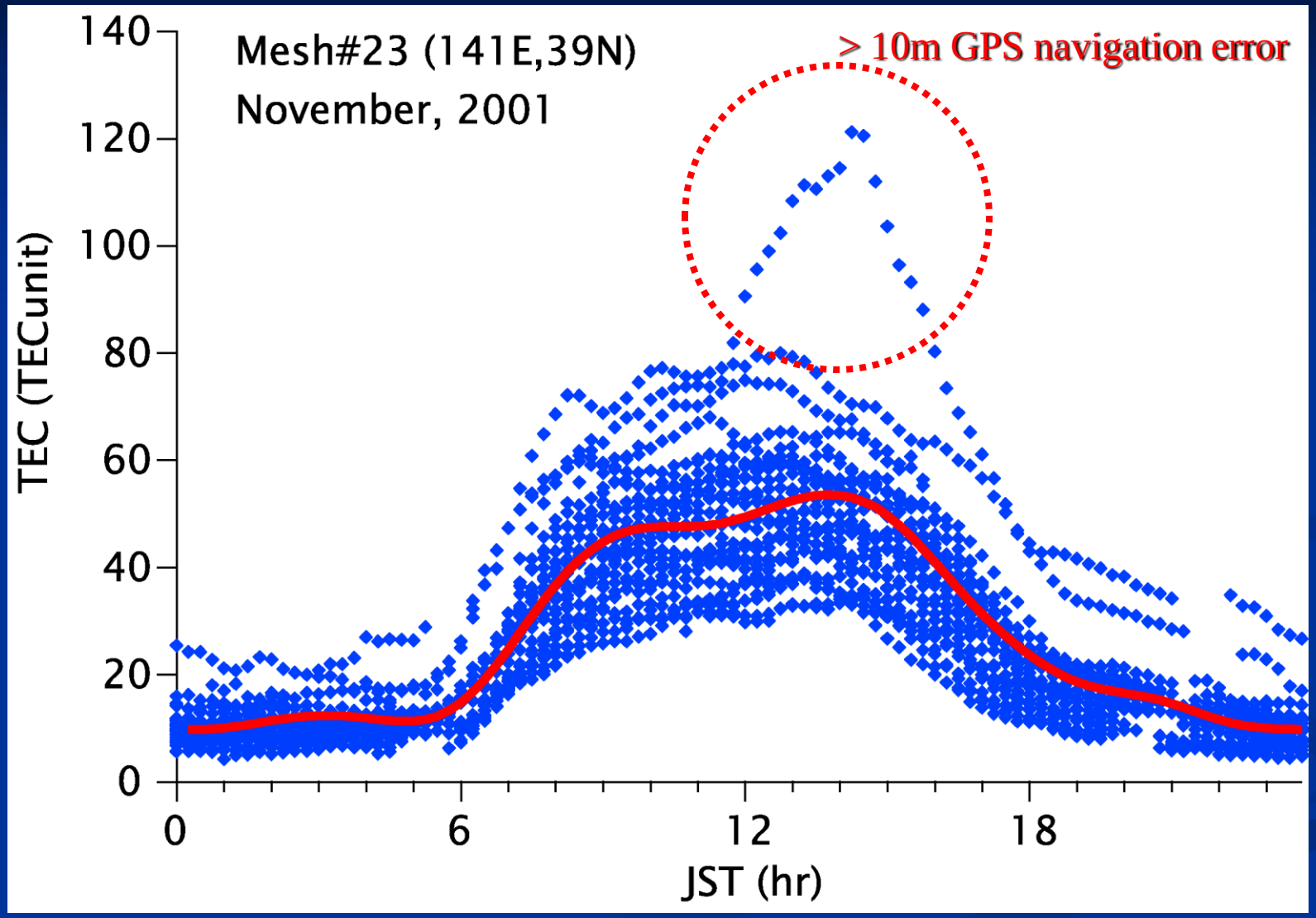

T. Maruyama (NICT)

Auroral substorm

佐藤夏雄氏撮影・提供

Equivalent currents for ground magnetic disturbances during the growth and expansion phases of substorms

[Iijima and Nagata, 1972]

Growth phase (DP2)

Expansion phase (DP1)

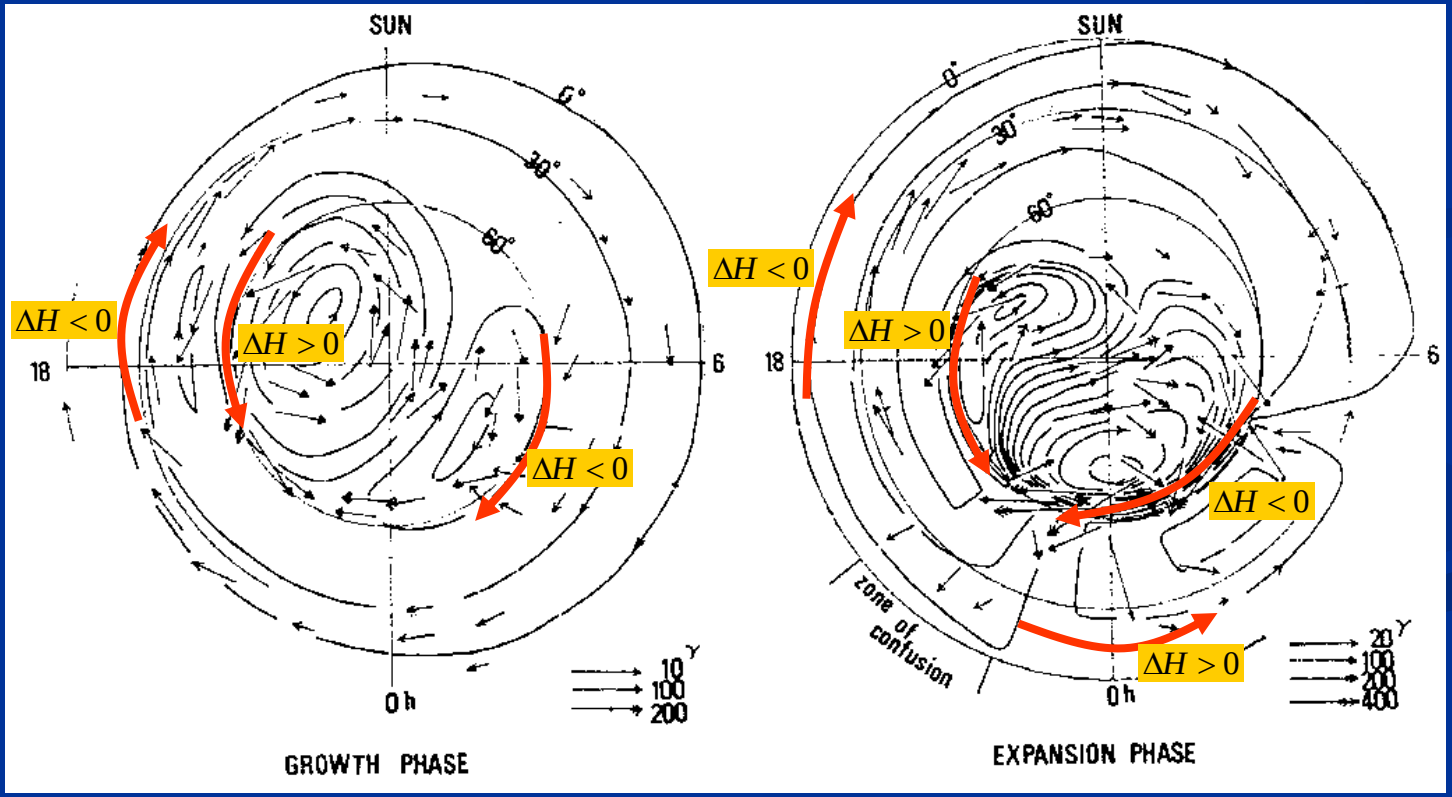

DP2 and overshielding currents during the substorm

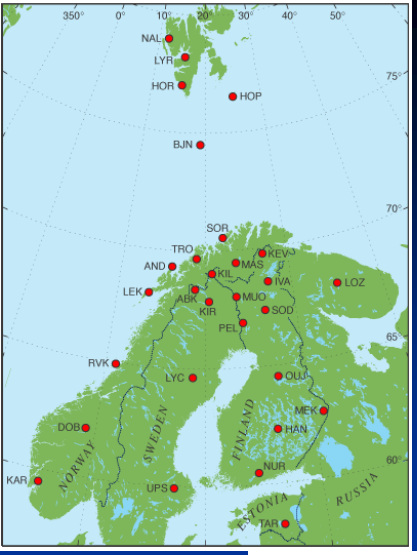

The magnetic perturbations are caused by the ionospheric Hall currents.

EISCAT

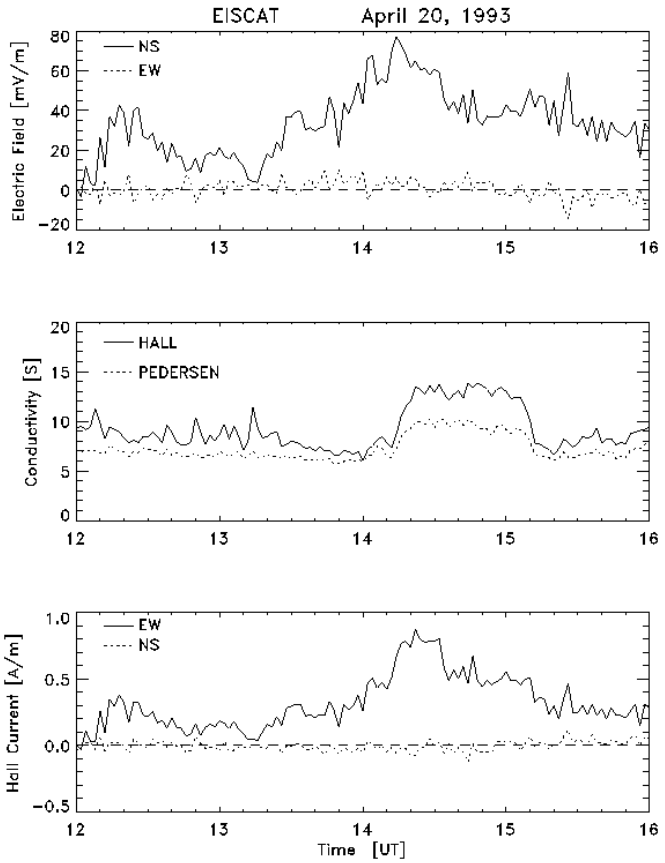

(Kikuchi et al., JGR 1996)

IMAGE Magnetometer chain

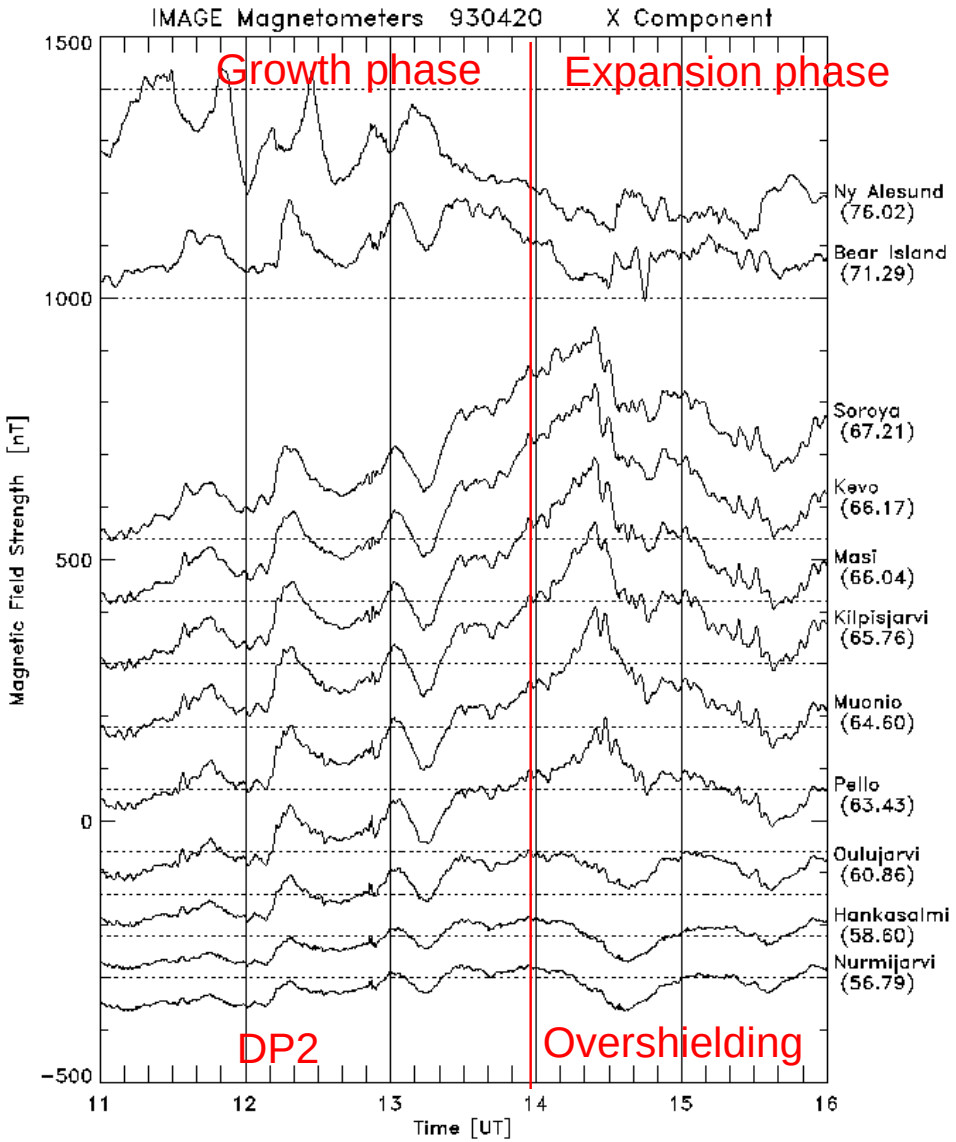

Equatorial DP2/overshielding during the substorm growth/expansion phase

Kikuchi et al. (JGR 1996, 2000)

Magnetometer chain in the afternoon sector

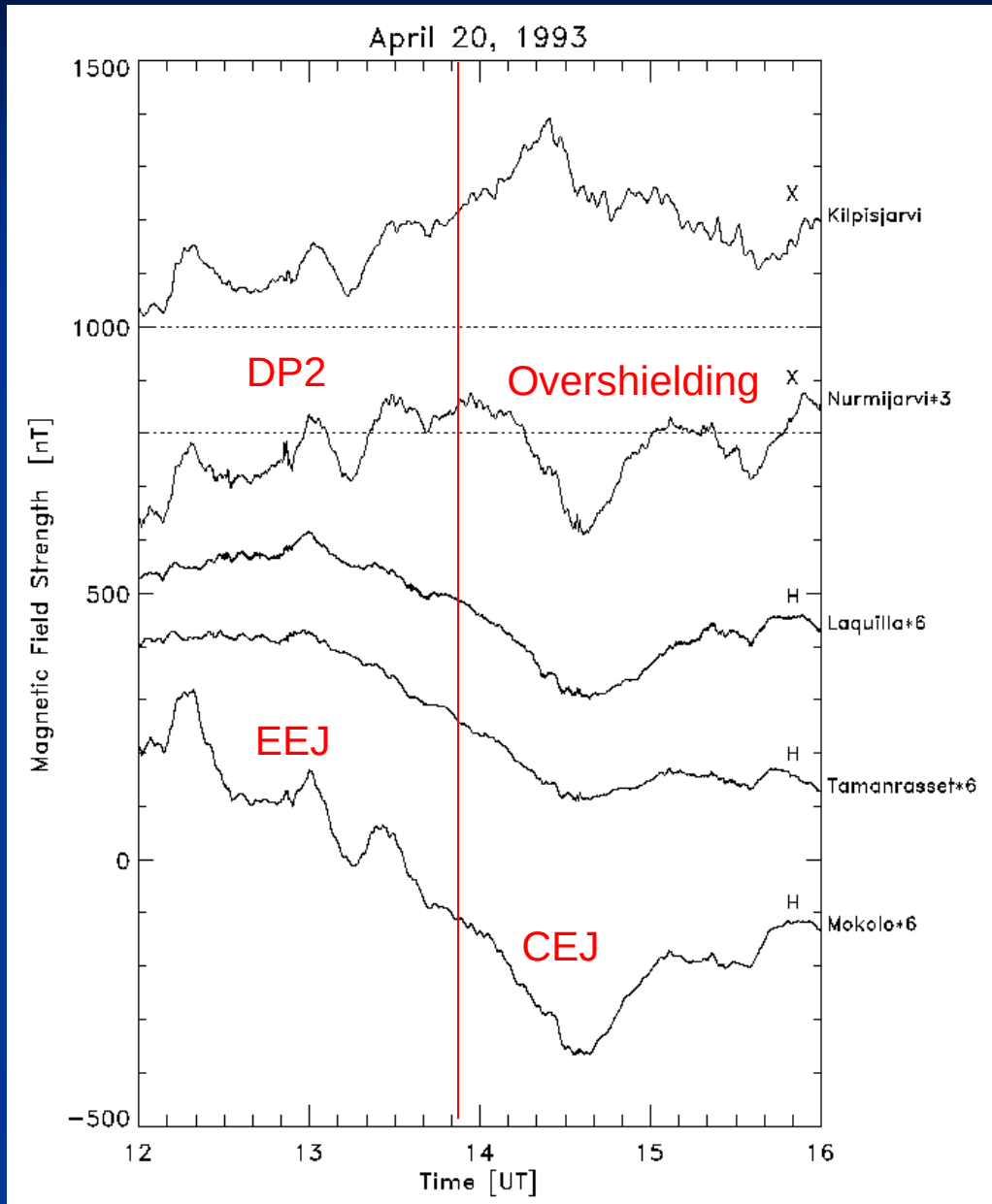

Latitudinal profile of the DP2

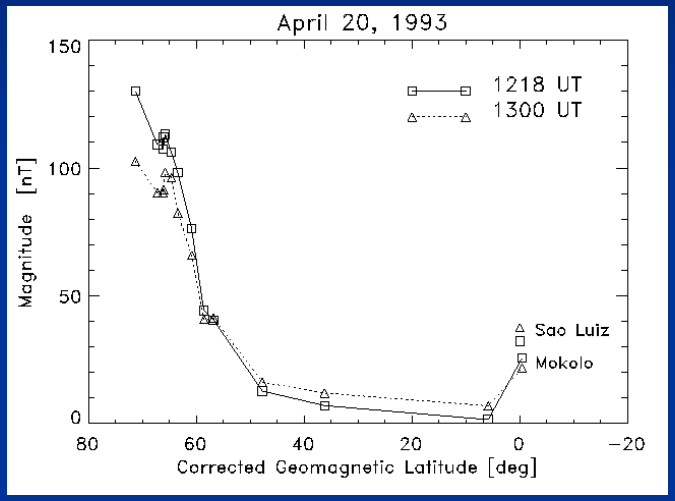

Latitudinal profile of the negative bay

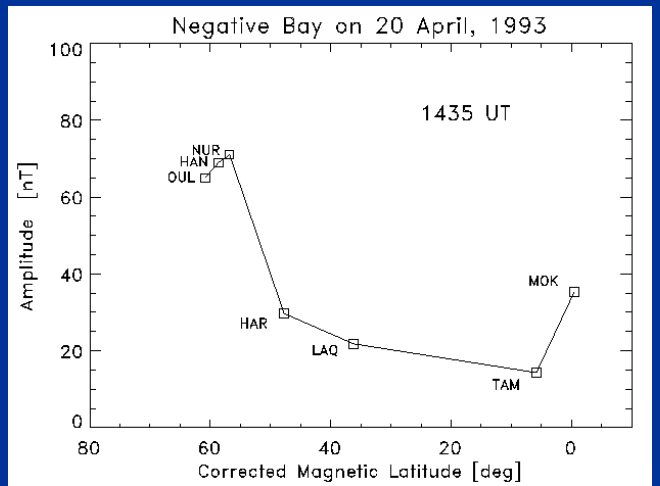

Overshielding at the onset of an isolated substorm

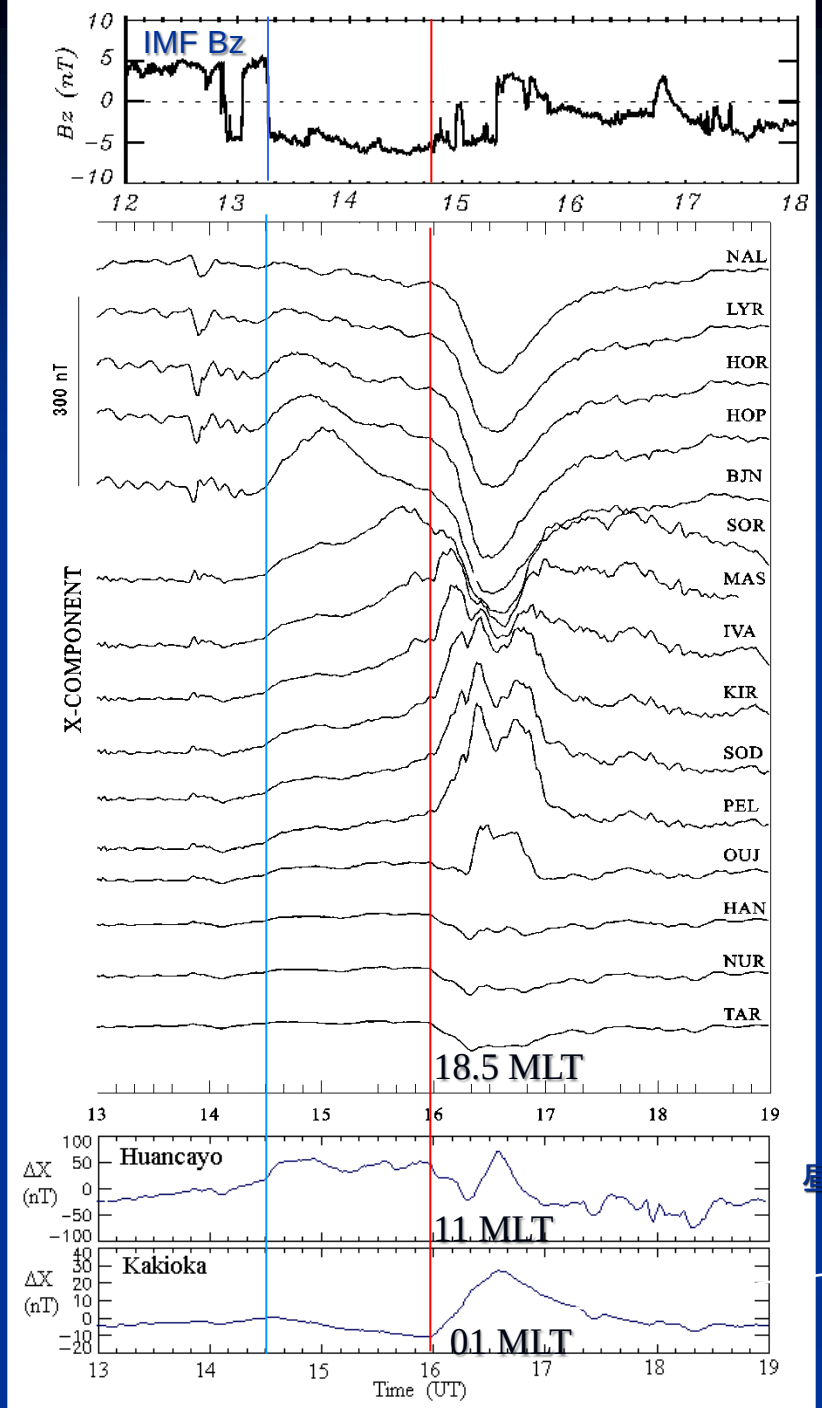

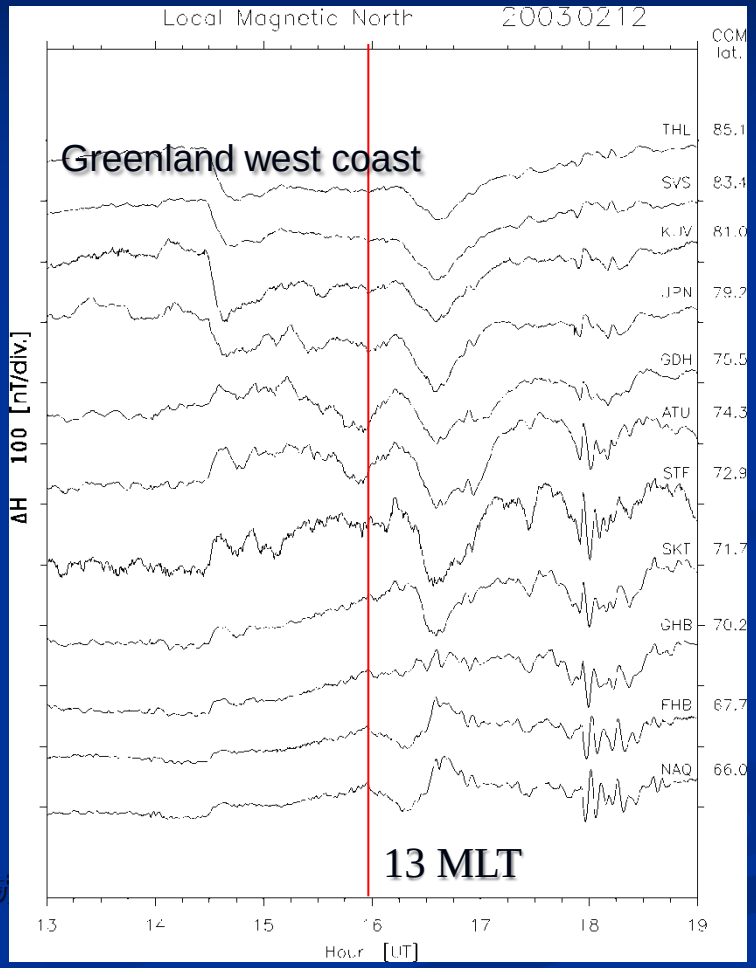

(Hashimoto et al., JGR 2011)

The equatorial CEJ begins 2 min earlier than the midnight positive bay

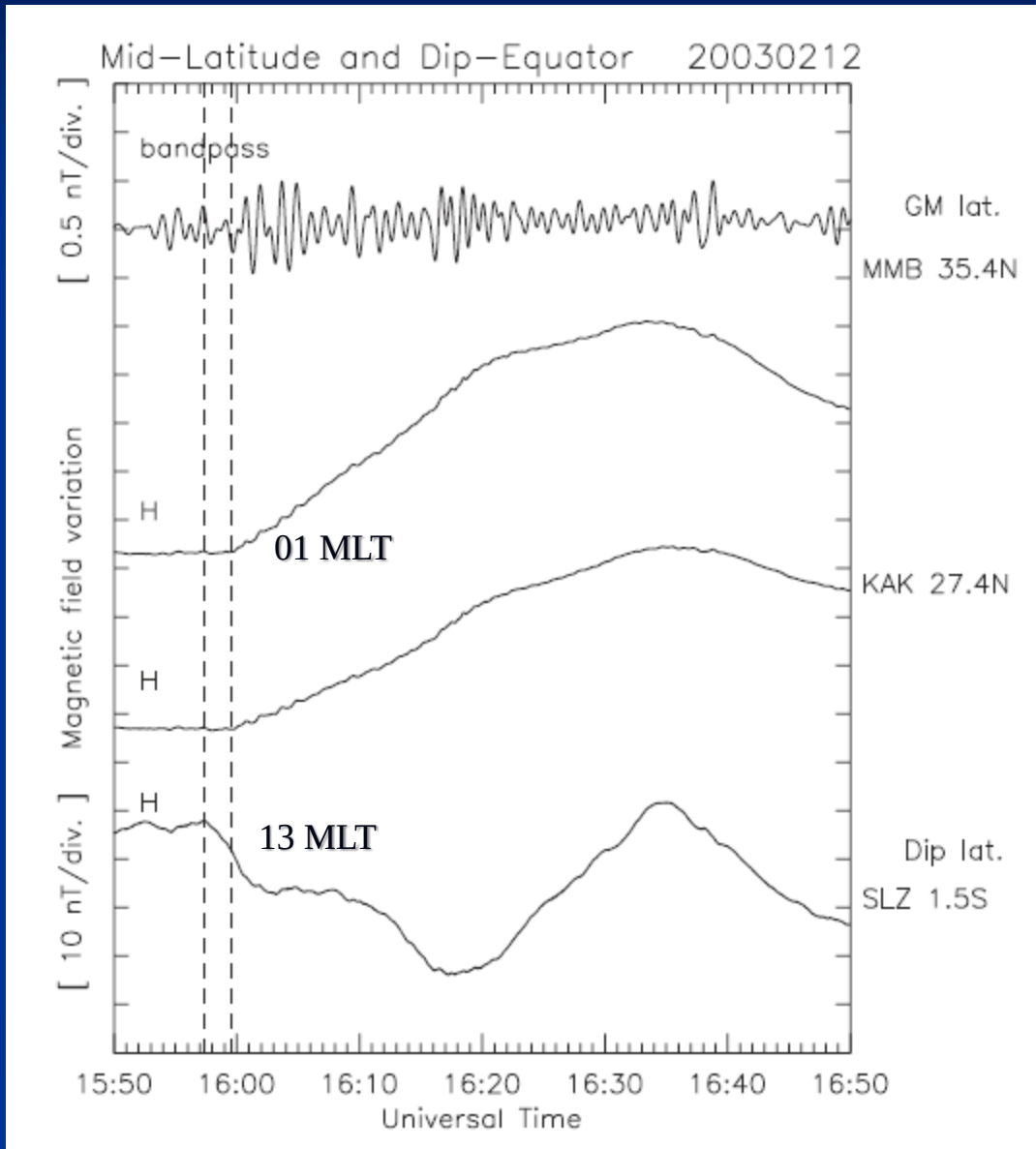

(Hashimoto et al., JGR 2011)

Global MHD simulation of the substorm current system

A ring current-R2 FAC current circuit is completed between the inner magnetosphere and auroral ionosphere at the onset of the substorm.

Substorm R1 FACs are generated by the dayside cusp dynamo

(Tanaka et al., JGR 2010)

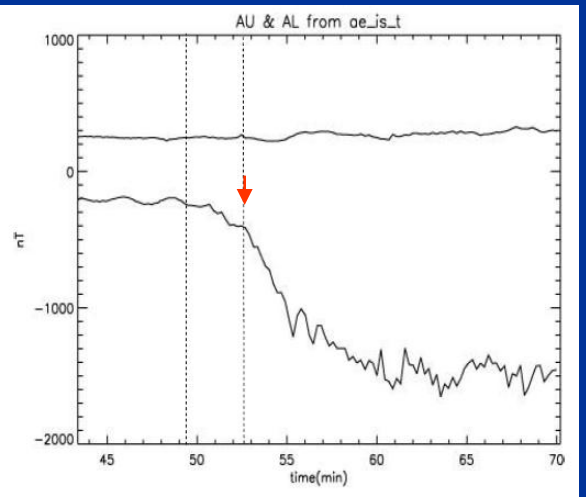

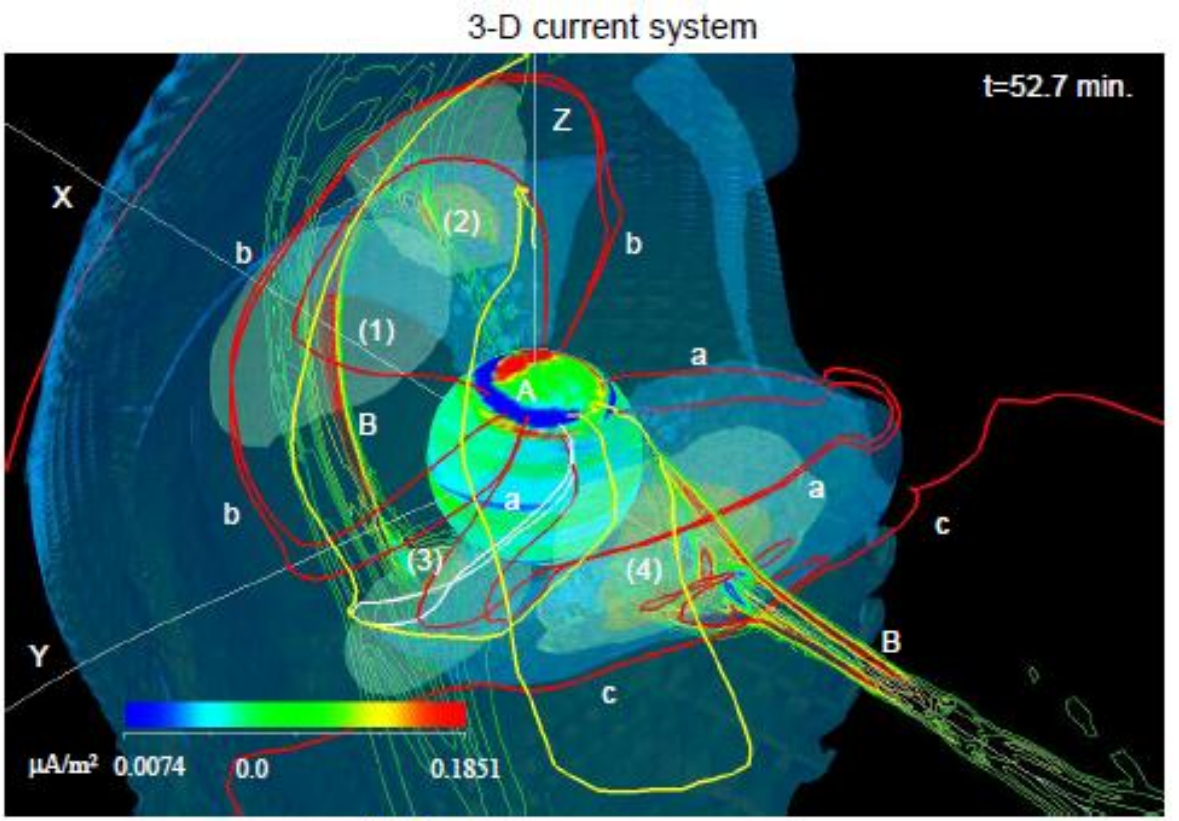

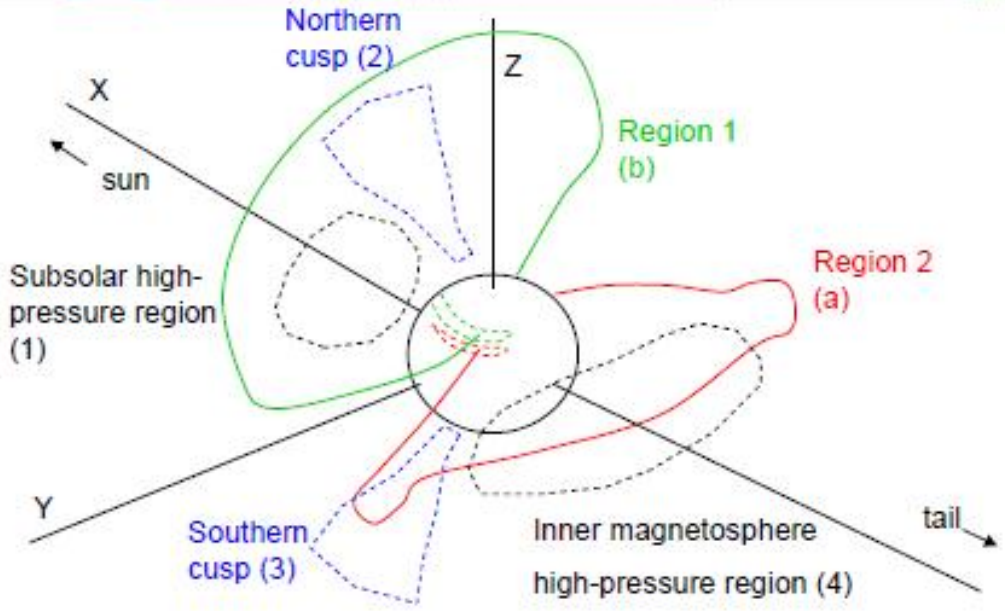

MHD simulation of the R1 and R2 field-aligned currents on the polar ionosphere during the substorm

(Tanaka et al., JGR 2010)

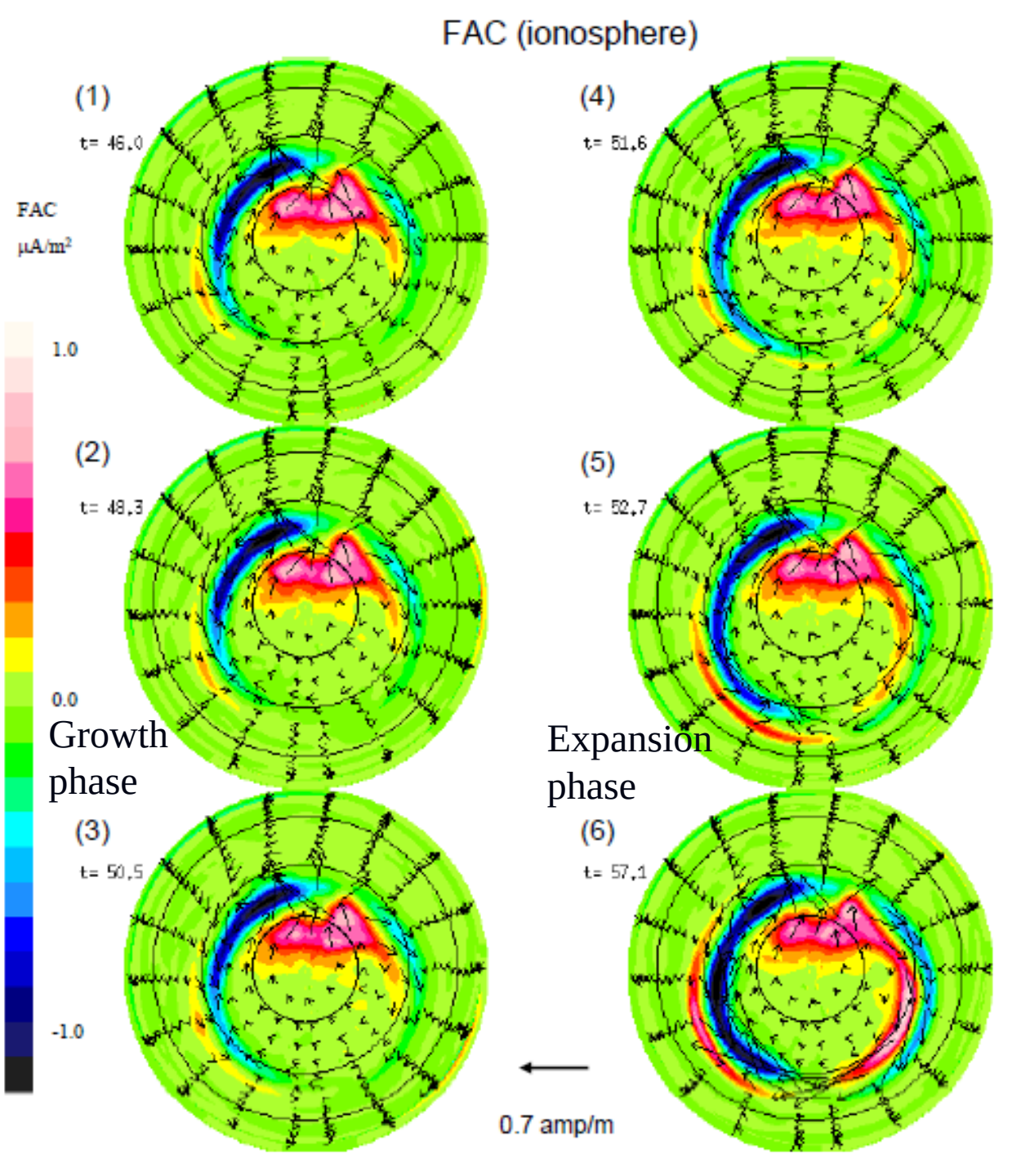

Integrated R1 and R2 FACs during the substorm

(Courtesy of Fujita and Tanaka)

Both the R1 and R2 FACs increase significantly during the expansion phase in agreement with the observations.

The R2 FACs are strong enough to cause the overshielding at low latitude.

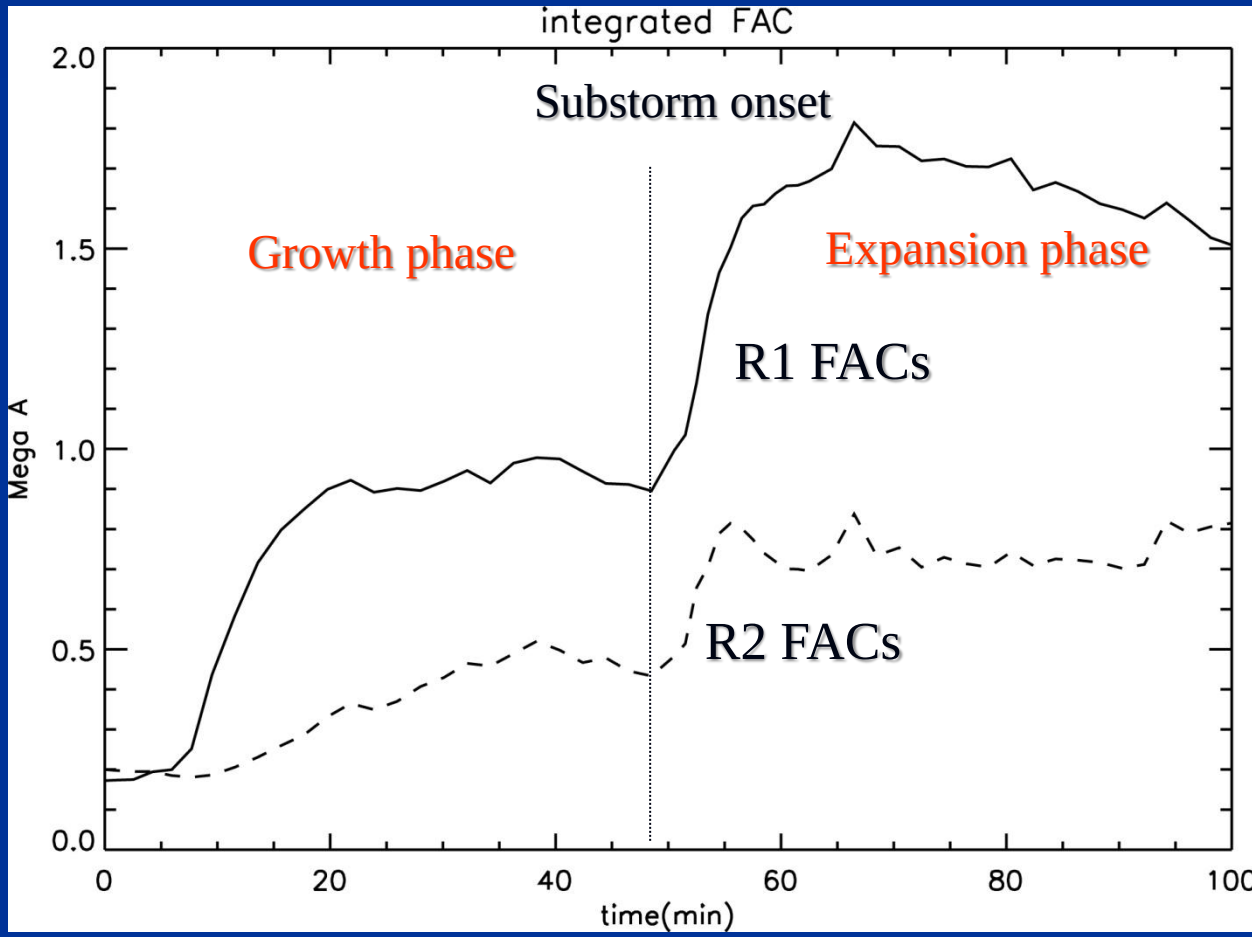

Dayside substorm currents driven by the R1 and R2 FACs

R1 FAC - EEJ
current circuit

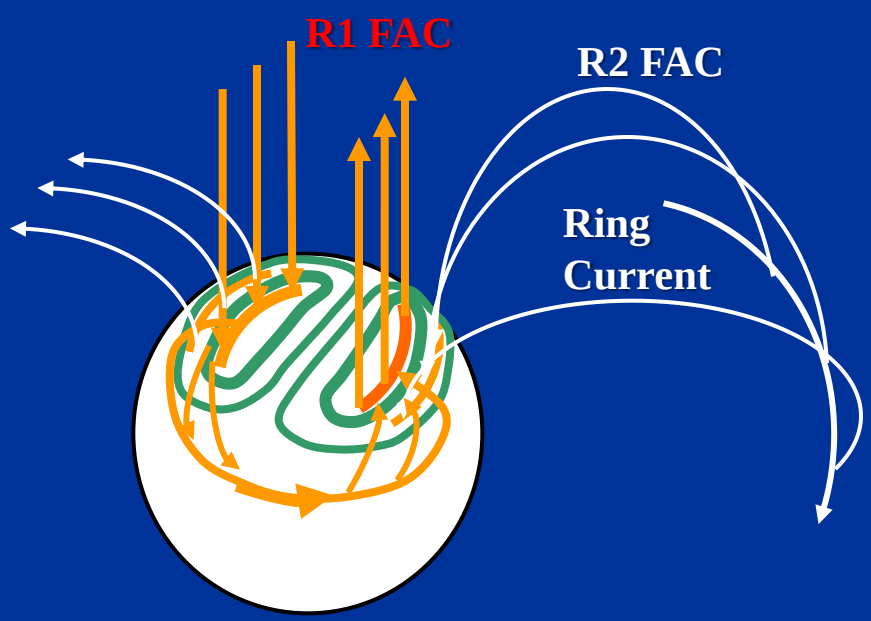

R2 FAC - CEJ
current circuit

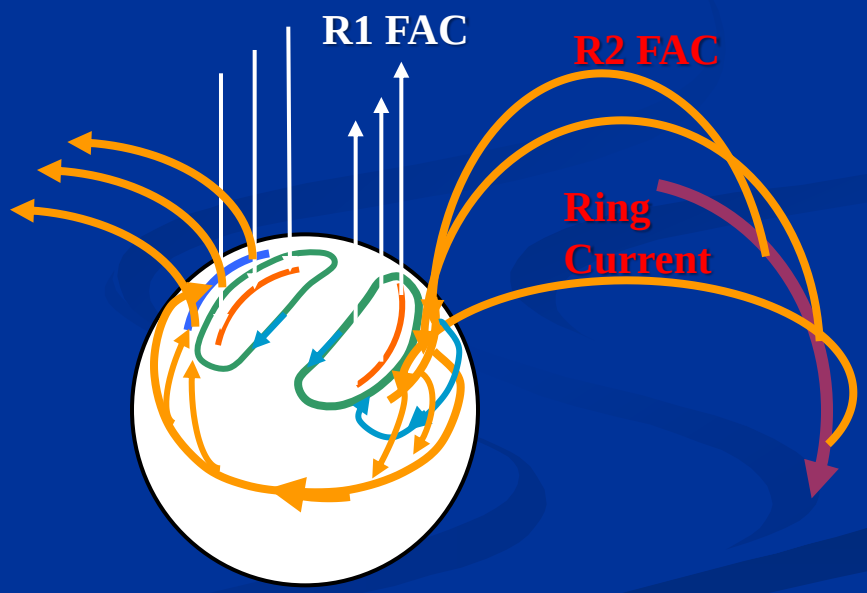

Substorm (auroral substorm)

Growth phase

Expansion phase

Recovery phase

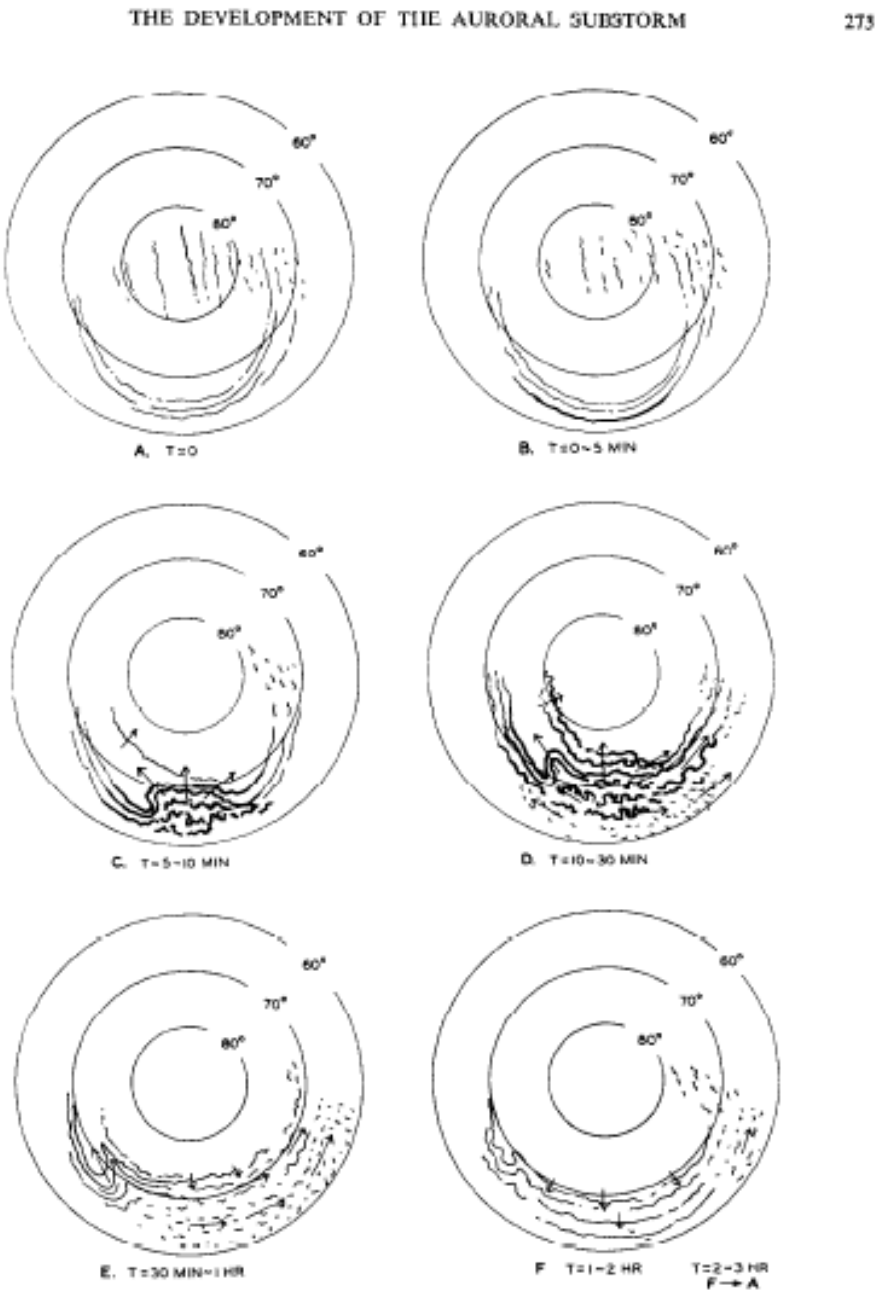

FIG. 1. SCHEMATIC DIAGRAM TO ILLUSTRATE THE DEVELOPMENT OF THE AURORAL SUBSTORM. THE CENTER OF THE CONCENTRIC CIRCLES IN EACH STAGE IS THE NORTH GEOMAGNETIC POLE, AND THE SUN IS TOWARD THE TOP OF THE DIAGRAM.

PBI and preexisting arc

(Toshi Nishimura)

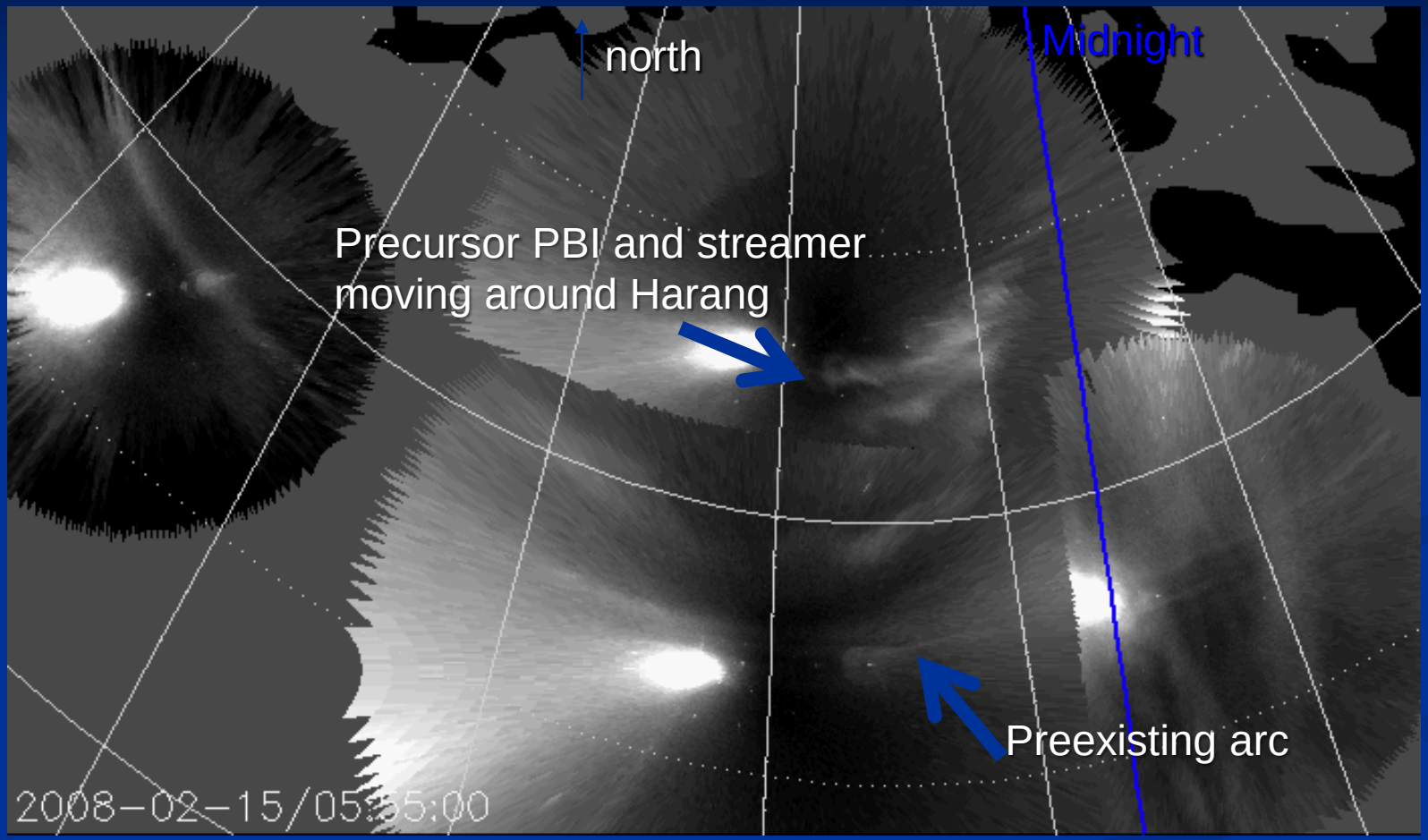

Multiple streamer sequences occurred but only the last one led to the onset.
Notice the thin arc formation associated with the previous streamer.

Pre-onset BBF and PBI

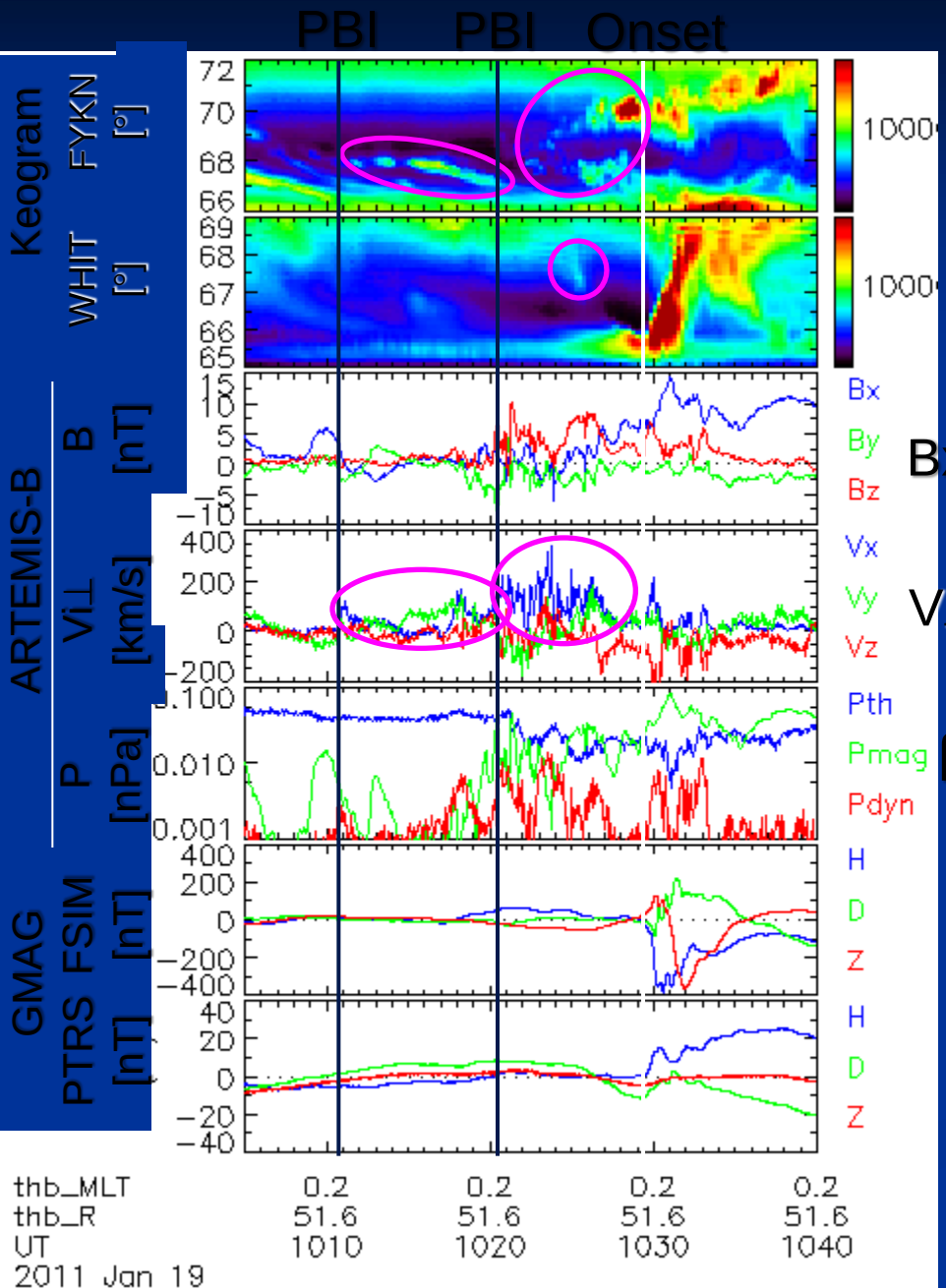

PBIs

Streamer

Bx~0

V⊥x>0

β>1

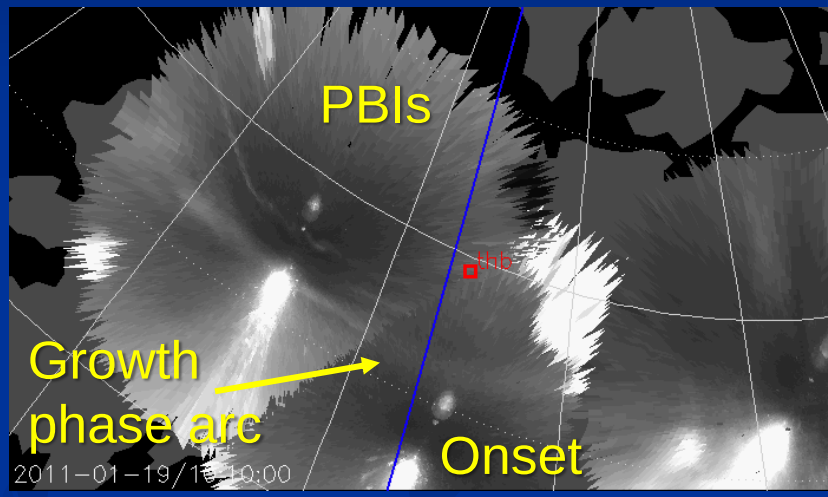

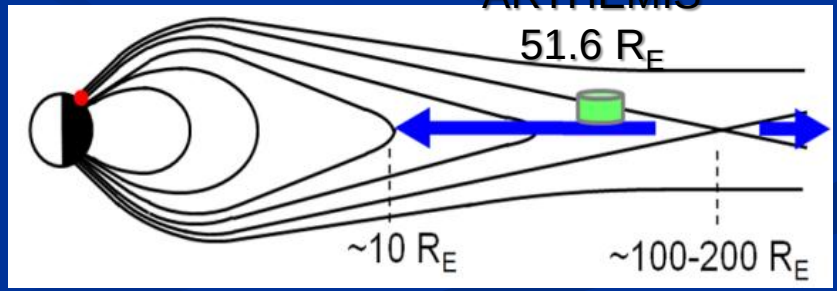

Earthward flow at 51.6 R_E, suggesting the flow originating from further downtail rather than NENL.

[Nishimura et al., 2011 pre-onset thin arc]

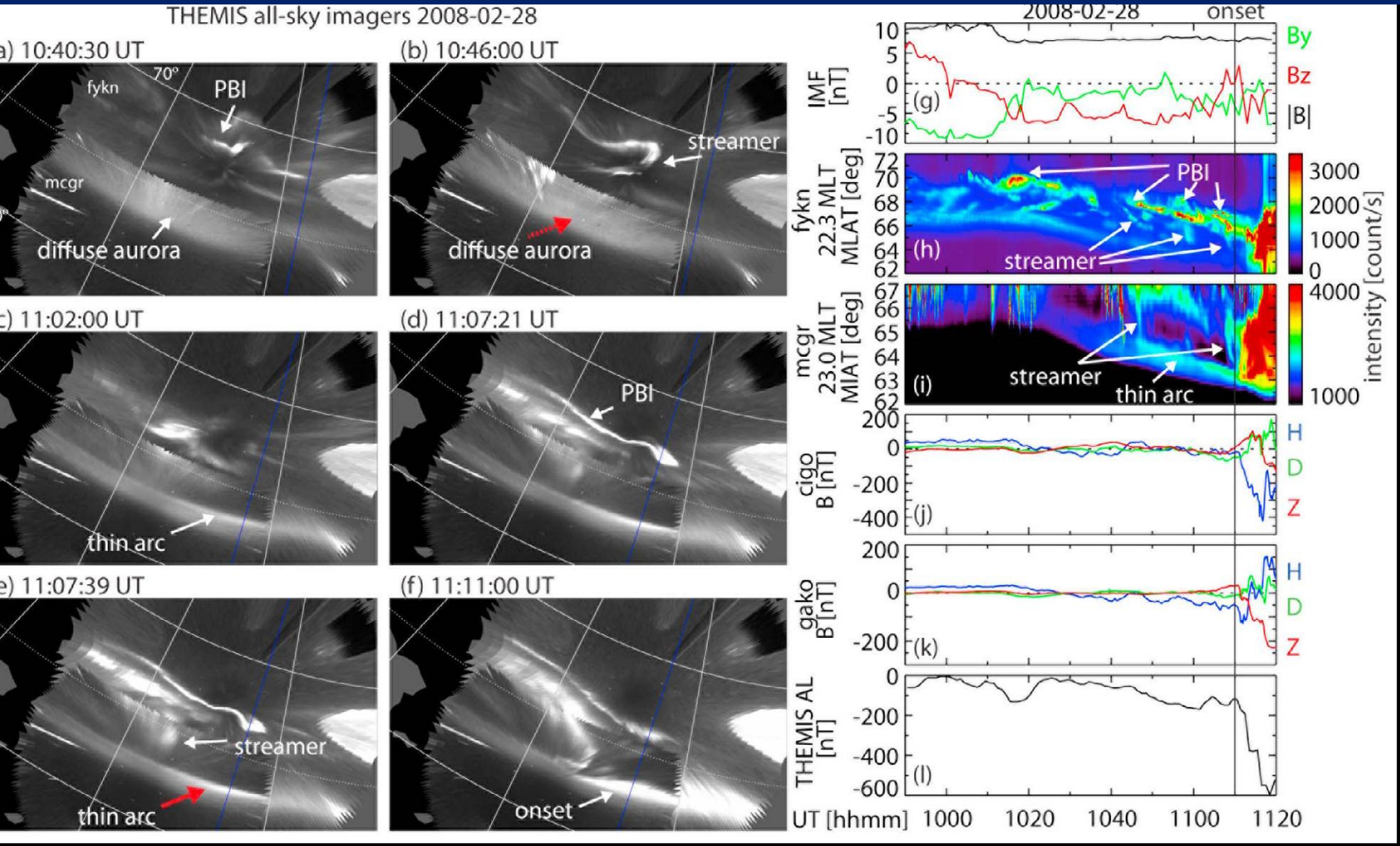

Suggested auroral sequence

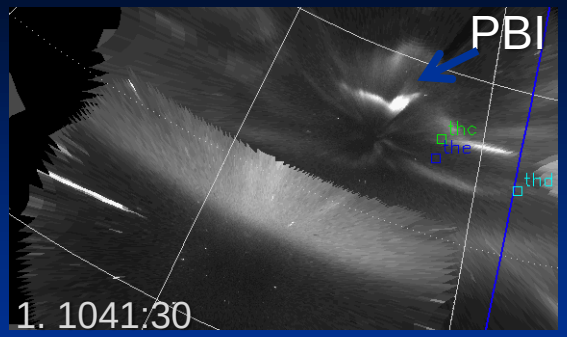

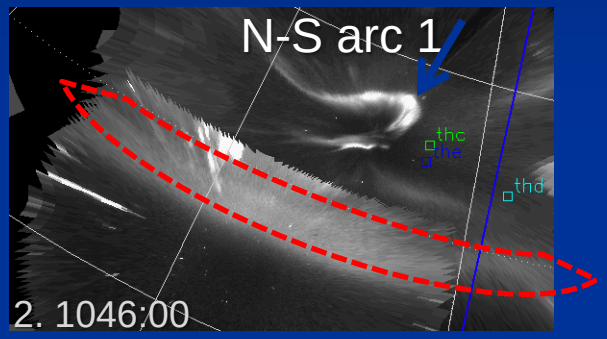

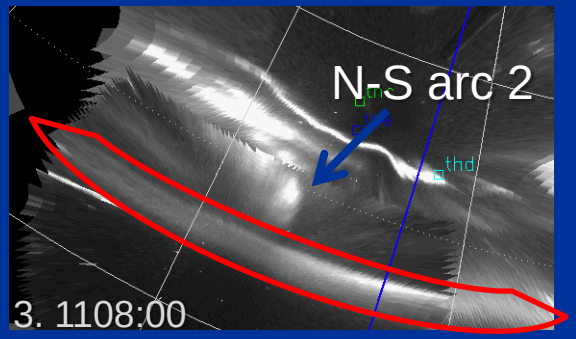

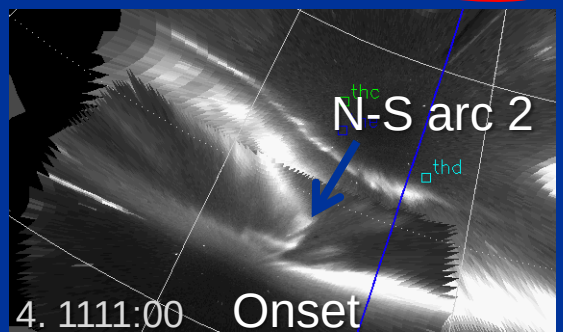

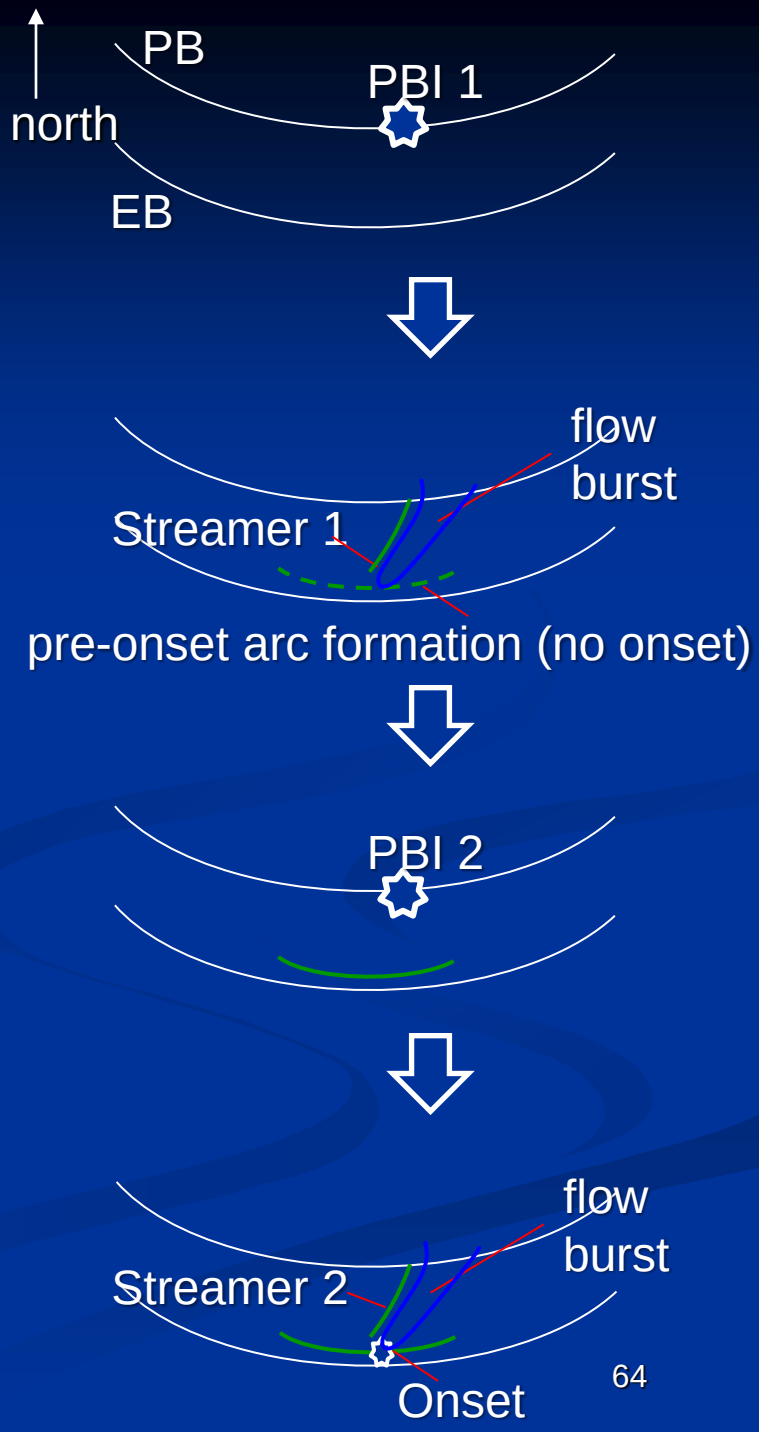

Onset arc FACs

[Nishimura et al., JGR2012 in press, onset FAC]

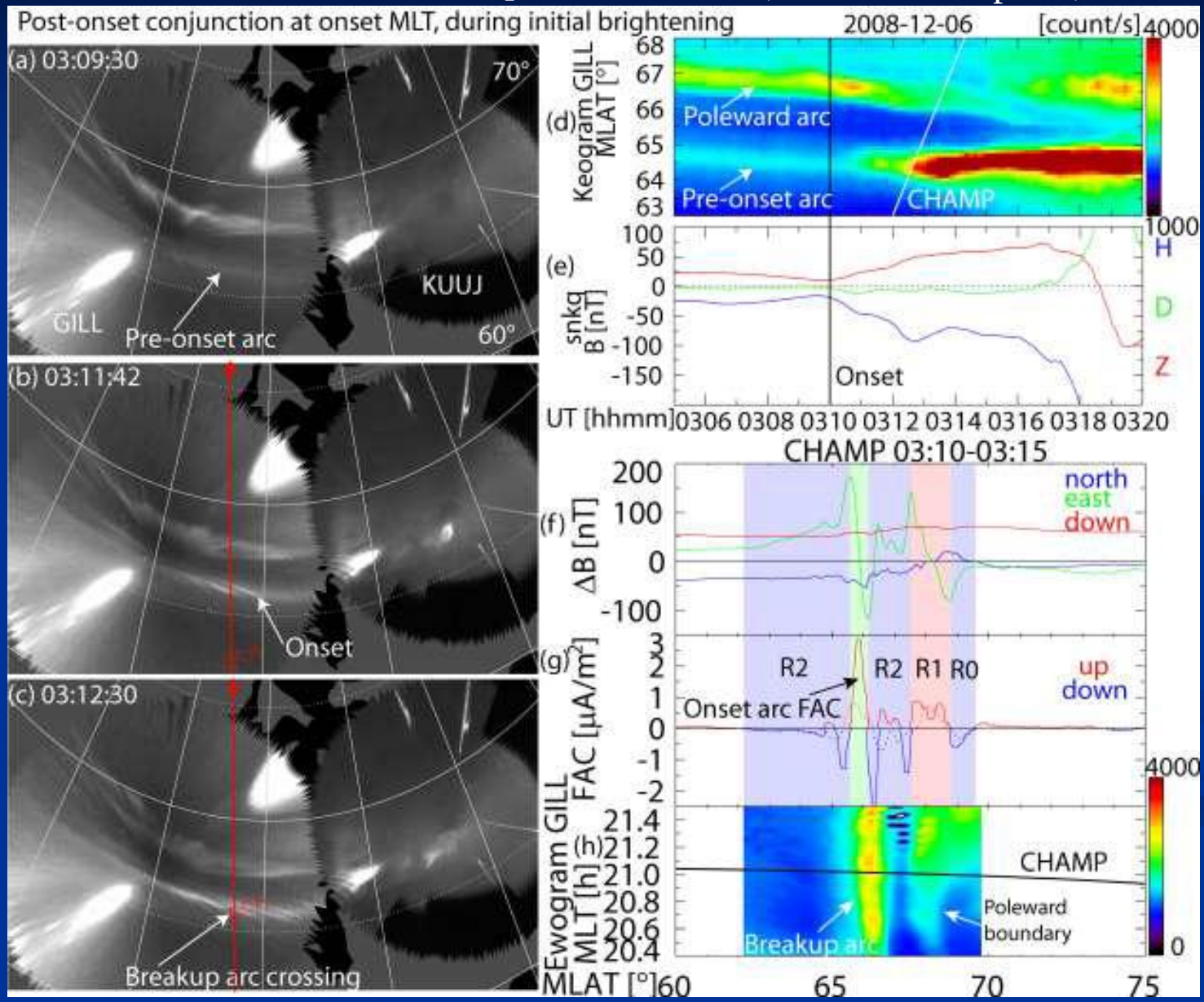

Breakup arc FACs

[Nishimura et al., JGR2012 in press, onset FAC]

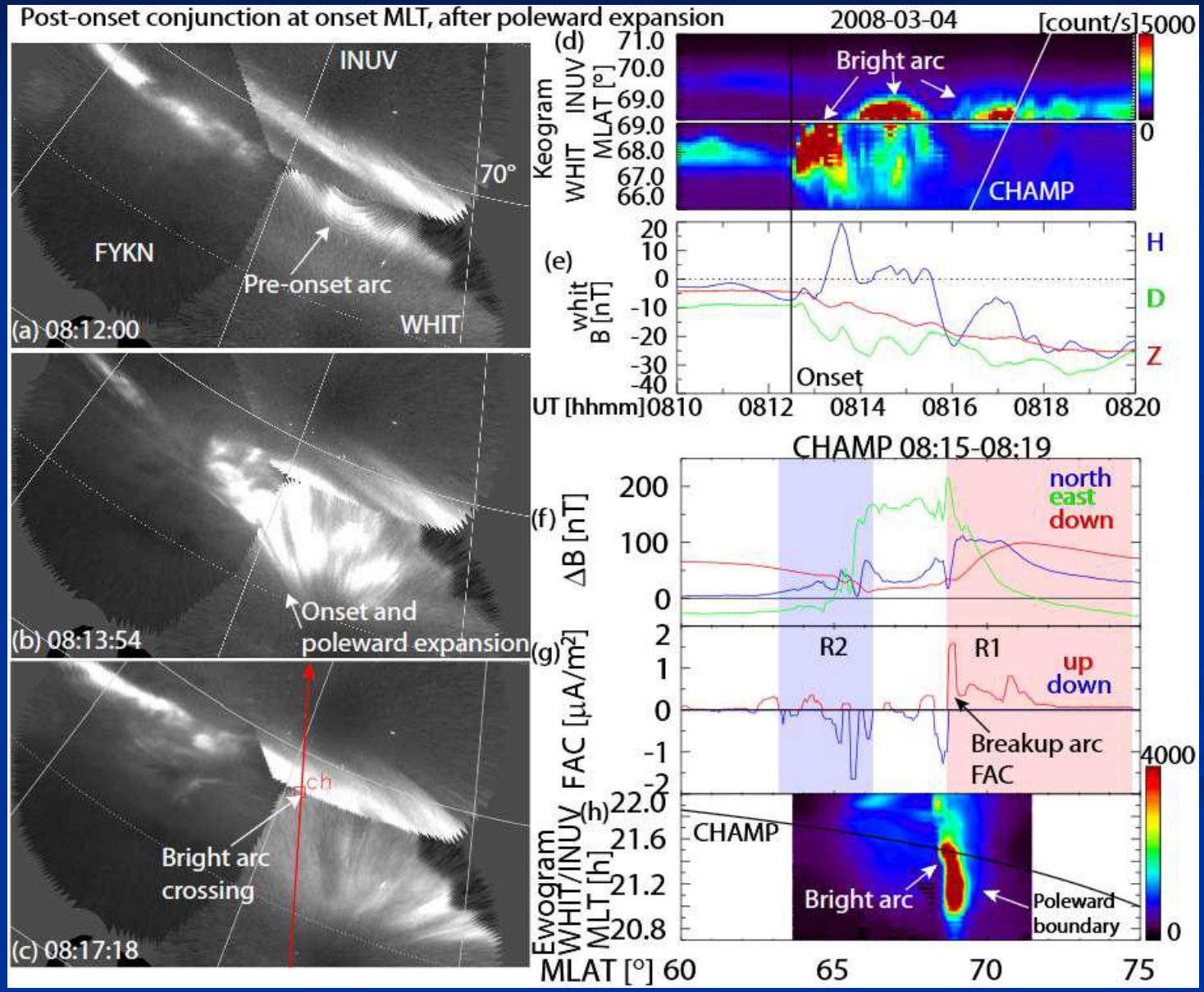

Post-breakup FACs

[Nishimura et al., JGR2012 in press, onset FAC]

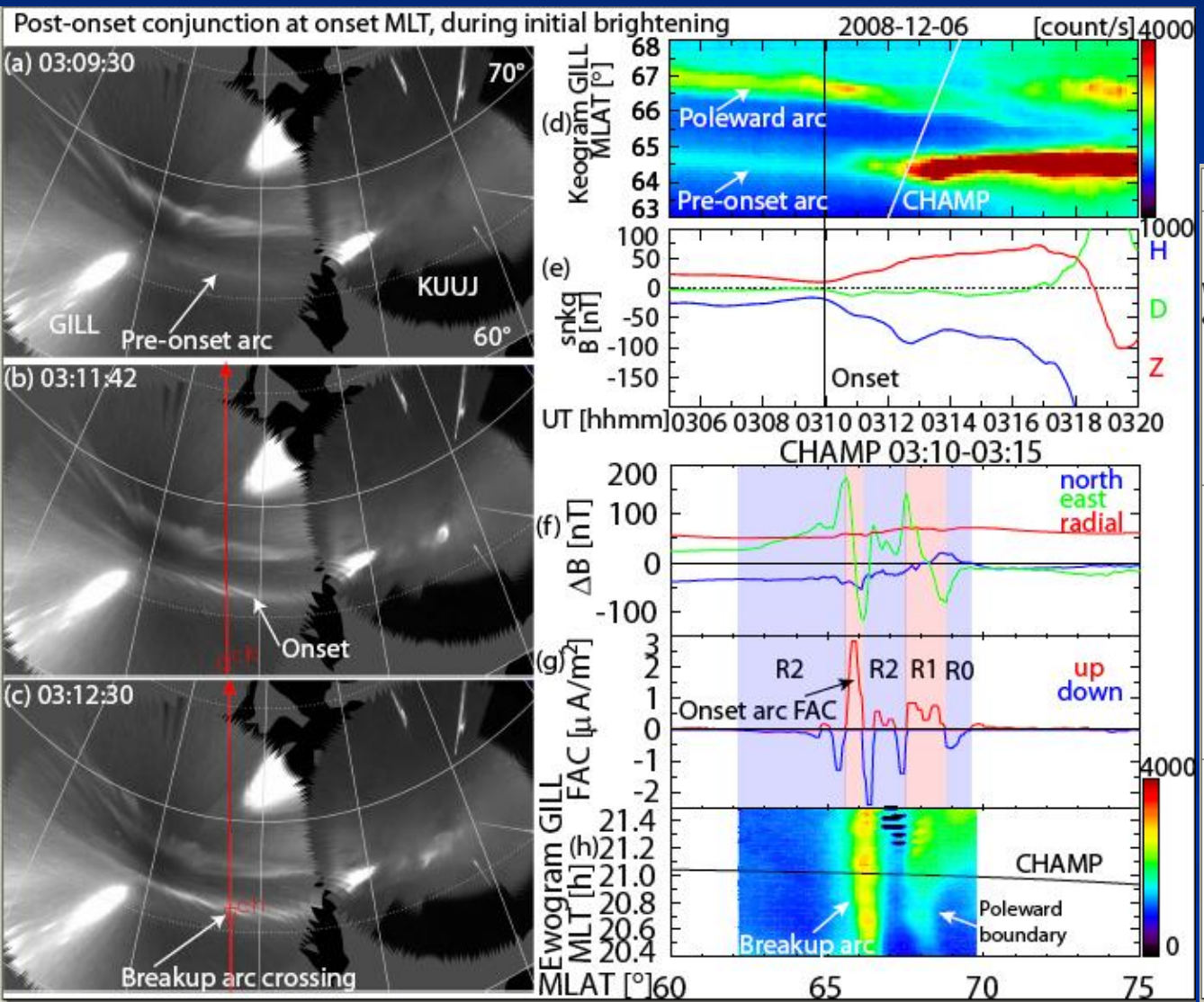

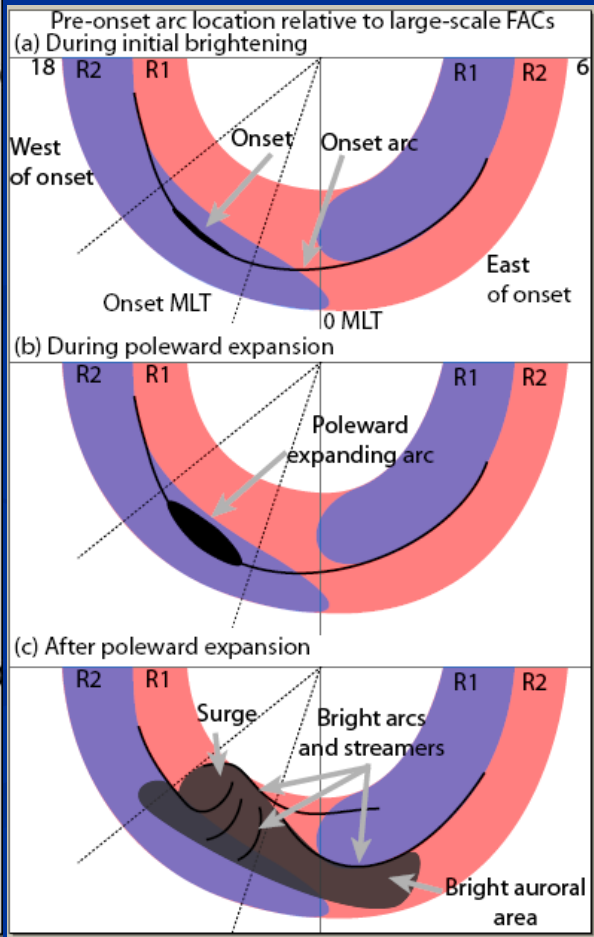

Summary (1)

- Different types of dynamos are activated in the magnetosphere during the geospace disturbances: magnetopause currents (SSC, PC5), diamagnetic currents in the cusp/mantle (R1 FACs), in the inner magnetosphere (ring currents, R2 FACs) and in the near-Earth magnetotail (substorm currents).
- The electric field and currents are transmitted along the magnetic field lines forming a pair of field-aligned currents to the polar ionosphere. They are transmitted to low latitude by the TM0 mode waves in the Earth-ionosphere waveguide, driving DP2 type ionospheric currents composed of two-cell Hall currents and Pedersen currents amplified by the Cowling effect at the dayside equator.
- The electric field is transmitted from the conducting ionosphere to the F-region and inner magnetosphere, causing quick response of the low latitude ionosphere and inner magnetosphere.

Summary (2)

- During the substorm growth phase and storm main phase, the convection electric field prevails down to the equator, causing significant ionospheric disturbances such as the EIA, PRE, TEC and so on.
- During the substorm expansion phase and storm recovery phase, overshielding occurs at mid-equatorial latitudes, suggesting that the energy deposited in the inner magnetosphere can make significant electrodynamic effects in the low latitude ionosphere.